Phenol and cresols treatment in aqueous solution by electro-Fenton process: Application to the mineralization of aeronautic wastewater industry

Marcio Pimentel

Université Paris-Est Marne-La-Vallée
Institut Francilien des Sciences Appliquées (IFSA)
Laboratoire Géomatériaux et Géologie de l'Ingénieur

THÈSE

pour obtenir le grade de
Docteur de l'Université Paris-Est Marne-la-Vallée

Spécialité : Sciences et Techniques de l'Environnement

présentée et soutenue publiquement par

Marcio PIMENTEL
le 24 septembre 2008

Etudes de l'oxydation de phénol et crésols par l'oxydation électrochimique avancée en milieu homogène. Application au traitement d'effluent de l'industrie aéronautique

Phenol and cresols treatment in aqueous solution by electro-Fenton process: Application to the mineralization of aeronautic wastewater industry.

Directeur de thèse : Prof. Mehmet A. OTURAN

Jury:

Président:	Prof. Jean Guillaume EON	Université Fédérale de Rio de Janeiro
Rapporteurs:	Dr. Maurice MÉDEBIELLE	Université Lyon 1
	Prof. Geraldo Lippel SANT´ANNA JR.	Université Fédérale de Rio de Janeiro
Examinateurs:	Prof. Márcia W. Carvalho DEZOTTI	Université Fédérale de Rio de Janeiro
	Dr. Nihal OTURAN	Université Paris-Est Marne-la-Vallée
	Prof. Tito Livio Moitinho ALVES	Université Fédérale de Rio de Janeiro

Remerciements

Cette thèse a été réalisée par une co-tutelle entre l'Université Féderal de Rio de Janeiro et l'Université Paris-Est de Marne-La-Vallée au laboratoire des Géomatériaux et Géologie de l'Ingénieur au sein de l'équipe chimie de l'environnement avec le financement de l'Armée de l'Air Brésilienne.

Je remercie l'Armée de l'Air Brésilienne par la confiance qui m'a été accordée.

Je tiens à dire un grand merci à Mehmet A. Oturan, Professeur à l'université de Marne-la-Vallée, pour les conseils précieux, ses commentaires et tout aide qu'il m'a apporté au cours de ce travail.

Je tiens à dire merci aussi à Marcia Dezotti, Professeur à l'Université Fédérale de Rio de Janeiro, pour les conseils et l'aide qu'il m'a apporté au cours de ce travail.

Je remercie très chaleureusement Nihal Oturan pour toute l'aide qu'elle m'a apportée pour mes expériences.

Un grand merci à mon épouse Marcela pour son amour et patience pendant tout ce temps.

Je voudrais également remercier toute l'équipe du laboratoire Géomatériaux, surtout les thésards et stagiaires, pour leur bonne humeur, leurs histoires et, particulierment, les commentaires sur football pendant les pauses. Merci à Beytül, Nacho, Samiha, Mababa, Aida, Mustapha, Minir. Vous étiez là quand j'en avais besoin et même pour les autreschoses.

Abstract of Thesis presented to COPPE/UFRJ as a partial fulfillment of the requirements for the degree of Doctor of Science (D. Sc.)

Phenol and cresols treatment in aqueous solution by “electro-fenton” process:
Application to the mineralization of aeronautic wastewater industry.

Marcio Antonio da Silva Pimentel

September/2008

Advisors: Mehmet A. Oturan
Márcia Walquíria de Carvalho Dezotti

Department: Chemical Engineering

The present work verified the efficiency of electro-Fenton to destroy phenolic compounds present in Stripping Aircraft Wastewater. This research aimed to elucidate the influence of the catalyst nature, its concentration and of electric current density in efficiency of electro-Fenton process using an indivisible cell with a carbon felt cathode and platinum or borod doped diamond anodes. The experiments compared the effect of these variables to destroy phenol, cresols and their intermediates. The compounds and many intermediates formed were identified in High Perfomance Liquid Chromatograph and allowed obtaining apparent and/or absolute constants and simplified degradation mechanisms. In optimum conditions, measures of Total Organic Carbon showed high mineralization rates. At the end, the application of electro-Fenton process to high organics loads of real Stripping Aircraft wastewater allowed obtaining almost complete mineralization replacing Pt anode by Boron Doped Diamond.

Key words: degradation, phenol, cresols, electro-Fenton.

SUMMARY

LIST OF FIGURES

LIST OF TABLES

ABREVIATIONS

AOPs – Advanced Oxidative Processes

HPLC – High performance liquid chromatography

TOC – Total Organic Carbon

Fig. – Figure

UNEP – United Nations Environment Programe

INTRODUCTION

Safety is one of the most important requirements in aeronautical industry. From the mechanical point of view, it is frequently necessary to remove all paint from the fuselage in order to verify the existence of corrosion points. Notwithstanding, the paint removers used in these processes have high concentrations of phenols and cresols, which are pollutants of considerable environmental risk. Releasing this waste in natura in the aqueous media constitutes environmental crime, because the waters generated from the washing (effluents) contain phenols' concentrations much higher than the release patterns defined by the environmental agencies (FRANCE, 2001; BRAZIL, 2005). The aeronautical activity also requires the use of extremely resistant paints, what makes impossible the use of less toxic removers. Hence, the *end of pipe* treatment becomes necessary, even if it means a higher cost.

Many studies show that the biological processes may degrade many effluents, which contain phenolic substances, satisfactorily. However, the acclimatization is very difficult in waters with high concentration of residuals; the retention time becomes very high (usually days), specific nutrients are needed, and the biggest part of aromatic intermediaries is persistent. (AHAMAD and KUNHI, 1999; PERRON and WELANDER, 2004).

Aiming at meeting the environmental legislation demands, which grow more and more severe since the 90's, a number of alternative techniques for residual water treatment were developed, these were called advanced oxidation processes (AOPs). The AOPs involve the in situ generation of hydroxyl radical ($^{\bullet}OH$), a very strong oxidizing agent, capable of destroying the organic molecules present in contaminated waters, converting them successively into carbon dioxide and water (BAIRD, 2002). Therefore, it is a clean technology that minimizes the transference of the pollutant mass from the liquid phase to the solid one. Moreover, the reactions between the radicals $^{\bullet}OH$ and the organic pollutants are quicker than the ones found in conventional chemical oxidants.

Among the most recent AOPs, the electrochemical advanced oxidation process (EAOP) was created, which made viable the electrochemistry production of the $^{\bullet}OH$ radical. Among the EAOPs, the electro-Fenton process has been efficiently applied to a large range of organic pollutants. The main advantages of this process lie on the fact that it presents high efficiency, low consumption of chemical products and it may be applied in high salinity and turbidity effluents.

The major applications of electro-Fenton process make use of iron (II) as catalyst. According to OTURAN *et al.* (2001), even when applying low electric currents at an optimum dose of Fe (II) of 0.1 mM, it is possible to degrade the biggest part of organic compounds and its aromatic intermediates. Nonetheless, new studies have presented interesting results using cobalt, cupper

and manganese as catalysts (ANIPSITAKIS and DIONYSIOU, 2004; SKOUMAL, 2006; IRMAK *et al.*, 2006).

Thus, the present research aims at verifying the efficacy of the electro-Fenton process for the treatment of the synthetic effluent, which contains phenol and cresols, used in the treatment of the actual effluent generated in the removal of paint from Air Force Command aircrafts. From the chemical composition of the products frequently used in aeronautical industry, and the characterization of the effluents originated in the paint removal processes, it was identified that phenol and the cresol isomers are the present chemical substances that demand more complexity in this effluent treatment.

As specific objectives we have: the identification of the most persistent aromatic compounds that was sought by obtaining the phenol and cresols degradation speed rates through the electro-Fenton process; the proposition of simplified mechanisms of degradation reaction by means of the identification of the most persistent intermediates; the study of nature influence on the electrodes (anodes), as well as of nature and catalysts concentration and current density in phenol degradation; and the optimization of operational parameters for the mineralization of the real effluent.

Many experiments were made applying the electro-Fenton process in synthetic samples containing phenol, cresols and some intermediates aiming at optimizing the operational parameters of the process. Lastly, the use of the process in real effluent, collected in November 2007 in the Park of Aeronautical Material of Galeão in Rio de Janeiro were made, under optimum conditions.

The development of this thesis was made through chapters, summarized in the following way: from the introduction and the research objectives presentation, followed the bibliographical review presenting the characteristics of the effluents typical from the aeronautical industry, the techniques of treating phenol and cresols and the influence factors in the Electro-Fenton Process. The third chapter presents experimental procedures, analytical methodologies, analytical techniques used in the treatments and in the chemical analysis. The results obtained in the experiments are presented and discussed in the fourth chapter. In the closing chapter the conclusions are presented and research lines for further studies are suggested.

CHAPTER I: BIBLIOGRAPHICAL REVIEW

1.1 Aircraft effluent characterization

The stages that generate effluents in aircraft maintenance processes are the decarbonization, remotion, degreasing, phosphatization, chromatization and the application of shampoo and brightener (INTERMETA, 2001).

Decarbonization consists of the application of phenol, cresols and methylene chloride based products, aiming the removal of grime accumulated on aluminium throughout time, especially nearby the engine and exhaust pipes (ARQUIAGA *et al.*, 1995).

Remotion encloses the fuselage paint removal by means of using products that contain methylene chloride (70-75%), phenol, cresols and surfactants (PENETONE CORPORATION, 2004), while the degreasing consists in the application of an alkaline solution of nonyl phenol ethoxylated based, usually heated, to remove contaminating substances, such as oils, grease and solids from the surface of the piece. Depending on the percentage of oil and grease in a piece, the degreaser may be diluted in kerosene (HANS, 1995).

According to NEUDER *et al.* (2003), phosphatization is a process of protecting metals, which consists of coating the metallic pieces with neutral phosphates and zinc, iron and manganese amino acids.

Chromatization consists in the application of chromate-based coating particularly on aluminium surfaces, aiming at guaranteeing protection against corrosion and providing a base for painting (PUMA and RHODES, 2002).

The application of neutral detergent-based shampoo aims at complementing the removal of previously applied chemical products, which were not removed by water.

The application of a brightener aims at recovering the oxidized aluminium surfaces using a balanced composition of organic acids with moisturizing and penetrating agents which guarantee residual and homogenous protection.

All these stages of aircraft maintenance are present in the washing, pickling and painting preparation processes indicated in Figures 1, 2 and 3.

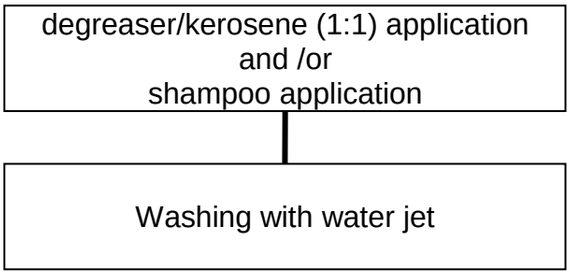

Figure 1. Typical flowchart from washing process.

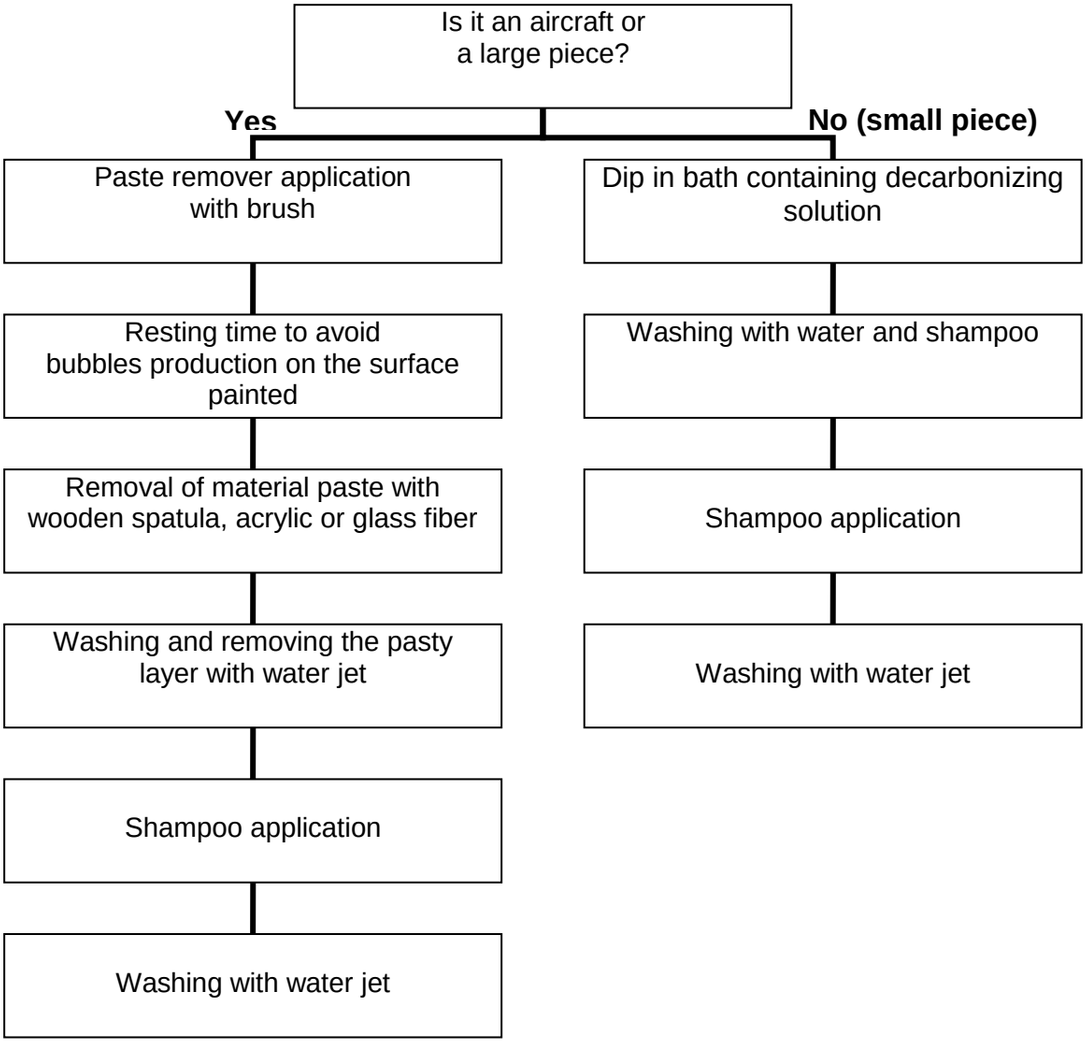

Figure 2. Typical flowchart of stripping process.

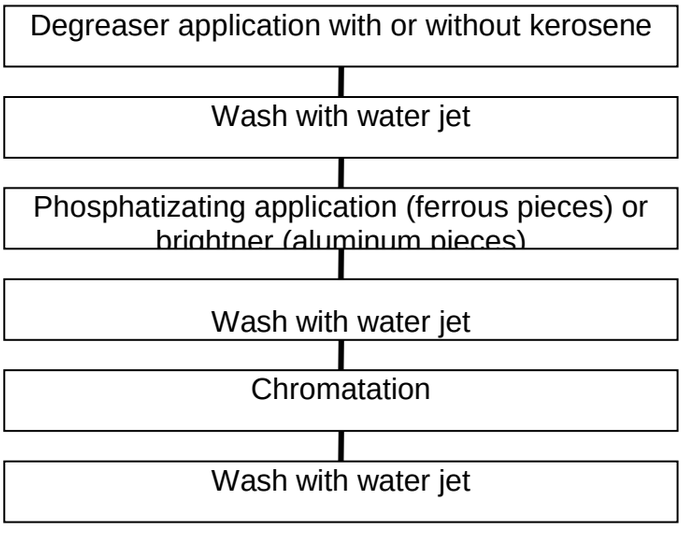

Figure 3. Typical flowchart of pre-painting process.

Figure 4 shows a fuselage pickling of T-25 aircraft in the Aeronautical Material Park of Lagoa Santa. It can be observed that, due to the nature of the chemical products used, protection gear for the individual are demanded.

Figure 4. Fuselage stripping of T-25 aircraft at PAMA-LS.

The frequency of the processes is extremely variable, and it is conditioned to the services demand promoted by maintenance routines. In general, an aircraft goes through many washing processes until it reaches the useful lifetime of painting. In this moment, after washing, paint stripping and pre-painting process, many kinds of painting with different chemical compositions are used. The paint film aims at protecting the fuselage from ultra-violet radiation and at providing it an aesthetical aspect. According to SHREVE and BRINK (1997), the phenolic and alchilic resins, as well as metallic pigments predominate in aeronautical industry.

Paint stripping tends to produce a more complex effluent because it contains chemical products with high phenols concentration, and by the presence of chemical products originated from the other processes of all film remotion from the fuselage. It also should be highlighted that paint stripping is a considerably important process as a security measure, because it allows checking the existence of any corrosion points at the fuselage.

Face this diversity of present chemical compounds; the Air Force Command hired two analyses set, done respectively in the Aeronautical Material Park of Lagoa Santa (PAMA-LS) (CETEC, 2000) and in the Aeronautical Material Park of Galeão (PAMA-GL) (HIDROQUÍMICA, 2007). These analyses aimed at characterizing the effluents originated from aircraft maintenance processes, identifying which organic compounds demanded more complexity in the process of

treating the effluents produced. Table 1 shows the results in the characterization from effluents produced in PAMA-LS and Table 2 presents the results in the characterization of effluents produced in PAMA-GL.

Table 1. Chemical analysis from wastewater produced at PAMA-LS

Place	PAMA-LS			
Date	11/12/2000			
Sample	Stripping Results	Washing	Pre-painting	Essay method
Ag (mg/L)	0.001	0.001	0.003	APHA 3120B
Al (mg/L)	1.63	0.29	27.85	APHA 3120B
Cd (mg/L)	0.80	0.054	4.34	APHA 3120B
Cr (mg/L)	33.11	2.94	4.46	APHA 3120B
Cr^{6+} (mg/L)	24.06	2.72	0.01	APHA 3500-CRD
Cu (mg/L)	0.043	0.04	0.65	APHA 3120B
COD (mg/L)	7317	20244	6537	ABNT NBR 10357/1988
Fe (mg/L)	0.47	0.16	____	APHA 3120B
Fe^{2+} (mg/L)	____	____	24.95	APHA 3120B
Phenols (mg/L)	2300	470	16	ABNT NBR 10740/1989
Ni (mg/L)	0.57	0.063	1.15	APHA 3120B
Oil and grease (mg/L)	566	96	12	APHA 5520B
Pb (mg/L)	1.07	0.42	0.55	APHA 3120B
pH	8.62	8.92	2.13	ABNT NBR 9251/1986
Settleable Solids (mL/L)	0.3	< 0.1	< 0.1	ABNT NBR 10561/1988
Sulfate (mg/L)	22.7	47.1	791.8	APHA 4500-SO_4^{2-} E
Anionic Surfactants (mg/L)	0.84	0.08	0.93	ABNT NBR 10738/1989
Zn (mg/L)	1.77	0.13	5.17	APHA 3120B

Among the metals analyzed, high concentrations of total chromium, hexavalent chromium, aluminium, cadmium and zinc can be observed. These metals are present in the paintings, in the many coatings base and, in the aluminium case, in the fuselage itself. The classic treatment for

hexavalent chromium comprises its reduction to trivalent chromium in alkaline pH and later precipitation in pH close to 9, with the aid of anionic polyelectrolytes. The other metals may be easily removed by precipitation in alkaline pH.

Table 2. Chemical analysis from wastewater produced at PAMA- GL

Place	PAMA-GL				
Date	14/12/2006		08/11/2007	09/11/2007	
Sample	Stripping	Stripping	Washing + Stripping + Pre-painting	Washing	Essay method
	Results				
Cr (mg/L)	65.6	75.0	_____	_____	APHA 3120B
Cr^{6+} (mg/L)	56.0	49.5	< 0.1	0.47	SM 3500
Phenols (mg/L)	_____	_____	157.68	10.1	MF 428
Óil and grease (mg/L)	_____	_____	42	65	MF 412
Anionic Surfactant (mg/L)	_____	_____	95.67	75.20	MF 417

The higher concentration of phenols, and of oils and greases, were detected in the paint stripping processes due to the remotion or decarbonization steps. The paint stripping process also presented high concentration of Chemical Oxygen Demand (COD), because besides the presence of phenols, cresols, anionic surfactants (detergents) and oils and greases, there is also high concentration of methylene chloride. Among the compounds present in the paint stripping process, the percentage of oils and greases, as well as the concentration of methylene chloride, can be reduced more easily. The oils and greases can be removed from physical processes breaking emulsions and passing through oil separators (NUNES, 19XX). According to *UNEP, ILO* and *WHO* (1996), the biggest part of methylene chloride evaporates in aqueous media, because it is extremely volatile (Henry's Constant = 2.57 x 10^{-3} atm m^3/mol) and the residual methylene chloride may be removed biologically.

Nevertheless, according to the International Programme on Chemical Safety (UNEP, ILO and WHO, 1994, 1995), many studies applied to humans, aquatic and terrestrial organisms and microorganisms prove phenol and cresols high level of toxicity.

The need of removing these compounds demands the knowledge of their main physical-chemical properties. According to BUDAVARI *et al.* (1989), phenol possesses white-colorless crystal shape with boiling point at 43° C. It has an acre smell and a pungent and spicy taste. When in liquid state it presents transparent, colorless and low viscosity character. A phenolic solution with approximately 10% of water is liquid at room temperature. Phenol is soluble in most organic solvent (aromatic hydrocarbonates, alcohols, ketones, ethers, acids, and halogen hydrocarbonates). However, it has its solubility limited whiled in aliphatic solvents.

Cresols are phenolic isomers with a methyl radical substituting the hydrogen in the *orto, meta* or *para* in relation to the hydroxyl group. According to DEICHMANN and KEPLINGER (1981), the commercial cresol, also known as cresilyc acid has the three isomers with low quantities of phenols and xylenes. From the physical point of view, the cresols consist in a solid white crystal or a yellowish liquid with pungent odor typical from phenols. Cresols are flammable and soluble in water, ethanol, ether, ketone and alkaline hydroxides.

The phenol and cresols' chemical properties are relatively close one to the other. According to SOLOMONS (1996), the main characteristic of these compounds is the presence of cyclic chains constituted by six atoms of carbon in hybridization type sp^2. Therefore, the high stability of the aromatic compounds would be related to the Bayer's Tensions Theory. The chemical reactions involve electrophilic substitution of the positions *orto* or *para* in relation to the hydroxyl group. Cloration, bromation, sulphonation and nitrations are typical examples of these reactions.

Phenol is sensitive to the action of oxidating agents. According to UNEP, ILO and WHO (1994), the removal of the hydrogen atom from the hydroxyl group is followed by the resonance and stabilization of the resultant phenoxy radical, which may be easily oxidized later. Depending on the oxidating agent and the reaction conditions, products like dihydroxy, trihydroxy-benzenes and quinones are formed. These properties make possible the use of phenol as an antioxidant, acting like a radical capturer (*trapping*). Phenol also reacts with the carbonyls in acid or alkaline media. In the presence of formaldehyde, phenol is easily converted into hydroxy-methyl-phenol and latter converted into resins by condensation.

According to FIEGE and BAYER (1987), cresols can also go through condensation reactions with aldehydes, ketones and dienes. The main physico-chemical characteristics of phenol and cresols are presented in Table 3.

Table 3. Some physical and chemical properties of phenol and cresols (FIESER, 1930; VIDIC, SUIDAN and BRENNER, 1993; UNEP, ILO and WHO, 1994, 1995)

COMPOUND	Molecular Mass (g/mol)	Critical Oxidation Potential (V)	Relative density (25 ºC)	Melting Point (ºC)	Boiling Point (ºC)	Solubility in water at 25ºC (g/L)	pK_a 25 ºC	Organoleptic Limits in water (mg/L)	
								Odour	Taste
Phenol	94.11	1.089	$1.071^{20ºC}$	43	181.75	93	9.89	7.9	0.3
o-cresol	108.14	1.040	1.135	30.94	191.0	25	10.20	1.4	0.003
m-cresol		1.080	1.030	12.22	202.32	26	10.01	0.8	0.002
p-cresol		1.038	1.154	34.74	201.94	23	10.17	0.2	0.002

Therefore, these effluents have pungent odor, unpleasant and high toxicity (LEMASTERS *et al.*, 1999), even when in low concentrations (Table 3). Considering the technical records of the remover used by the Air Force Command (PENETONE CORPORATION, 2004), the mass rate of the present aromatic compounds (phenol– 7.4%, 2-hydroxytoluene – 1.6%, 3-hydroxytoluene– 3.1%, 4- hydroxytoluene – 2.3% and xylenes – 0.4%), the toxicity and the physico-chemical properties of these compounds (Table 3), the amount of chemical analysis already made (Tables 1 and 2) and the environmental discharge limit for phenols (BRASIL, 2005), it can be concluded that phenol and cresols constitute the greatest challenge in the treatment of effluents in aeronautical industry.

Thus it becomes necessary, to know the techniques normally used in the treatment of these phenolic compounds.

1.2 *Treatment Techniques to remove phenol and cresols*

The techniques in the treatment of effluents which contain phenols may be divided in biological, conventional physico-chemical and advanced oxidative processes (AOP's).

1.2.1 Biological Processes

A great effort has been made to remove phenols by biological treatment. Table 4 presents some published studies that made use of aerobic, anoxic and anaerobic processes.

Table 4. Efficiencies obtained during biological treatment of phenol and cresols

Medium	Degraded (s) Compound(s) (removal %)	Initial Conc. (mg/L)	Retention time (d)	Remaining percentage (%)	Authors
AEROBIC	Phenol (99%) *o*-cresol (99%) *m*-cresol (99%) *p*-cresol (99%)	150	> 2	____	PERRON and WELANDER (2004)
	o-cresol (100%)	600	0.23	____	MAEDA *et al.* (2005)
ANOXIC	*o*-cresol (< 70%)	< 5.7	> 2	51% of TOC	FLYVBJERG *et al.* (1993)
ANAEROBIC	Phenol (87.2%) *o*-cresol (80%) *p*-cresol (100%)	11760	0.50	18.2% of COD	MEHROTRA *et al.* (2003)
	Phenol (< 75%)	< 900	10	____	ZHOU and HERBERT (1997)
	m-cresol (< 33%)	< 320			
	Phenol (< 95%)	<1500	1	15 – 20% of COD	FANG and ZHOU (2000)

However, as it can be observed, most studies do not make clear if all aromatic intermediates formed are eliminated. Actually, in effluents which present a high concentration of phenols, the results obtained by means of biological treatment presented problems, such as a long detention time (frequently several days), need of nutrients and aromatic intermediates persistence (FLYVBJERG *et al.* 1993; PERRON and WELANDER, 2004).

1.2.2 Conventional Physico-Chemical Processes

The conventional physico-chemical processes use as a base the removal by mass transfer or chemical oxidation. Among these, the most frequently used processes for the removal of phenols are: the activated carbon absorption, chemical precipitation and chemical oxidation.

1.2.2.1 Activated Carbon Absorption

Despite the fact that countless studies (CATURLA *et al.*, 1988; JUANG *et al.*, 1996) report the removal of phenolic compounds from industrial effluents by means of activated carbon filters, the available project parameters (DABROWSKI, 2005) are limited to the use in diluted solutions (< 20 mg/L).

Besides, some researchers state that there is no way to regenerate the filtering media in the applications of activated carbon that contain elevated charges of phenols (GRANT and KING, 1990). Hence, the use of activated carbon to remove phenols is more recommended as a tertiary process.

1.2.2.2 Chemical precipitation

According to RICHTER and AZEVEDO NETO (1991), chemical precipitation is frequently applied in the removal of organic matter while in suspension or under colloidal shape, being anteceded by coagulation and flocculation.

SOLOMONS (1996) states that phenols may be precipitated by means of bromation reactions, forming precipitates as the 2, 4, 6-tribromophenol. Nevertheless, according to KURAMOCHI *et al.* (2004), the solubility of this precipitate (59-61 mg/L in water at 25 ºC) exceeds the environmental discharge limit for phenols, being necessary to make additional post-treatment steps. Moreover, bromophenols present acute and chronic toxicity in seaweeds, protozoans and fish (UNEP *et al.,* 2005), even while under low concentrations (0.1 mg/L).

1.2.2.3 Conventional chemical oxidation

Chemical oxidation generally refers to the use of oxidizing agents aiming at destroying toxic, refracting compounds or those which inhibit the growing of microorganisms (ECKENFELDER, 2000). Considering the critical potential of phenol (1.089 V) oxidation (Table 3), of the cresols (1.038 at 1.080 V) and the potential of conventional oxidation power, the ozone has one of the higher reduction potentials (2.07 V, 25º C), being the most conventional oxidant used in oxidating phenols.

Ozone stability in aqueous media is greatly influenced by factors such as pH, UV irradiation, the presence of catalysts and ozone dosages. In acid media, in the absence of UV or catalysts, high ozone dosages favor its action as a direct oxidant, that is, via molecular ozone. In

these cases, phenol (KUSIC *et al.*, 2006), *o*- *m*- and *p*-cresol (ZHENG *et al.*, 1993) oxidation rates are respectively equal to 1300, 32240, 60870 and 45460 M^{-1} s^{-1}.

Although, under these conditions, the ozone presents high selectivity towards the phenolic compounds, the removal efficiency and the kinetic constants of ozone and other conventional oxidants are too low while compared to •OH produced in AOP's.

1.2.3 Advanced Oxidative Processes (AOPs)

1.2.3.1 Conventional AOPs

The main principle of AOPs is the production of hydroxyl radical, •OH, oxidizing agent with high oxidation potential (2.80 V), what grants a lot of similarities to these processes. The high potential of •OH justifies the efficacy of AOPs from the thermodynamic point of view.

Besides, the reaction rate constants between the •OH and the organic pollutants are very high (10^8 to 10^{10} M^{-1} s^{-1}, ESPLUGAS *et al.*, 2002), what guarantees the AOPs efficacy in what concerns the kinetic point of view. The reactivity and instability of these radicals demand processes able to assure *in situ* production. The reactions presented in Table 5 show how the •OH is generated by different processes.

The efficacy of these processes in phenol (ph) and cresols (*o*-cr, *m*-cr and *p*-cr) oxidation may be confirmed from the destruction of these compounds forming other intermediates presented in Table 6 and 7.

The rate constants of the reactions between hydroxyl radicals and phenol, o-, m-, p-cresols (BUXTON *et al.*, 1988; RODER *et al.*, 1999) are respectively equal to 6.6 x 10^9, 1.1 x 10^{10}, 1.44 x 10^{10} and 1.2 x 10^{10} $M^{-1}s^{-1}$. These values assure AOP's high efficiencies during phenol and cresols degradation as it may be observed in all studies presented in Table 8.

Taking in consideration the absolute constants high rates of the reactions between phenols and •OH and that the hydroxyl concentration remains between 10^{-10} and 10^{-12} M, the organic compounds degradation may be approximated to a pseudo first order kinetic constant with values between 1 and 10^{-4} s^{-1}.

Table 5. Reactions of production of •OH by AOP's.

Reagents			Main reactions (Equation)		Source
O_3	OH^-		$2O_3 + OH^- \rightarrow O_2^{\bullet-} + 2O_2 + {}^{\bullet}OH$	(1)	GLAZE (1987)
O_3	H_2O_2		$O_3 + H_2O_2 \rightarrow {}^{\bullet}OH + HO_2^{\bullet} + O_2$	(2)	
H_2O_2	UV		$H_2O_2 + h\nu \rightarrow 2\ {}^{\bullet}OH$	(3)	BELTRAN (2003)
O_3	UV		$O_3 + h\nu + H_2O \rightarrow H_2O_2 + O_2$	(4)	KUSIC *et al.* (2006)
				(2)	
O_3	H_2O_2	UV		(2- 4)	
H_2O_2	Fe^{2+}		$H_2O_2 + Fe^{2+} \rightarrow FeOH^{2+} + {}^{\bullet}OH$	(5)	NEYENS and BAYENS (2003)
			$H_2O_2 / R^{\bullet} + Fe^{3+} \rightarrow HO_2^{\bullet} / R^+ + FeOH^{2+}/Fe^{2+}$	(6)	
			$HO_2^{\bullet} + Fe^{2+} \rightarrow Fe^{3+} + HO_2^-$	(7)	
H_2O_2	Fe^{2+}	UV	$FeOH^{2+} + h\nu \rightarrow Fe^{2+} + {}^{\bullet}OH$	(8)	PIGNATELLO (1992)
			$Fe^{+3}(RCO_2)^{+2} + h\nu \rightarrow Fe^{+2} + CO_2 + R^{\bullet}$	(9)	
				(5- 7)	
O_3	Fe^{2+}		$O_3 + Fe^{2+} + H_2O \rightarrow O_2 + FeOH^{2+} + {}^{\bullet}OH$	(10)	SÁNCHEZ *et al.* (2003)
O_3	Fe^{2+}	UV		(2-4, 8, 10)	
UV	TiO_2		$TiO_2 + h\nu \rightarrow h^+ + e^-$	(11)	AL-EKABI *et al* (1989)
			$h^+ + H_2O_{(ads)} \rightarrow OH^{\bullet} + H^+$	(12)	
			$O_2 + e^- \rightarrow O_2^{\bullet-}$	(13)	
			$O_2^{\bullet-} + H^+ \rightarrow HO_2^{\bullet}$	(14)	
			$HO_2^{\bullet} + HO_2^{\bullet} \rightarrow H_2O_2 + O_2$	(15)	
			$O_2^{\bullet-} + HO_2^{\bullet} \rightarrow HO_2^- + O_2$	(16)	
			$HO_2^- + H^+ \rightarrow H_2O_2$	(17)	
			$H_2O_2 + e^- \rightarrow {}^{\bullet}OH + OH^-$	(18)	
			$H_2O_2 + O_2^{\bullet-} \rightarrow {}^{\bullet}OH + OH^- + O_2$	(19)	
				(3)	
H_2O	^{60}Co g-rays		$2H_2O \rightarrow H_3O^+ + {}^{\bullet}OH + e^-$	(20)	BUXTON *et al.* (1988)
H_2O	Ultrasound		$H_2O \rightarrow H^{\bullet} + {}^{\bullet}OH$	(21)	
H_2O	e^-		$H_2O \rightarrow {}^{\bullet}OH + H^+ + e^-$	(22)	COMINELLIS (1994)
O_2	H_2O	e^-	½ $O_2 + H_2O \rightarrow 2{}^{\bullet}OH$	(23)	OTURAN (2000)
O_2	H_2O	e^- UV		(8-9, 23)	FLOX *et al.* (2007)

Table 6. Aromatic intermediates identified during phenol and cresols degradation by AOP's.

AOP	Degraded compound				Intermediates	Authors
	Ph	o-cr	m-cr	p-cr		
Fenton (∘)	∘ ●∗ ▷				Catechol	ZAZO et al. (2005)
Fenton (●)	∘ ●∗ ▷				Hydroquinone	BREMNER et al. (2006)
UV / H2O2 (∗)	∘ ●∗ ▼				1, 4 –Benzoquinone	TRYBA et al.(2006)
Photo-fenton (▲)	∘ ∆				Resorcynol	ARAÑA et al. (2001)
O_3 (▷)	▷	◥	◥		1, 2, 4-benzenetriol 3-methylcatechol	HSU et al. (2007)
O_3 O_3 / H_2O_2 UV / H2O2 (∆) UV / O3 UV/O3/H2O2		◥			2-methylresorcynol	KUSIC et al. (2006)
Anodic oxidation (▼)		◢ ◥	◢ ◥		Methylhydroquinone	TORRES et al. (2003)
Anodic oxidation (▽)		◢ ◥	◢ ◥		Methyl-p-benzoquinone	LI et al. (2005)
Photo-electro-Fenton (◢)				◢	5-methyl-2-hydroxi-p-benzoquinone	FLOX et al. (2007)
UV/TiO_2 (◥)		◥			2-hydroxybenzaldehyde	WANG et al. (1998)
			◥		3-hydroxybenzaldehyde	
				◥	4-hydroxybenzaldehyde	
		◥	◥		2,5-dihydroxybenzaldehyde	
			◥		5-methyl-resorcynol	
			◥	◥	4-methyl-catechol	

Table 7. Carboxylic acids identified during phenol and cresols degradation by AOP's.

AOP	Degraded compound				Intermediates	Authors
	Ph	*o*-cr	*m*-cr	*p*-cr		
Fenton (∘)	∘ ▷				Muconic	ZAZO *et al.* (2005)
Fenton (●)	● ▽ ∘ ▷	◢	◢	◢	Maleic	BREMNER *et al.* (2006)
Anodic oxidation (▽)	∘ ▷	◢	◢	◢	Fumaric	LI *et al.* (2005)
Photo-electro-Fenton (◢)	▽				Succinic	FLOX *et al.* (2007)
Fenton (◣)	▽ ∘				Malonic	KAVITHA and PALANIVELU(2005)
O_3 (▷)		◢	◢	◢	Pyruvic	HSU *et al.* (2007)
		◢	◢	◢	Glycolic	
	∘	◢ ◣	◢ ◣	◢ ◣	Acetic	
	▽ ∘ ▷	◢ ◣	◢ ◣	◢ ◣	Oxalic	
	∘	◢	◢	◢	Formic	

Table 8. Efficiencies obtained during phenol (Ph) and cresols (Cr) degradation by AOP's.

AOP	$[Conc]_0$ (mM) Ph	Cr	t (h)	Analysis	Efficiency (%)	Authors
O_3	1.06	——	1	DOC	44	CANTON *et al.* (2003)
O_3/Fe^{+3}					52	
O_3/UV					56	
O_3/UV/Fe^{+3}					90	
O_3/H_2O_2			1.5	Phenol	37	ESPLUGAS *et al.* (2002)
O_3/UV			1		60	
O_3/H_2O_2/UV			2		45	
H_2O_2/Fe^{2+}			1		10	
O_3	2.12		1.5	DOC	60-87	BESSA (2003)
UV/TiO_2			168		88-92	
UV/H_2O_2				Phenols	1	KAVITHA and PALANIVELU (2004)
Fenton			2		82	
Photo-Fenton					99	
UV/TiO_2		0.1	2.5	Cresols	98 88 93	WANG. *et al.* (1998)
Fenton		1.85	2	Cresols DOC	82 42	KAVITHA and PALANIVELU (2005)
Anodic Oxidation (Ti/TiO_2-RuO_2-IrO_2/CF)	——	2.78	8		49.3 - 67.9	RAJKUMAR and PALANIVELU (2003)
Anodic Oxidation (Pt/graphite)		0.66	5	DOC	20	FLOX *et al.* (2005)
Anodic Oxidation (BDD/graphite)			4		100	4-6 dinitro-o-cresol
Photo-electro-Fenton(BDD/FC)		1.12	2		87-90	FLOX *et al.* (2007)

While observing Table 8, presented above, it can be verified that the higher efficiencies were observed in AOPs combined at ultraviolet irradiation. However, despite some AOPs, like the photo-catalysis of ozone (CANTON *et al.,* 2003), the photo-Fenton process (KAVITHA and

PALANIVELU, 2004) and the photo-electro-Fenton process (FLOX *et al.* 2007) present high degradation rates of phenol and cresols, the cost of chemical products or the turbidity augmentation may limit the efficiency of these processes.

Since the last decade, electrochemistry offers a new technology of advanced oxidative processes that allows reducing the parasite reactions and the restrictive operational parameters, consequently increasing the efficiency of degradation and mineralization of organic compounds. In electrochemical advanced oxidation processes (EAOP), $^{\bullet}OH$ may be produced by direct (BRILLAS *et al.*, 2005; FLOX *et al., 2005*), indirect (OTURAN, 2000; OTURAN *et al.* 2001) and coupled oxidation (FOCKEDEY and VAN LIERDE, 2002; SIRÉS *et al.*, 2007a).

1.2.3.2 Electrochemical Advanced Oxidation Processes

1.2.3.2.1 Direct EAOP: Anodic Oxidation

In these processes, the $^{\bullet}OH$ is produced and transferred directly from the electrode originated from the water oxidation in the anode, for this reason, it is frequently referred to as anodic oxidation.

In anodic oxidation, GANDINI *et al.* (2000) state that $^{\bullet}OH$ are produced from the water oxidation in different anodes (Pt, PbO_2, SnO_2, boron doped diamond, etc). However, according to OTURAN and BRILLAS (2007), the most frequently used anodes in EAOP's are platine and boron doped diamond (BDD). According to FLOX *et al.* (2006), the anodic oxidation by BDD in acid media may be represented in a simplified manner by Equation 24.

$$BDD(H_2O) \rightarrow BDD(^{\bullet}OH) + H^{+} + e^{-} \quad (24)$$

However, in all these processes, water is competitively oxidized by other mechanisms. COMINELLIS (1994) proposes a generalized scheme that presents the typical oxidating processes of water in anodes compound or coated by oxides layers. In the first stage, the water is oxidized in its anodic surface (MO_x) to produce adsorbed hydroxyl radicals, later oxidized according to Equations (25) and (26).

$$MO_x + H_2O \rightarrow MO_x(^{\bullet}OH) + H^+ + e^- \quad (25)$$

$$MO_x(^{\bullet}OH) \rightarrow MO_{x+1} + H^+ + e^- \quad (26)$$

In the absence of any oxidizable agent, oxygen is produced from Equations (27) and (28).

$$MO_x(^{\bullet}OH) \rightarrow MO_x + ½\ O_2 + H^+ + e^- \quad (27)$$

$$MO_{x+1} \rightarrow MO_x + ½\ O_2 \quad (28)$$

Therefore, adding the Equations (25) to (28), the equation of water degradation may be obtained, under the absence of any oxidizable agent (29).

$$2H_2O \rightarrow 4H^+ + O_2 + 4e^- \quad (29)$$

On the other hand, in the presence of oxidizable organic compounds (R), the reactions described in Equations (30) and (31) may occur:

$$R + MO_x(^{\bullet}OH)_n \rightarrow CO_2 + nH^+ + ne^- + MO_x \quad (30)$$

$$R + MO_{x+1} \rightarrow MO_x + RO \quad (31)$$

TORRES *et al.* (2003) proposed a mechanism similar to the phenol anodic oxidation in platine electrodes. In this mechanism, the oxidation mechanisms occur throughout the following reactions presented in Equations (32 – 35).

$$Pt + H_2O \rightarrow Pt(^{\bullet}OH) + H^+ + e^- \quad (32)$$

$$Pt(^{\bullet}OH) \rightarrow PtO + H^+ + e^- \quad (33)$$

$$RH + Pt(^{\bullet}OH) \rightarrow Pt + mCO_2 + H^+ + e^- \quad (34)$$

$$RH + PtO \rightarrow Pt + ROH \quad (35)$$

Therefore, anodic oxidation functions as EAOP in Equations (24, 25, 30, 32 and 34). The decisive factors to reduce the concurrent reaction of water oxidation to oxygen (Equation 29) are related to the oxidizing power of the electrode (OTURAN and BRILLAS, 2007) and to the presence of oxidizable substances according to Equation 34 (COMINELLIS, 1994; TORRES *et al.*, 2003). However, the anodic oxidation of high concentrations of phenol may lead to the formation of polymers, as Figure 5 shows.

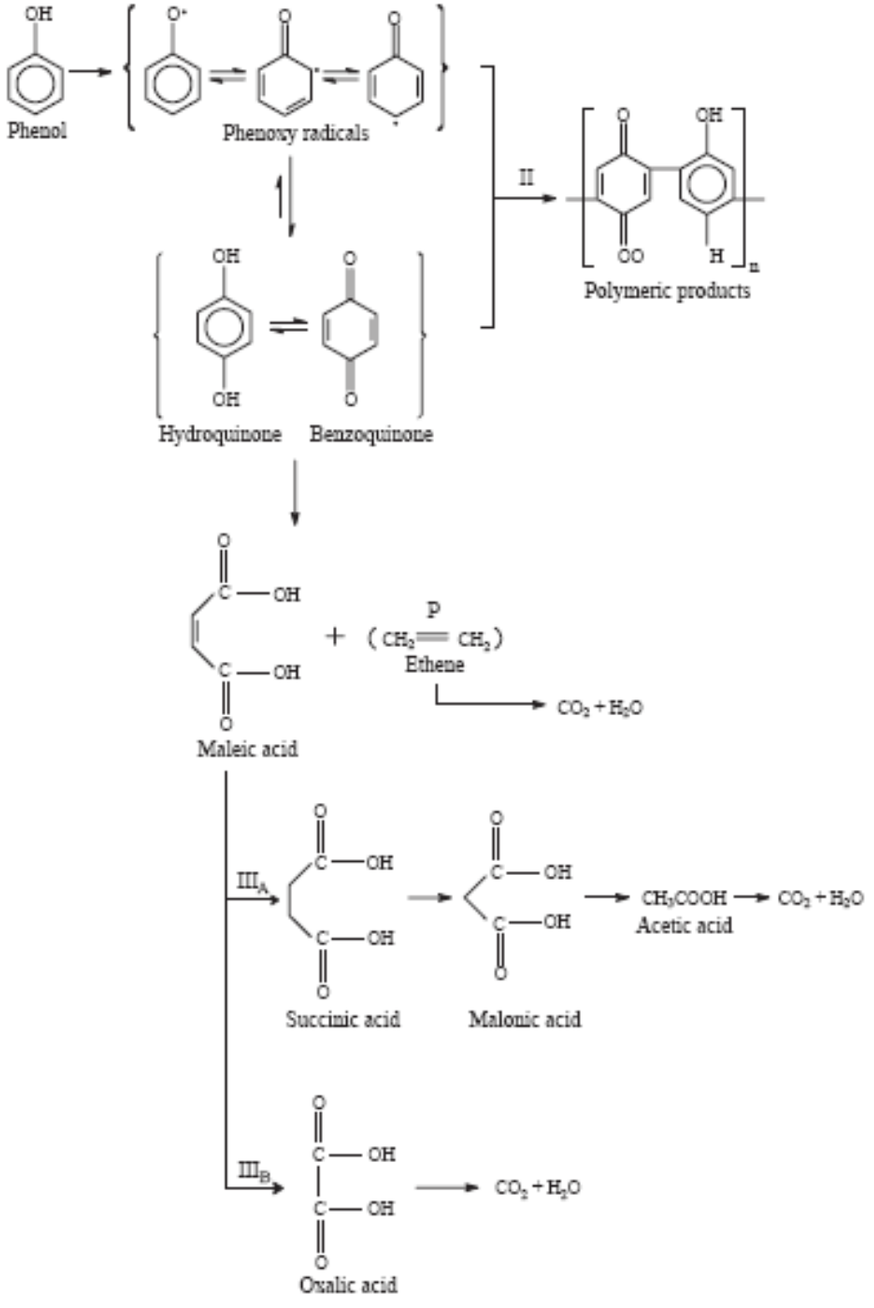

Figure 5. Reaction pathway during electrochemical phenol degradation. Experimental conditions: anodic oxidation in indivisible cells with cathodes of stainless steel and anodes of Ti/SnO_2-Sb, Ti/RuO_2 or Pt (LI *et al.* 2005).

In the case of platine electrode, the transference of $^{\bullet}OH$ to the media is little according to its low oxidating power (BRILLAS *et al.*, 2007) because $^{\bullet}OH$ is strongly adsorbed to Pt surface. On the other hand, BDD has one of the highest O_2-overpotential, what justifies the fact that this electrode presents the highest removal efficiency of organic compounds (GANDINI, 2000; COMINNELLIS, 2001; BRILLAS *et al.*, 2007). However, while applying more elevated electric charges in the BDD anode, the relative generation of $^{\bullet}OH$ by the Equation (20) is reduced

(PANIZZA and CERISOLA, 2005; FLOX *et al.*, 2006) due to the increase in oxygen production (Equation 29) and other weaker oxidants such as ozone (Equation 36), peroxydisulfate (Equation 37) and peroxide (Equation 38).

$$3H_2O \rightarrow O_3 + 6H^+ + 6e^- \quad (36)$$

$$2HSO_4^- \rightarrow S_2O_8^{2-} + 2H^+ + 2e^- \quad (37)$$

$$2H_2O \rightarrow H_2O_2 + 2H^+ + 2e^- \quad (38)$$

Nevertheless the attack of the $^{\bullet}OH$ produced in the anodic oxidation only occurs in the anodes surface, what limits the speed of the process (OTURAN and BRILLAS, 2007) in relation to indirect EAOP's.

1.2.3.2.2 Indirect EAOP: Electro-Fenton

The most used electrochemical advanced oxidation processes by indirect oxidation are the electro-Fenton process and its variants (peroxi-coagulation) or combinations (coupling the anodic oxidation and/or UV irradiation). The degradation of organic compounds (generically represented as an organic compound R) by the electro-Fenton process is summed up as follows (Figure 6).

The electro-Fenton process, simultaneously developed in France (OTURAN *et al.*, 1992) and in Spain (BRILLAS *et al.*, 1996), is based on the *in situ* electrochemical production of the Fenton reagent, a mixture of hydrogen peroxide and iron ions (or other catalysts), capable of producing hydroxyl radicals as shows Equation 5.

$$H_2O_2 + Fe^{2+} (M^{n+}) \rightarrow FeOH^{2+} / (M^{(n+1)+}) + {}^{\bullet}OH \quad (5)$$

where:

M^{n+} – Reduced form of $M^{(n+1)}/M^{n+}$ redox catalyst couple;
$M^{(n+1)+}$ – Oxidized form of $M^{(n+1)}/M^{n+}$ redox catalyst couple.

The fact that the $^{\bullet}OH$ has been produced throughout all media (Equation 5 and Figure 6) and not only in the anode gives to the electro-Fenton process an oxidizing power more elevated than the anodic oxidation (OTURAN and BRILLAS, 2007).

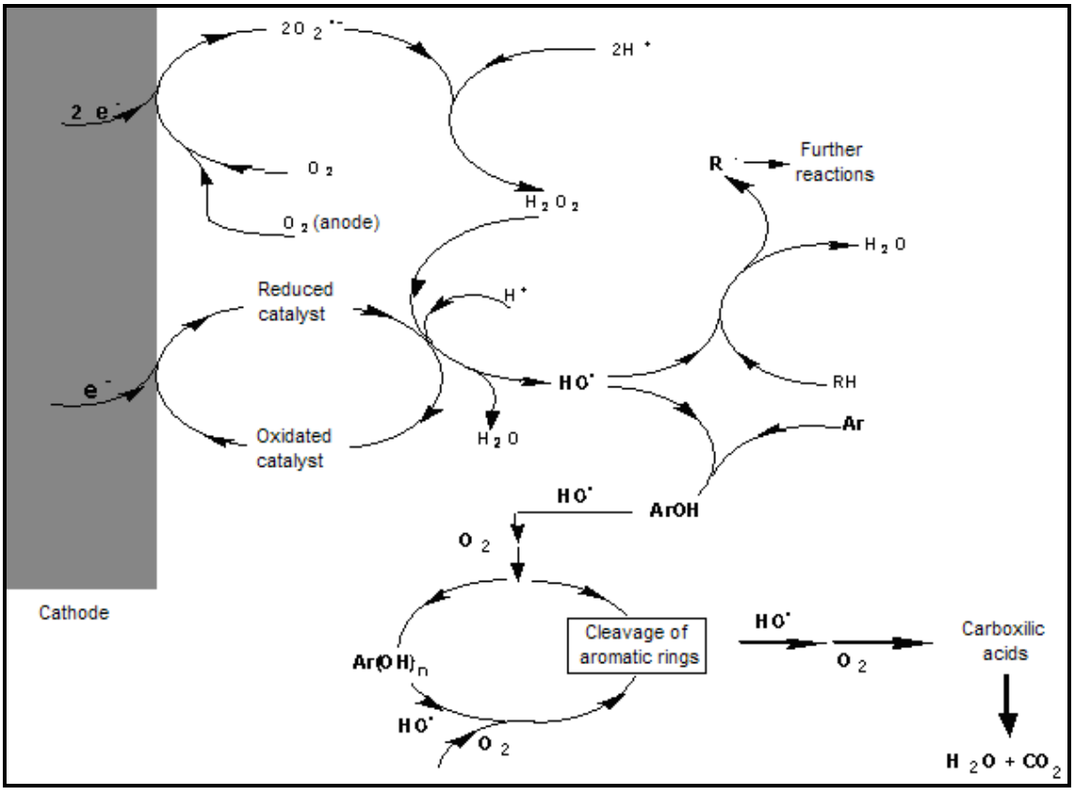

Figure 6. Electro-Fenton process (Source: adapted from OTURAN e PINSON, 1992).

The hydrogen peroxide is continually generated in acid media from the electrochemical reduction of the oxygen dissolved in solution, using mercury cathodes (OTURAN *et al.*, 1992; OTURAN and PINSON, 1995), carbon felt (OTURAN *et al.,* 1999; OTURAN, 2000; OTURAN *et al.,* 2000; OTURAN *et al.,* 2001) and diffuse oxygen composed by polytetra-fluoroethylene carbon (BRILLAS *et al.*, 1996; BOYE *et al.*, 2002; BRILLAS *et al.*, 2003; BRILLAS *et al., 2004a*) as showed in Equation (39) as well as Figure 6.

$$O_2 + 2H^+ + 2e^- \rightarrow H_2O_2 \quad (39)$$

The addition of a small amount of Fe^{2+} or Fe^{3+} (or any transition metal that can act as a catalyst) increases sensibly the oxidating power of the hydrogen peroxide produced electrochemically, because it makes the production of $^{\bullet}OH$ possible, from the Fenton's reagent represented by reaction (5). In the electro-Fenton process, the regeneration of the ferrous ion is sensibly increased in relation to the Fenton's reagent, because, beside the chemical regeneration (reactions 6 and 7), the ferrous ion becomes regenerated electrochemically. In pH 3 (optimum value for reaction 39), the electrochemical regeneration of the iron ion is represented by equation 40. The sum of equations (39) and (40) in acid media indicates the electrocatalytic production of the Fenton's Reagent (41).

$$Fe(OH)^{2+} + e^- \rightarrow Fe^{2+} + OH^- \quad (40)$$

$$O_2 + 3H^+ + Fe(OH)^{2+} + 3e^- \rightarrow H_2O_2 + Fe^{2+} + H_2O \quad (41)$$

Taking in consideration the reaction occurred on the cathode (reaction 41) and in the solution (reaction 5), it can be observed that the concentration of dissolved oxygen is an essential factor in the efficiency of electro-Fenton process.

Platine and BDD are the most used anodes in the electro-Fenton process (OTURAN *et al.* 2001; BRILLAS *et al.*, 2007). Within these anodes, in the absence of any oxidizing agent (COMINELLIS, 1994), an increment of the concentration of the dissolved oxygen in the media by means of the following reaction occurs.

$$2H_2O \rightarrow 4H^+ + O_2 + 4e^- \quad (29)$$

Thus, while adding the reactions present on the cathode (41), on the anode (29) and in the media (5) and keeping the electrical charge balanced, the electro-Fenton global reaction is obtained:

$$O_2 + 2H_2O \rightarrow 4^{\bullet}OH \quad (42)$$

In the peroxi-coagulation, the principle is similar to the electro-Fenton process. The difference resides in the use of a sacrificial iron anode, which allows its oxidation, producing mainly the iron ion as equation 43 shows (BRILLAS *et al.*, 1997).

$$Fe \rightarrow Fe^{2+} + 2e^{-} \quad (43)$$

Hence, while adding the reactions present in the cathode (41), in the anode (43) and in media (5), keeping the electrical charge balanced, the peroxi-coagulation global reaction is obtained:

$$2O_2 + 6H^{+} + 3Fe \rightarrow 2^{\bullet}OH + 3Fe^{2+} + 2H_2O \quad (44)$$

Therefore, while comparing the electro-Fenton process (42) to the peroxi-coagulation (44) it can be verified in this case, an excessive production or ferrous ion that ends up to be transformed to the ferric ion with the pH increase and to act like a coagulant in the final products (BRILLAS and CASADO, 2002).

OTURAN and BRILLAS (2007) claim that the substitution of the Pt anode by BDD allows increasing considerably the efficiency of the electro-Fenton process, due to the supplementary $^{\bullet}OH$ produced by equation (24). In this case, there is a combination of the electro-Fenton process with the anodic oxidation (FOCKEDEY and VAN LIERDE, 2002).

Another possible combination comprises the use of the electro-Fenton process coupled to the simultaneous radiation of ultraviolet light. This combination, also known as photo-electro-Fenton process (BOYE *et al.*, 2003; BRILLAS *et al.*, 2003), allows accelerating the mineralization process by:

a) Regeneration of the ferrous ion by the photo-reduction of ferric ions (reaction 8) and/or;

b) Photo-decomposition of Fe^{3+} complexes with some products such as oxalic acid (reaction 9).

Theoretically, the use of BDD anode in the photo-electro-Fenton process corresponds to the combination of the electro-Fenton with higher oxidizing power (BRILLAS and OTURAN, 2007) and has made possible to obtain high rates of mineralization during cresols oxidation. Figure 7 presents the photo-electrochemical degradation mechanism of the cresols isomers proposed by FLOX *et al.* (2007) while making use of the photo-electro-Fenton process in a reactor containing an oxygen diffusion cathode, a BDD anode and a UV-A lamp.

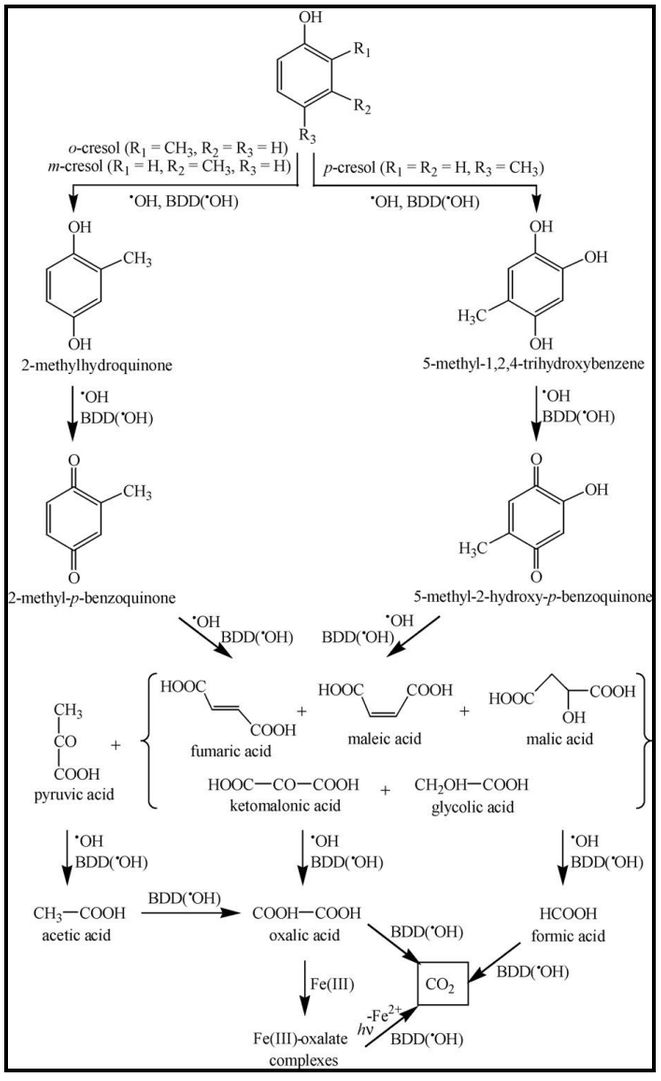

Figure 7. Proposed reaction sequence for the electro-Fenton and solar photoelectro-Fenton degradations of o-cresol, m-cresol and p-cresol in acid medium using a BDD anode. The hydroxyl radical is denoted as •OH or BDD(•OH) when it is formed from Fenton's reaction or at the BDD surface from water oxidation, respectively (FLOX *et al.,* 2007).

Face so many present parameters in the electro-Fenton process, it becomes necessary to perform a detailed analysis of the main influent parameters.

1.3 Influential parameters in the Electro-Fenton process

1.3.1 Electrode nature

According to OTURAN and BRILLAS (2007), Pt and BDD are the most used electrodes as anodes. However, the cathode is the working electrode in the electro-Fenton process and currently the carbon felt (CF) (HANNA *et al.*, 2005; OTURAN and OTURAN, 2005; DIAGNE *et al.*, 2007) and the oxygen diffusion (OD)PTFE electrodes (BRILLAS *et al.*, 2003; BRILLAS *et al.*, 2004b) are the most frequently used cathodes. Aiming to maximize the efficiency of the electro-Fenton process about the electrodes used, SIRÉS *et al.* (2007b) have studied in detail the effect of the electrodes Pt-CF, BDD-CF, Pt-OD and BDD-OD combination use in the electro-Fenton process during the degradation of the antimicrobiotics tryclosan. Figure 8 presents the kinetic degradation of Tryclosan under different combination of electrodes (Pt-CF, BDD-CF, Pt-OD and BDD-OD).

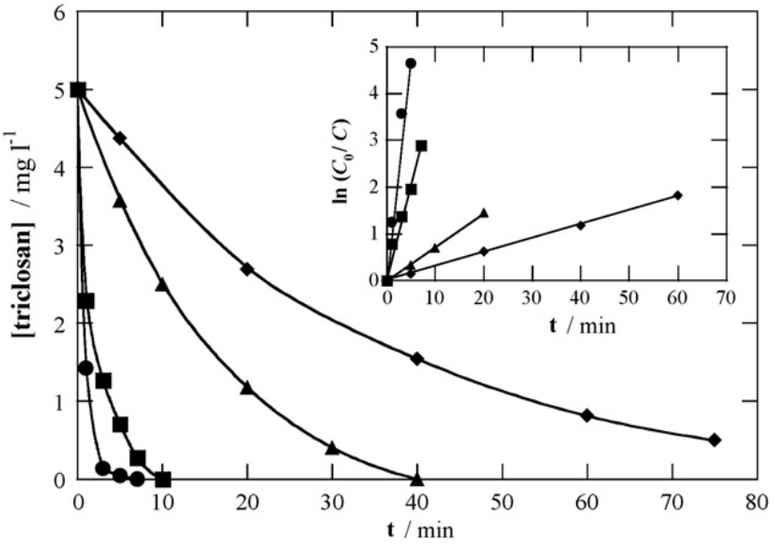

Figure 8. Triclosan degradation (V_0 = 200 mL, C_0 = 5 mg triclosan/L, pH = 3 e I = 60mA) in aqueous solution containing 0.05M of Na_2SO_4 and 0.20 mM of Fe^{3+}. Electrochemical cells: (●) Pt/FC, (■) BDD/FC, (▲) Pt/O_2 and (◆) BDD/O_2 (SIRÉS *et al.*, 2007b).

In this study, the *tryclosan* degradation rates followed the following order: Pt-CF > BDD-CF > Pt-OD > BDD-OD. Therefore, the Pt anode and the carbon felt cathode (CF) presented the highest efficiency. The higher efficiency of the Pt/CF cell was justified due to the fact that this system has

proportioned the highest capacity of regeneration of the ferrous ion. The biggest area of the carbon felt cathode and the smaller oxidation power of the Pt anode made possible the presence of a higher concentration of Fe^{2+}, increasing the production of $^{\bullet}OH$.

In another study, SIRÉS *et al.* (2007a) have studied the use of the same electrodes combinations (Pt-CF, BDD-CF, Pt-OD and BDD-OD) during the degradation of 200 mL of aqueous solution containing 84 mg/L of the chlorophene antimicrobials by electro-Fenton process. The degradation rates obtained followed the order: Pt-CF > BDD-CF > BDD-OD > Pt-OD.

Consequently, the electrode combinations that allowed highest efficiency in the electro-Fenton process were carbon felt cathode (CF) and platinum anode (Pt), followed by carbon felt cathode (CF) and boron doped diamond (BDD) anode (SIRÉS *et al.*, 2007a, 2007b).

1.3.2 pH

The pH is one of the main factors to be considered in the electro-Fenton process. According to MIOMANDRE *et al.* (2005), the oxygen transfer is the limiting stage in the electrochemical production process of hydrogen peroxide (equation 39). Taking in consideration the saturation of oxygen dissolved in media ($[O_2] \cong 0.25$ mM), the reaction of oxygen consumption (39: $[H^+]/[O_2] = 2$) and the electrocatalysis of the Fenton's reagent (41: $[H^+]/[O_2] = 3$), it can be observed that the pH 3.0 ($[H^+]/[O_2] \cong 4$) maximizes the efficiency of the process (PIMENTEL *et al.*, 2008). Thus, the acidity reduction (pH > 3), makes the peroxide production more difficult, as it can be observed in Figure 9.

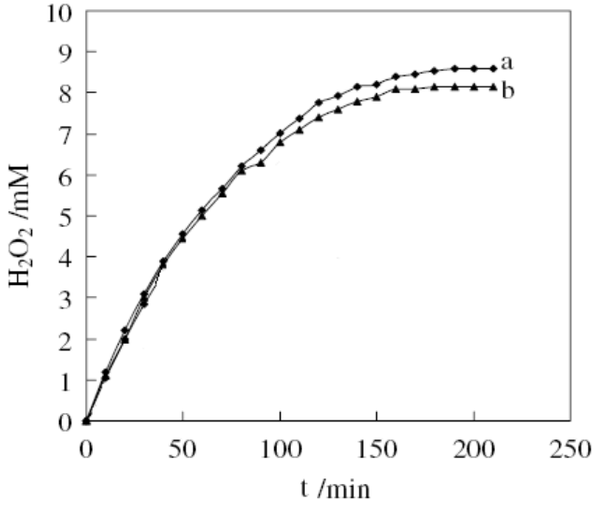

Figure 9. Change of accumulated H_2O_2 concentration with time during electrolysis of 50 mL of 0.1 M phosphate buffer solution in an undivided cell of Pt/graphite at: (a) pH=3.0, (b) pH=4.0 (CHEN *et al.*, 2003).

On the other hand, the acidity increase (pH < 2.8), also disturbs the peroxide production, because it enhances peroxide and sulphate complexes formation (OTURAN and BRILLAS, 2007).

Moreover, the pH has a specific effect depending on the catalyst adopted, what will be soon exposed.

1.3.3 Nature and Catalyst Concentration

The classical electro-Fenton process is conducted with the reduced form of the redox system Fe^{3+}/Fe^{2+} (E^0 = 0.77 V/SHE). Nonetheless, any proper redox system $M^{(n+1)+}/ M^{n+}$ can be used according to the equation (45). In these cases, the electro-Fenton efficiency is related to the standard reduction potential and to the scavenging effect of the reduced species of the redox system used (PIMENTEL *et al.*, 2008).

$$M^{n+} + H_2O_2 \rightarrow M^{(n+1)+} + OH^- + {}^{\bullet}OH \qquad (45)$$

In fact, some other transition metals have been tested as catalysts. Among these cobalt ($E^0(Co^{3+}/Co^{2+})$ = 1.92 V), cupper ($E^0(Cu^{2+}/Cu^{+})$ = 0.16 V) and manganese ($E^0(Mn^{3+}/Mn^{2+})$ = 1.50 V) have been the transition metals most frequently used (ANIPSITAKIS and DIONYSIOU, 2004; BARRET and MCBRIDE, 2005; TÜRK and ÇIMEN, 2005; IRMAK *et al.*, 2006; SKOUMAL, 2006). All these redox pairs can be used, once the cathode interface potential in relation to the solution (OTURAN and PINSON, 1995) is approximately equal to -0.25V (SHE).

FOCKEDEY and VAN LIERDE (2002) have studied the iron concentration effect in the electrochemical degradation of phenol coupling the electro-Fenton process to the anodic oxidization by means of a Sb-SnO_2-Ti/ reticulated vitreous carbon cell, as Figure 10 shows.

It can be observed in Figure 10, that 50 mg/L of iron made possible the highest degradation of phenol. The reduction of iron concentration revealed less efficiency in the process, because there was no catalyst to produce OH radicals, as reaction 5 shows. On the other hand, the increase in iron concentration reduced the efficiency by the presence of parasite reactions as reaction 46.

$$Fe^{2+} + {}^{\bullet}OH \rightarrow Fe^{3+} + OH^- \qquad k = 4.3 \times 10^8\ M^{-1}\ s^{-1} \qquad (46)$$

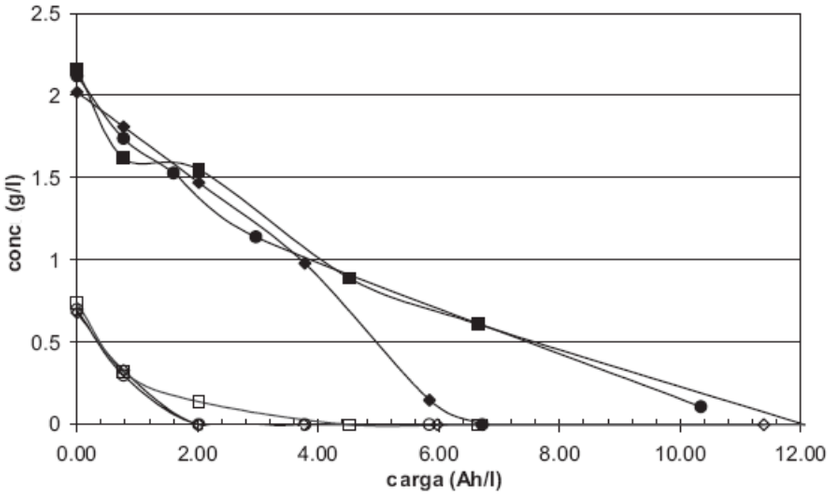

Figure 10. Evolution of COD (filled symbols) and phenol concentration (outlined symbols) vs. electrical charge for coupled oxidation at various iron concentrations (■: 5. ◆: 50 e ●: 200 mg/L). Operating conditions: 100 A/m^2, 20 mg/L O_2, and pH 3 (FOCKEDEY and VAN LIERDE, 2002).

1.3.4 Effect of the medium

DIAGNE *et al.* (2007) have recently studied the effect of the nature of the acid used to set the pH in the mineralization of the methyl-parathion pesticide (MP) in the electro-Fenton process (Pt/carbon felt) using Fe^{3+} as catalyst. The results obtained are presented in Figure 11.

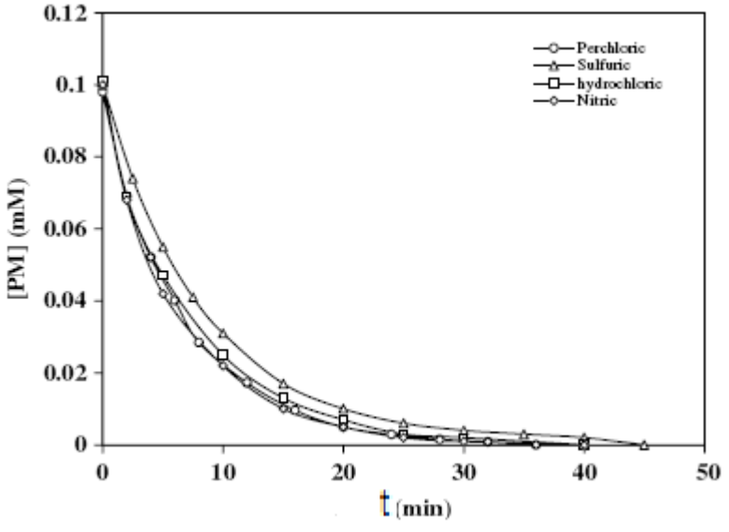

Figure 11. Degradation kinetics of methyl parathion in several acidic media by electro-Fenton process: (○): perchloric, (△): sulfuric, (▫): hydrochloric, and (◇):nitric media. C_0 = 0.13 mM, [Fe^{3+}] = 0.1 mM, V = 0.150 L, I = 100 mA, DIAGNE *et al.* (2007).

The higher degradation was obtained in pH 3, for perchloride acid as for sulphuric acid, confirming the expected results. The efficiency of the process was lower when the sulphuric acid was used for all studied values of pH, probably due to the bigger amount of added acid, because the sulphuric acid is a weaker one. Additionally, the sulphuric acid has a lower oxidation state, making parasite reactions easier, such as reaction 47 (BUXTON *et al.*, 1988).

$$OH^{\bullet} + HSO_4^{-} \rightarrow SO_4^{\bullet -} + H_2O \qquad k = 1.7 \times 10^6\ L\ M^{-1}\ s^{-1} \qquad (47)$$

Considering the observed effect while making use of different acids, even when in low concentrations (pH = 3, [acids] < 2mM), the influence of the electrolytes in the solution must be taken in consideration, normally used in higher concentrations.

1.3.5 Electrolytes

DUTTA *et al.* (2001) have studied the effect of different electrolytes in the degradation of the methylene blue coloring by the Fenton's reagent as it can be observed in Figure 12.

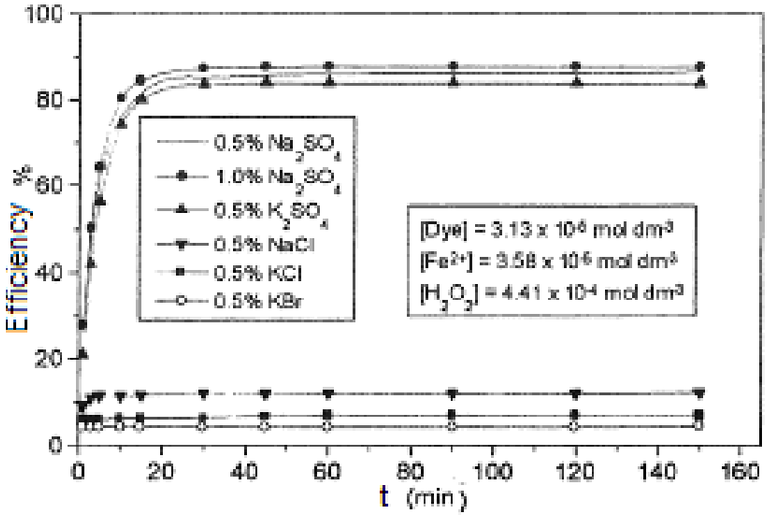

Figure 12. Effect of eletrolytes on blue methylene degradation by Fenton process (DUTTA *et al.*, 2001).

While observing Figure 12, it can be verified that sodium sulphate propitiates the highest degradation efficiency in methylene blue, what can be justified by the highest rates observed in the

reaction between halogen ions and $^{\bullet}OH$ (BUXTON *et al.,* 1988) according to Equations (48) and (49).

$$^{\bullet}OH + Br^{-} \rightarrow BrOH^{-} \qquad k = 1.1 \times 10^{10}\ L\ M^{-1}\ s^{-1} \qquad (48)$$

$$^{\bullet}OH + Cl^{-} \rightarrow ClOH^{-} \qquad k = 4.3 \times 10^{9}\ L\ M^{-1}\ s^{-1} \qquad (49)$$

Considering the global reaction of the electro-Fenton process (42), the dissolved oxygen concentration in the media and the current intensity used are essential parameters in the process.

1.3.6 Dissolved Oxygen concentration

FOCKEDEY and VAN LIERDE (2002) have studied the effect of dissolved oxygen concentration (DO) in the electrochemical degradation of phenol, coupling the electro-Fenton process to the anodic oxidation using a Sb-SnO_2-Ti/ reticulated vitreous carbon cell. The concentration of DO was altered including different emissions of pure oxygen, as it can be seen in Figure 13.

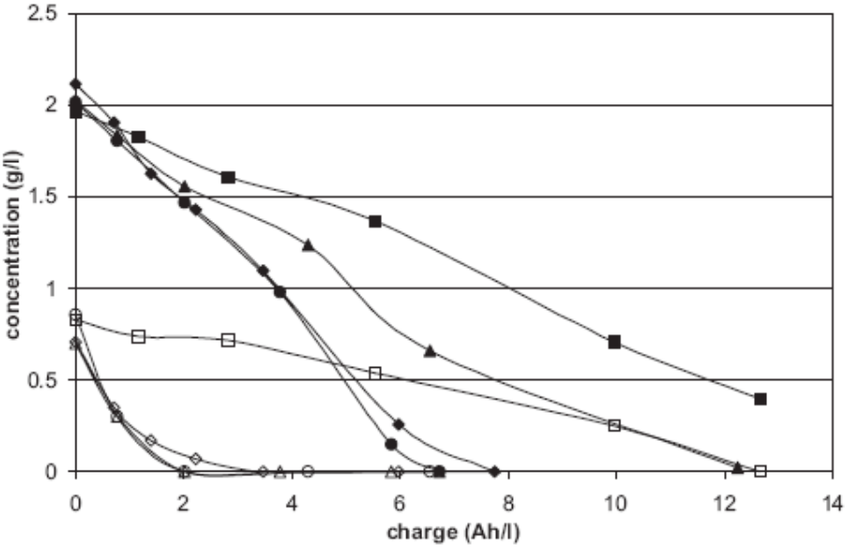

Figure 13. Evolution of COD (filled symbols) and phenol concentration (outlined symbols) vs. electrical charge for coupled oxidation at various dissolved oxygen concentration (■: 4 mg/L, ▲: 10 mg/L, ●: 20 mg/L, and ◆: 27 mg/L). Operating conditions: 100A/m^2, 50 mg/L Fe, and pH 3 (FOCKEDEY and VAN LIERDE, 2002).

While observing Figure 13, it can be verified that the optimum concentration of DO was equal to 20mg/L. There was a small reduction in the phenol degradation efficiency when the DO concentration was reduced from 20 to 10 mg/L. However, the reduction of the efficiency was significant when the DO concentration was reduced to 4 mg/L. For the authors, the DO concentration reduction favors competitive reactions in the cathode, reducing the peroxide production (equation 39) over the hydrogen production (by the acidity reduction) and/or the organic compounds reduction.

On the other hand, the increase in the DO concentration also reduced the process efficiency. According to FOCKEDEY and VAN LIERDE (2002), in this case, the increment of very high releases of pure oxygen reduced the hydrodynamic performance of the electrolytic cell

1.3.7 Current Density

The electrical current density corresponds to the ratio between the applied current and the surface of the working electrode. Therefore, the current density can be altered by changing the current and/or the surface of the working electrode. The electro-Fenton process is an electrochemical process ruled by equation 42. So, the current increase maintaining a constant working electrode area, allows improving the degradation rate by the increase of the $^{\bullet}OH$ production rate, as Figure 14 shows.

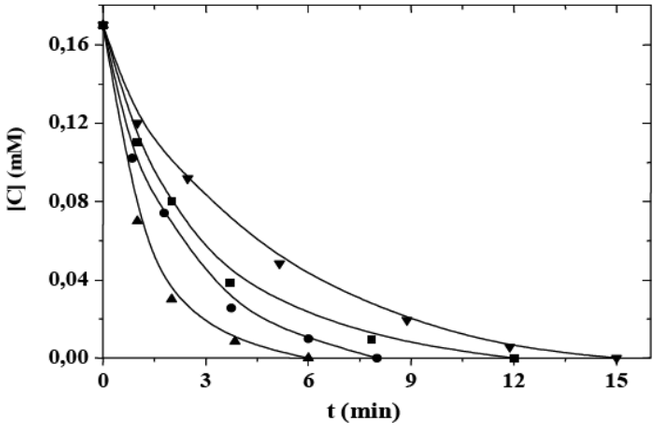

Figure 14. Effect of current increase (▼: 60. ■: 100. ●: 200 e ▲: 300 mA) on kinetics degradation of diuron herbicide in aqueous solution containing 0.05M Na_2SO_4 and 0.5mM Fe^{2+} in an indivisible Pt/CF cell. Experimental conditions: cathodic surphace equal to 60 cm^2 and volume equal to 150 ml (EDELAHI *et al.*, 2004).

Therefore, at first analysis, Figure 14 shows that the higher the current, the higher the tendency to increase the degradation rate, what is naturally expected in an electrochemical process.

However, in the electro-Fenton process, the dissolved oxygen, the water and the product to be degraded (Figure 6) are consumed once the electrical current is applied. Thus, the enhancement in the electrical productivity from the current increase has a limit that tends to be defined by the dissolved oxygen concentration or by the concentration of the product to be degraded in the media. This current is normally defined in relation to the working electrode area and is known as limit current (i_{lim}). The use of currents greater than limit current will promote the increase of parasite reactions, which reduces the electrical productivity. Considering the use of three-dimensional electrodes (FOCKEDEY and VAN LIERDE, 2002), the limit current (i_{lim}) occurs when the reaction becomes controlled by the mass transference process, being defined by the Equation 50.

$$i_{lim} = n \times F \times \lambda \times K_m \times C_l \quad (50)$$

where:

i_{lim} – limit current (A);
n – number of exchanged electrons;
F –Faraday's constant (96485 C/mol);
λ - ratio of the real area of the electrode to the projected area;
k_m – diffusion coefficient divided by the thickness of the boundary layer (m/s);
C_l – Limit concentration (mol/m^3).

Considering, for instance, phenol mineralization by $^{\bullet}OH$ during electro-Fenton process, molecules may be simplified by reaction 51.

$$C_6H_5OH + 28\ ^{\bullet}OH \rightarrow 6CO_2 + 17H_2O \quad (51)$$

Considering the electro-Fenton process general reaction (42) and the reaction (51), the phenol degradation mechanism by the electro-Fenton process can be represented by equation 52.

$$C_6H_5OH + 7\ O_2 \rightarrow 6CO_2 + 3H_2O \quad (52)$$

Considering equation 52, the reaction rate in electro-Fenton process is limited by mass (O_2 - rapid or reversible system) or electronic (e^- - slow or irreversible system) transfer. Hence, in the electro-Fenton process, the increase of the cathode area increases the value of limit current to be applied, improving the electrical productivity specially while making use of higher currents. Additionally, the augmentation of cathodic surface in the electro-Fenton process improves the contact between the working electrode and the focused chemical species (O_2 and Fe^{2+}, reaction 41), increasing the regeneration of the ferrous ion (QIANG, CHANG and WANG, 2003) and the production of hydrogen peroxide (PIMENTEL *et al.*, 2008).

1.3.8 Temperature

While studying the temperature effect on cresols destruction by Fenton's reagent, KAVITHA and PALANIVELU (2005) verified the increase in the apparent rate constants with the increase in temperature, becoming stable at 30º C. Moreover, QIANG *et al.* (2003) revealed that the increase in temperature improves the electrochemical regeneration of the ferrous ion.

On the other hand, the temperature increase reduces the concentration of dissolved oxygen saturation in the media, limiting the efficiency of the electro-Fenton process globally. Therefore, considering the dissolved oxygen in media concentration, equation 50 shows that the increase in temperature causes the decrease in the density of limit current, reducing the electrical productivity of the process.

1.3.9 Transport Phenomena

In all electrochemical process, mass transport, charge and heat transfer are closely related. In the electro-Fenton process, the reaction of hydroxyl radicals production occurs in homogenous medium according to the equation 5 and, both dissolved oxygen, as the catalyst, need to establish contact with the cathode. Therefore, it is necessary to apply a mechanical potency (P) that supplies a hydraulic gradient sufficiently high ($G > 700\ s^{-1}$) to promote an adequate agitation degree (RICHTER and NETTO, 1991). The mechanical potency (P) in laboratory scale is introduced by using magnetic stirrers and by the introduction of pure oxygen or compressed air in media, according to the following equations.

$$P = \mu \times V \times G^2 \quad (53)$$

where:

P – Mechanical potency applyed (W),
μ – Absolute viscosity (kg m^{-1} s^{-1}),
V – Volume (m^3),
G – Hydraulic gradient (s^{-1}).

$$P = P_{ms} + P_{ca} \quad (54)$$

where:

P_{ms} – Mechanical potency due to magnetic stirrers (W),

P_{ca} – Mechanical potency due to bubbles produced during air diffusion (W).

These potencies are respectively obtained by means of the Equations presented as follows.

$$P_{ms} = v_{ms} \times r_{H2O} \times g \times L_{ms} \times n / 9.555 \quad (55)$$

where:

P_{ms} (W) – Potency supplyed by magnetic stirrer;
v_{ms} –magnetic stirrer volume (m^3);
r_{H2O} – water specific mass (kg/m^3);
g –gravity aceleration (9.81 m/s^2);
L_{am} – magnetic stirrer length;
n – rotations par minute.

$$P_g = Q_g \times r_{H2O} \times g \times h_i \quad (56)$$

where:

P_g (W) – Potency supplyed by gas injection;
Q_g – Gas flow (m^3/s);

h_i – imersion profundity of gas diffusor.

As a result, the applied hydraulic gradient is obtained from Equations 54, 55 and 56, as shown in Equation 57.

$$G = [g/(V \times n_{H2O}) \times (0.10466 \times v_{ms} \times L_{ms} \times n + Q_g \times h_i)]^{1/2} \quad (57)$$

n_{H2O} – Water dynamic viscosity (m^2/s).

CHAPTER II: MATERIALS AND METHODES

2.1 Chemical Products

The names, uses, formulae and purities of the chemical substances are presented in Table 9.

Table 9. Name, use, formula and purity of chemical substances used in this work

Product	Use	Formula Purity (%)	Product	Use	Formula Purity (%)
Ferrous sulfate heptahydrate	Catayst	$FeSO_4.7H_2O$ 99	Methanol	Eluent	CH_3OH 99.7
Cobalt(II) sulfate pentahydrate		$CoSO_4.5H_2O$ 99	*p*-hydroxy-benzoic	Absolute constants	$C_6H_4(COOH)(OH)$ 99.5
Cupper(II) sulfate pentahydrate		$CuSO_4.5H_2O$ 99	Sodium sulfate	Electrolite	Na_2SO_4 99
Manganese(II) sulfate monoh.		$MnSO_4.H_2O$ 98	Potassium cloride		KCl 99
Phenol	Degraded compounds	C_6H_5OH 99	Maleic (*cis*) and Fumaric (*trans*)	I	$C_4H_4O_4$ 99
o-cresol		$C_6H_4CH_3OH$ 98	Succinic	D E	$C_4H_6O_4$ 99
m-cresol		$C_6H_4CH_3OH$ 99	Malonic	N T	$C_3H_4O_4$ 99
p-cresol		$C_6H_4CH_3OH$ 99	Pyruvic	I F	$C_3H_4O_3$ 98
Catechol		$C_6H_4(OH)_2$ 99	Glycolic	I E	$C_2H_4O_3$ 99
Hydroquinone	Identified products	$C_6H_4(OH)_2$ 99	Glyoxylic monohidrate	D	$C_2H_2O_3$ 98
Benzoquinone		$C_6H_4O_2$ 99.5	Oxalic	A C	$C_2H_2O_4$ 98
3-methylcatechol		$C_6H_3CH_3(OH)_2$ 99	Acetic (also used as eluent)	I D	CH_3COOH 99.7
2-methyl-hydroquinone		$C_6H_3CH_3(OH)_2$ 99	Formic	S	CH_2O_2 98

2.2. Solutions Prepared

Synthetic effluent solutions with variation volumes between 100 and 400 mL were prepared with deionised water (conductivity < 6×10^{-8} S cm^{-1} at 25 °C), except for final experiments

conducted with real wastewater. Although phenols' concentrations in effluents swing between 10 and 2300 mg/L (Table 1 and 2), in this work, phenol's concentrations were between 31.3 and 419 mg/L (1 and 4 mM).

2.3. Analytical Techniques

Analytical techniques used are described above.

2.3.1 High performance liquid chromatography (HPLC)

Phenol, cresols and all other intermediates were identified by reversed phase liquid chromatography, using a Merc-Hitachi high performance liquid chromatograph, Lachrom-Elite model, controlled by an EZCHROM elite program. It was composed of a quaternary pump MH L-7100, a diode array detector L-7455 and a Merck column L-7360 with thermostat.

The analyses were made by injecting 20 μL aliquots and the oven temperature was fixed at 40°C. The column, the wavelenght and the mobile phase were changed in the case of aromatic compounds or carboxylic acids, according with the desired analyse.

Aromatic compounds were identified by a RP-C18 (5 mm, 250 mm x 4.6 mm) column coupled with the diode array detector at 280 nm and a flow rate of 0.8 mL/min. Two different mixtures of water/methanol/acetic acid were used as mobile phase at a flow rate of 0.8 mL/min during phenol and cresol degradation (phenol: 79.2/19.8/1, v/v; cresols: 59.4/39.6/1 v/v).

Carboxylic acids were identified and measured by ion-exclusion chromatography fitted with a Supelcogel H (250 mm x 4.6 mm) column at 40 °C. The detection was performed at 210 nm with a mobile phase of 4 mM H_2SO_4 at a flow rate of 0.2 mL/min.

2.3.2 Total Organic Carbon (TOC)

Total Organic Carbon (TOC) amounts in aqueous solutions were obtained with a Shimadzu VCSH carbon analyser. During all experiments, samples were collected and immediately measured without using any filter.

2.4 Electrochemical Reactor

Experiments were performed at room temperature (25 ± 1 ºC) in an open undivided cylindrical glass cell of diameter intern of 6 mm presented in Figure 15.

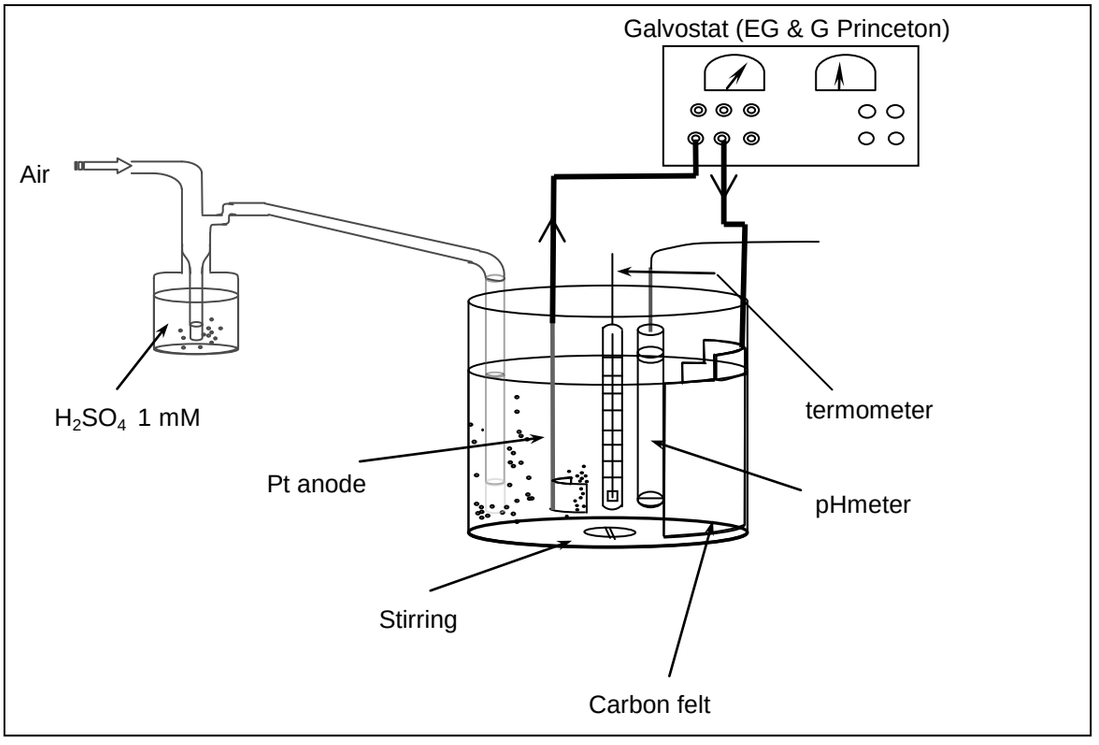

Figure 15. Electrochemical reactor used in electro-Fenton experiments.

Figure 15 presents an undivided cell with two electrodes totally immersed in the solution. The cathode was a piece of carbon-felt (7 cm x 8 cm x 0,6 cm), placed on the inner wall of the cell. Anode was a piece of Pt (1.5 cm x 2 cm) placed on the centre of the cell. Solutions were always stirred magnetically in a a rate of 500 rpm. During experiments to study the effect of current density, it was used a larger piece of carbon-felt (7 cm x 16 cm x 0,6 cm).

A control experiment was also conducted in 125 mL solution, using a cathode of a larger surface (7 cm x 16 cm x 0.6 cm), in order to quantify external losses like phenol adsorption in carbon-felt electrode.

Experiments were monitored by an EG&G Princeton Applied Research 273A potentiostat/galvanostat that assured the application of different currents ($60 \leq I \leq 500$ mA).

Prior to the electrolysis, compressed air was bubbled through the solution for 15 minutes. This proceeding was maintained during all experiments to garantee oxygen saturation in aqueous media and to let the solution homogeneous.

A catalytic quantity of metal ion (catalyst) was added to solutions before starting the electrolysis. Current remained constant during electrolysis and samples were withdrawn at different coulometric charges.

The initial pH of solutions was adjusted in a range of 2.8 to 3.0 by the addition of concentrated sulphuric acid (in experiments to identify intermediates) or hidrocloridric acid (in experiments to measure TOC). In fact, pH remained almost constant, confirming the equations 40, 51 and 52. This pH range was chosen to optimize the hydrogen peroxide production in an acid media saturated of dissolved oxygen ($[O_2] \cong 0.25$ mM, PIMENTEL *et al.*, 2008), according to the equation 37. The pH was measured by a pH glass electrode calibrated with standard buffers at pH values of 4 and 7. Temperature changes were measured by a thermometer and were not significant.

During synthetic experiments with higher electric currents (I / 200 mA), the ionic strength was maintained constant by the addition of 50 mM of Na_2SO_4 (carboxilic acids evolution) or 75 mM of KCl (mineralization experiments) to improve the conductivity of the medium. This procedure was not necessary during experiments with real wastewater.

The experimental procedures are presented below.

2.5 Experimental Procedures

This work was developed at *Laboratoire des Géomatériaux et Géologie de l'Ingénieur at Université Paris-Est Marne la Vallée, in Noysy le Grand*, in France. Each experiment was repeated at least once a time. Data were presented only if the difference between results was above 5% (five per cent). Experiments were made with the application of electrolysis in solutions with different proportions of phenol, *o*- *m*- e *p*-cresol and some of their intermediates. Final experiments were conducted with real effluent. The sequence of experiments was presented as follow.

2.5.1 Obtention of absolute rate constants

The competitive kinetics method (HANNA *et al.,* 2005; DIAGNE *et al.*, 2007) was used to obtain phenol and *o*-cresol absolute constants at pH 3. These compounds were chosen because they are the most persistent phenols present in the real effluent. This method considers that

hydroxyl radicals react mainly with the degradated compound (R) and with the reference substrate (S). In this case, the degradation rate is presented by the equations 58 and 59.

$$-d[R]/dt = k_R[^{\bullet}OH][R] = K_{app(R)}[R] \quad (58)$$

$$-d[S]/dt = k_S[^{\bullet}OH][S] = K_{app(S)}[S] \quad (59)$$

where:

k_{app} – Apparent rate constant.

As the hydroxyl radicals are very reactive and present a very short life-time, it does not accumulate in media and, consequently, they promote a pseudo first order kinetic behavior. Therefore, as we divide the equation (58) by (59), integrating from the beginning of the experiment (t_0) to a generic time (t), it was obtained the equation 60:

$$\ln([R]_0/[R]_t) = k_R/k_S \times \ln([S]_0/[S]_t) \quad (60)$$

This method used equal initial concentrations of the compound and of the reference substract (4-hydroxybenzoic acid — 4-HBA) and allowed obtaining the absolute constants of phenol and *o*-cresol degradation by hydroxyl radicals at pH 3. These results aimed to confirm phenol as the most resistant compound in relation to hydroxyl radicals attack at pH 3. The value used like reference absolute constant (4-HBA) was equal to 1.63×10^9 M^{-1} s^{-1} (BUXTON *et al.*, 1988). The others experiments intended to maximize the conditions to the compounds more persistent (s).

2.5.2 Influence of the catalyst nature

The effect of catalysts was compared by the observation of TOC removal measures obtained through experiments made with four different catalysts (iron, cobalt, cupper, manganese). Three experiments, for each catalyst, with three different concentrations were used to identify optimal concentration range for each catalyst. These twelve experiments could be accelerated increasing the current (I=100 mA) and decreasing phenol start concentration ($[phenol]_0$ = 0.33 mM with theoretical initial TOC_0 = 24 mg/L). When the experiments ended, it was possible to compare mineralization rates. The catalysts tested and their experimental concentrations are presented in Table 10.

Table 10. Metal ions and salt concentrations used during catalyst's experiments.

Catalysts	Salt used	Concentrations used (mM)
Co^{2+}	$CoSO_4.5H_2O$	0.05
		0.10
		1.00
Cu^{2+}	$CuSO_4.5H_2O$	1.00
		5.00
		10.00
Fe^{2+}	$FeSO_4.5H_2O$	0.05
		0.10
		1.00
Mn^{2+}	$MnSO_4.H_2O$	0.10
		0.50
		1.00

2.5.3 Effect of catalyst concentration and anodic oxidation

After obtaining the most efficient catalyst, kinetics experiments were conducted under specific conditions (I = 60 mA and V_0 = 125 mL) that allowed to identify the effect of catalyst concentration during degradation of 1 mM of phenol and *o*-cresol. One additional experiment with phenol electrochemical degradation without the presence of a catalyst, allowed to study the effect of Pt anode in anodic oxidation. Two others additional experiments allowed to obtain apparent constants of *m*- and *p*-cresol.

2.5.4 Identification of intermediates and oxidation reactions

When optimum conditions of the catalyst were obtained, some intermediates produced during phenol and cresols degradation could be identified. Then, with the injection of samples (volume = 20 μL) in High Performance Liquid Chromatograph (HPLC), phenol, o-, m-, p-cresol and the intermediates were separated, identified according to reaction time and quantifed according to obtained areas. The retention times of the identified compounds are presented as follow.

Table 11. Retention times obtained during compounds identification

Compound	Retention time (min.)	Compound	Retention time (min)
Hydroquinone	4.20	Malonic acid	11.86
p-hydroxy-benzoic	5.00	*o*-cresol	12.20
2-methyl-hydroquinone	6.30	*m*-cresol	14.30
Benzoquinone	6.70	Succinic acid	14.30
3-methylcatechol	7.12	*p*-cresol	14.40
Oxalic acid	7.52	Glycolic acid	15.10
Catechol	7.60	Phenol	15.90
Maleic acid	9.20	Formic acid	16.02
Pyruvic acid	10.60	Fumaric acid	17.00
Glyoxylic monohidrate acid	11.40	Acetic acid	17.40

Additionally, to clarify the predominant degradation mechanisms, some intermediates were degraded separetely.

2.5.5 Effect of current density and volume

The effect of the current density and treated volume were studied during experiments of phenol and *o*-cresol degradation, keeping a constant current. The current density, in this case, could be changed by the increase of the working electrode area (cathode). In this experiment, it was used carbon-felt electrode with 112 cm^2 (7 cm x 16 cm x 0.6 cm).

The effect of the current density has been also studied, increasing the current without any variation in the area of the working electrode (cathode area = 56 cm^2: 7 cm x 8 cm x 0.6 cm) in an equimolar mixture of phenol and cresols.

2.5.6 Real wastewater treatment

After the experiments with synthetic samples of phenol, cresols and the identified intermediates, a real wastewater sample (10 L) was collected during stripping process at Parque de Material Aeronáutico do Galeão in november of 2007. This sample was immediately transported by Brazilian Air Force to Université Paris-Est Marne-la-Vallée. Four electrochemical experiments were made to optimize the efficiency of the electro-Fenton process, using electrolytic cells containing carbon felt cathode and Pt or boron-doped diamond (BDD) anodes. These

experiments also studied the influence of chrome and other possible present metals in catalyst efficiency of added iron.

CHAPTER III: ELECTRO-FENTON TREATMENT OF PHENOL, CRESOLS AQUEOUS SOLUTIONS AND REAL "STRIPPING PROCESS" EFFLUENTS

The analysis of the results aimed to highlight the relationship between the phenomena studied and other factors in each stage defined in the experimental procedures. With the exception of the experiments with the real effluent, the other experiments were conducted with an undivided cell that contain Pt as anode and carbon-felt as the cathode. During real effluent treatment, Pt anode was replaced by boron-doped diamond (BDD) in three experiments.

3.1 Kinetics studies

Absolute rate constants of phenol and o-cresol degradation by hydroxyl radicals at pH 3 were obtained by the competitive kinetics method (HANNA *et al.,* 2005; DIAGNE *et al.*, 2007). The concentrations of phenol (or o-cresol) and 4-hydroxybenzoic acid (4-HBA), used as standard competition substrate, were equal to 0.5 mM. Experiments were conducted during thirty minutes using 0.1 mM of ferrous ions as catalyst. The value used as hydroxybenzoic acid (4-HBA) absolute constant was equal to 1.63 x 10^9 M^{-1} s^{-1} (BUXTON *et al.*, 1988) and allowed obtaining phenol and o-cresol absolute constants.

Three experiments, including phenol and 4-hydroxybenzoic acid (4-HBA) oxidation by electro-Fenton process, generated thirteen points that allowed obtaining a straight and fit line (R^2=0,999), as it is shown in Figure 16.

These thirtheen points (Figure 16) allowed obtaining the angular coefficients's standard deviation (s = 0.09). The application of distribution student's t with a degree of freedom equal to 12 and a probability of 95% ($t_{12,\ 0.95}$ = 1.78) produced the angular coefficients's confidence interval ($IC_{0.95}$ = 0.013). The multiplication between the angular coefficient obtained (1.61 6 0.01) and 4-HBA absolute constant (1.63 x 10^9 M^{-1} s^{-1}) showed that the value of phenol absolute constant in pH 3 was equal to (2.62 6 0.02) x 10^9 M^{-1} s^{-1}.

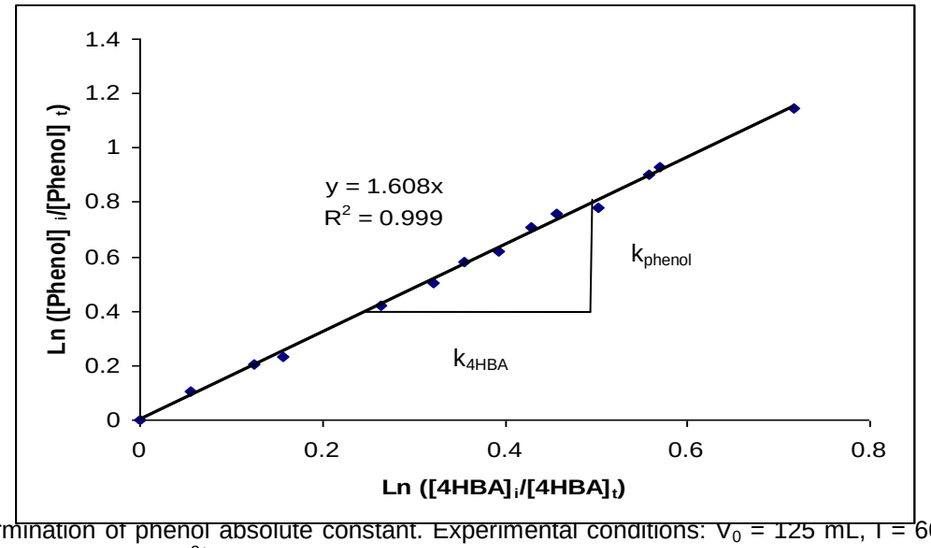

Figure 16. Determination of phenol absolute constant. Experimental conditions: V_0 = 125 mL, I = 60 mA, $[phenol]_i \cong [4HBA]_i \cong$ 0.5 mM, $[Fe^{2+}]$ = 0.1 mM, reaction time = 30 minutes and Pt (1.5 cm x 2 cm) / CF (7 cm x 8 cm x 0,6 cm) electrodes.

Similarly, two experiments including o-cresol and 4-hydroxybenzoic acid (4-HBA) oxidation by hydroxyl radicals during electro-Fenton process, generated nine points that allowed obtaining a straight and fit line (R^2=0,999), as it is shown in Figure 17.

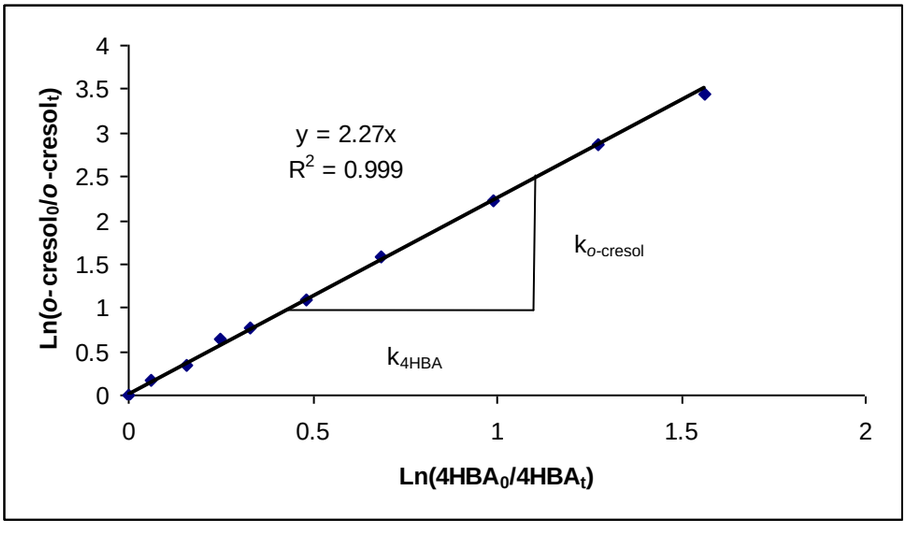

Figure 17. Determination of *o*-cresol absolute constant. Experimental conditions: V_0 = 125 mL, I = 60 mA, $[phenol]_i \cong [4HBA]_i \cong$ 0.5 mM, $[Fe^{2+}]$ = 0.1 mM, reaction time = 30 minutes and Pt (1.5 cm x 2 cm) / CF (7 cm x 8 cm x 0,6 cm) electrodes.

These nine points (Figure 17) allowed obtaining the angular coefficients's standard deviation (s = 0.19). The application of distribution student's t with a degree of freedom equal to 8

and a probability of 95% ($t_{8,\ 0.95}$ = 1.86) produced the angular coefficients's confidence interval ($IC_{0.95}$ = 0.12). The multiplication between the angular coefficient obtained (2.27 6 0.12) and 4-HBA absolute constant (1.63 x 10^9 M^{-1} s^{-1}) showed that the value of *o*-cresol absolute constant in pH 3 was equal to (3.70 6 0.19) x 10^9 M^{-1} s^{-1}.

High values of correlation coefficient (R^2) obtained in Figures 16 and 17 evidenced the pseudo first order kinetic, typical of AOP's. The absolute rate constants obtained were close, but phenol was more persistant than o-cresol. Additionally, phenol concentration is usually four times higher *o*-cresol concentration in commercial paint strippers (PENETONE CORPORATION, 2004), therefore, most experiments aimed to optimize the removal of phenol and its intermediates.

3.2 Influence of the catalyst nature

From the experiments using Co^{2+} ($E^0(Co^{3+}/Co^{2+})$ = 1.92 V), Cu^{2+} ($E^0(Cu^{2+}/Cu^{+})$ = 0.16 V), Fe^{2+} ($E^0(Fe^{3+}/Fe^{2+})$ = 0.77 V) and Mn^{2+} ($E^0(Mn^{3+}/Mn^{2+})$ = 1.50 V) ions, it was possible to study the influence of the catalyst in phenol mineralization, as shows Figure 18. In these experiments (V_0 = 330 mL, I = 100 mA, pH = 3, with theoretical TOC_0 = 24 mg/L), different behaviours could be observed to iron and cobalt experiments in relation to cupper and manganese. TOC removal rates from the experiments including iron and cobalt are really different when compared with copper and manganese (Figure 18). Higher rates (about 80% and 78% for iron and cobalt respectively in 4 h of electrolysis) were obtain when 0.1 mM of iron(II) or cobalt(II) ions was employed as catalyst. Stronger changes in color were also observed, which can be explained by the formation of quinones (AZEVEDO, 2003; MACIEL *et al.,* 2004). In these cases, catalyst concentrations greater than 0.1 mM harmed the efficiency of the treatment, which can be explained by scavenging reactions between iron(II) and / or cobalt(II) ions and hydroxyl radicals (Equations 46 and 61).

$$Fe^{2+} + {}^{\bullet}OH \rightarrow FeOH^{2+} \qquad k = 4.3 \times 10^8\ M^{-1}\ s^{-1} \qquad (46)$$

$$Co^{2+} + {}^{\bullet}OH \rightarrow CoOH^{2+} \qquad k = 8 \times 10^5\ M^{-1}\ s^{-1} \qquad (61)$$

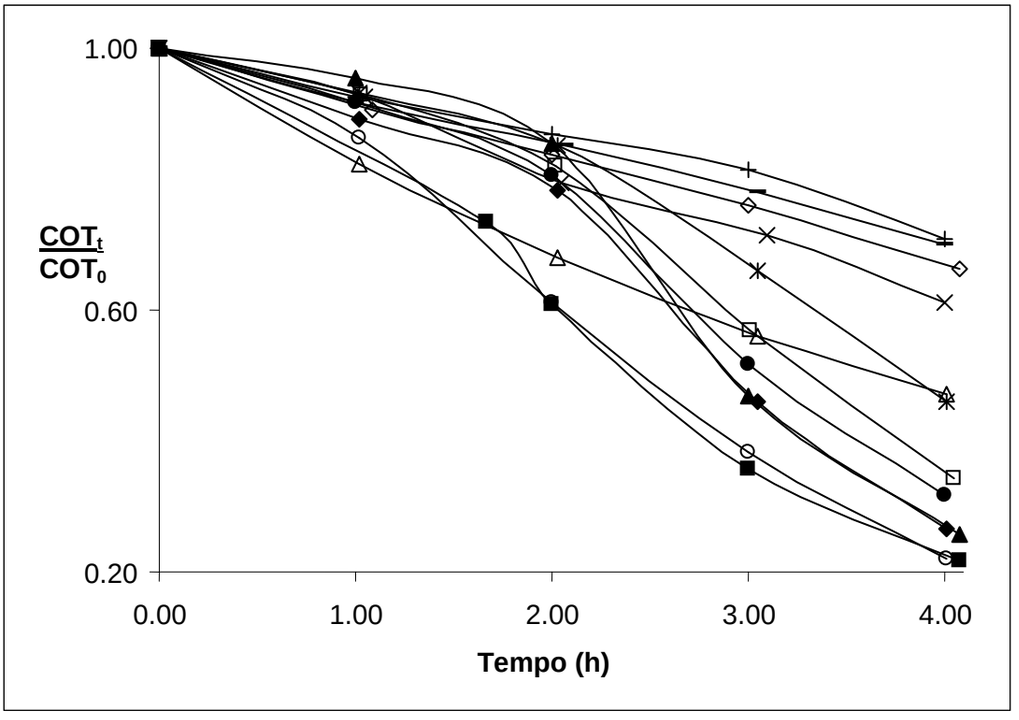

Figure 18. TOC removal with electrolysis time for the mineralization of 0.33 mM (TOC_0 = 24 mg L^{-1}) phenol aqueous solution with different catalysts during electro-Fenton treatment: [Fe^{2+}]: 0.05 mM (-□-), 0.10 mM (-■-), 1.00 mM (-Δ-); [Co^{2+}]: 0.05 mM(-▲-), 0.10 mM (-○-), 1.00 mM (-♦-); [Mn^{2+}]: 0.10 mM (--), 0.50 mM (◊), 1.0 mM (-∗-); [Cu^{2+}]: 1.0 mM (-+-), 5 mM (-●-),10 mM (-x-). Experimental conditions: Initial volume (V_0) = 330 mL, I = 100 mA, pH = 3 and Pt (1.5 cm x 2 cm) / CF (7 cm x 8 cm x 0.6 cm) electrodes.

When copper or manganese is used as catalyst, optimum catalyst concentration is higher (5 mM for Cu^{2+} and 1 mM for Mn^{2+}) in comparison with the optimal concentrations of Fe^{2+} and Co^{2+}. In fact, the reduction in catalyst concentration decreased considerably the efficiency in relation to iron and cobalt (about 35% to 1 mM of Cu^{2+} and 0.1 mM of Mn^{2+}). Although mineralization rates were optimized to 5 mM of Cu^{2+} and 1 mM of Mn^{2+}, they remained lowers in comparison to the rates obtained from the experiments with cobalt and iron. Loss of eficiency can be justified by metallic deposition on electrodes, observed in both cases. It evidenced reduction in catalyst concentration and, consequently, decrease of hydroxyl radical production (Equation 45).

Cupper deposition on carbon-felt cathode can be justified by the high values of standard reduction potentials to Cu(II) ($E^0Cu^{2+}/Cu(s)$ = 0.34 V/SHE) and Cu(I) ($E^0Cu^{+}/Cu(s)$ = 0.52 V/SHE) ions**.**

During experiments with manganese**,** it was observed a reddish oxide deposition on Pt anode. This phenomena is frequent in electrochemical experiments conducted with Pt in acid

media and can be justified by the chemical reaction presented in Equation 58 (GHAEMI *et al.*, 2001; WU and CHIANG, 2006).

$$Mn^{2+} + 2H_2O \rightarrow MnO_2\,(s) + 4H^+ + 2e^- \quad (62)$$

In the other hand, cathode potential (≅ -0.25 V/SHE, OTURAN and PINSON, 1995) did not favor iron ($E^0_{Fe^{2+}/Fe(s)}$ = -0.44 V, $E^0_{Fe^{3+}/Fe(s)}$ = -0.04 V) neither cobalt ($E^0_{Co^{2+}/Co(s)}$ = -0.28 V) deposition, optimizing catalyst action of these ions. Considering that iron presented a higher eficiency and that cobalt is more toxic for the environment, iron was selected for the other experiments.

3.3 Effect of catalyst concentration and anodic oxidation

Kinetic experiments were carried out in aqueous solutions containing 1.05 mM of phenol or o-cresol in the presence of Fe(II) ions to study the effect of the catalyst concentration. They were conducted with Fe^{2+} ions because Fe^{2+} presented better results as catalyst during phenol mineralization at previous experiments.

Figure 19 shows kinetic curves in function of electrolysis time with Iron (II) concentrations from 0.05 to 1.00 mM. The insert of Figure 19 ($Ln([fenol]_0/[fenol]_t)$ in function of time) allowed obtainin all apparent rate constants during phenol degradation. In this case, an additional and fast experiment (duration of fifteen minutes) was conducted in the lack of iron (II), obtaining phenol aparent rate constant during anodic oxidation.

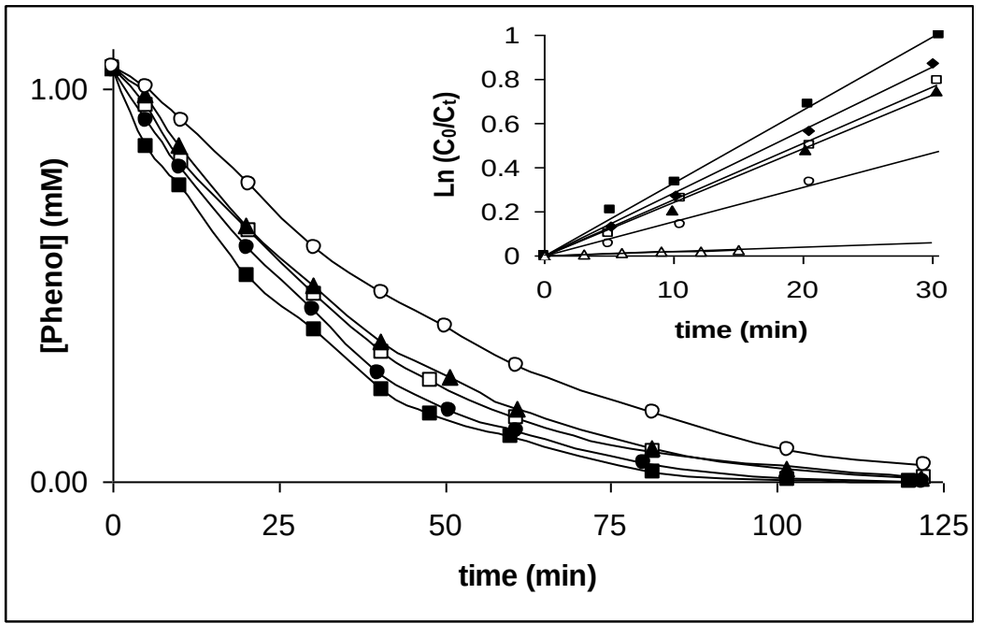

Figure 19. Effect of catalyst (Fe^{2+}) concentration on the degradation kinetics of phenol at pH 3 during current controlled electrolysis by electro-Fenton process at 60 mA: (-△-): [Fe^{2+}] = 0 mM (R^2=0.997); (-□-): [Fe^{2+}] = 0.05 mM (R^2=0.997), (-■-); [Fe^{2+}] = 0.1 mM (R^2=0.998); (-●-): [Fe^{2+}] = 0.25 mM (R^2=0.999); (-▲-): [Fe^{2+}] = 0.5 mM (R^2=0.998); (-O-): [Fe^{2+}] = 1.0 mM, (R^2=0.997). Experimental conditions: V_0=125 mL and Pt (1.5 cm x 2 cm) / CF (7 cm x 8 cm x 0,6 cm) electrodes.

In experiments with Fe^{2+} concentrations higher than 0.1 mM, it was observed an increase in degradation rates with the reduction of iron concentration ($k_{app\ 1mM}$ = 0.01560.005 < $K_{app\ 0.5mM}$ = 0.02460.005 < $k_{app\ 0.25mM}$ = 0.02860.001 < $k_{app\ 0.10mM}$ = = 0.03760.003 min^{-1}). Probably, in these conditions, the reduction of iron concentration decreased parasite reactions, consuming hydroxyl radicals particularly due to the equation (46).

On the other hand, in experiments with iron concentrations lower than 0.1 mM, the reduction of iron concentration decreased the degradation rates ($K_{app\ 0.10mM}$ = 0.03760.003 < < $k_{app\ 0.05mM}$ = 0.02560.003 < $K_{app\ 0mM}$ = 0.00260.001 min^{-1}). In these conditions, iron concentration was insufficient to catalyze the electro-Fenton system efficiently according to equation (5). The great difference between apparent constants obtained through experiments with 0 and 0.1 mM of iron evidenced that the production of hydroxyl radicals in Pt electrode (anodic oxidation) was despicable.

These results underline once again that under our experimental conditions a concentration of 0.1 mM ferrous iron constitute the optimal value for an effective oxidation of phenol in aqueous medium. Under these conditions, the complete degradation of a concentrated phenol solution

(1.05 mM) took place in less than 100 minutes, even when the applied current was relatively small (60 mA).

The effect of iron concentration in kinetic degradation of *o*-cresol has also been studied as presented in Figure 20. In optimum conditions, the apparent rate constants of *m*- and *p*-cresol were determined.

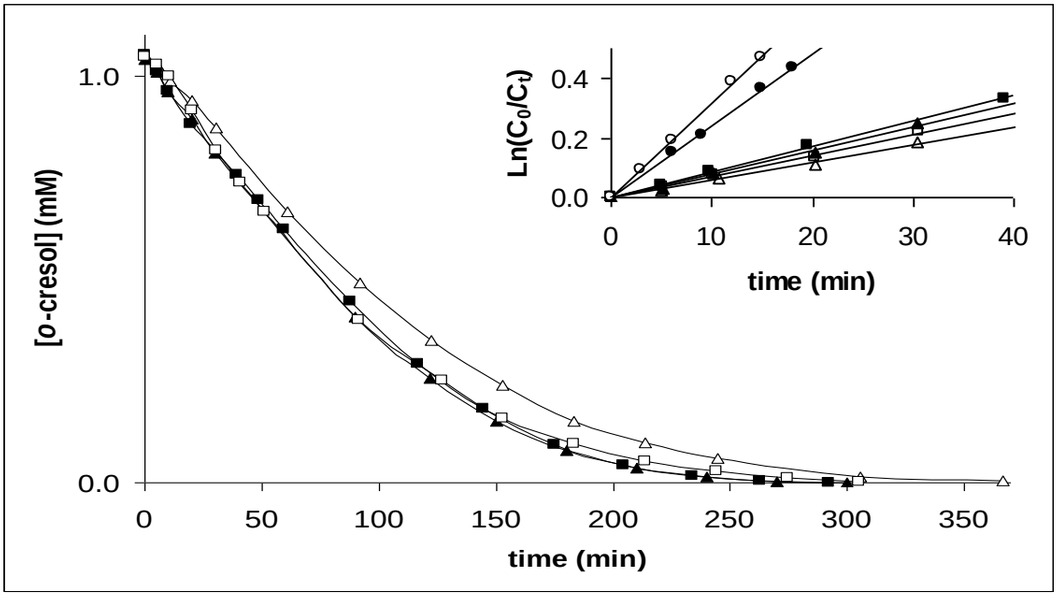

Figure 20. Effect of catalyst (Fe^{2+}) concentration on the degradation kinetics of *o*-cresol: (-□-) $[Fe^{2+}]$ = 0.05 (R^2=0.997), (-■-) $[Fe^{2+}]$ = 0.10 (R^2=0.999), (-▲-) $[Fe^{2+}]$ = 0.25 (R^2=0.997) and (-△−) $[Fe^{2+}]$ = 1 mM (R^2=0.996); m-cresol: (-○-) $[Fe^{2+}]$ =0.10 mM (R^2=0.999) and p-cresol: (-●-) $[Fe^{2+}]$ = 0.10 mM (R^2=0.998) at pH 3 during current controlled electrolysis at 60 mA by electro-Fenton process. Experimental conditions: V_0=125 mL and Pt (1.5 cm x 2 cm) / CF (7 cm x 8 cm x 0,6 cm) electrodes.

During kinetic experiments involving *o*-cresol degradation, catalyst optimum concentration obtained was also equal to 0.1 mM of Fe^{2+}. In these conditions, the apparent constants obtained during the degradation of 1.05 mM *m*-cresol ($k_{app\ 0.1mM}$ = 0.03260.001 min^{-1}) and 1.05 mM *p*-cresol ($k_{app\ 0.1mM}$ = 0.02460.001 min^{-1}) fortified the major persistence of o-cresol ($k_{app\ 0.1mM}$ = 0.00960.001 min^{-1}) between the cresols (BUXTON *et al.*, 1988; RODER *et al.*, 1999). Probably, the presence of a greater number of *orto* and *para*-positions relatives to hydroxyl radical can justify greater degradation rates obtained with *m*-cresol.

However, apparent constants obtained during *o*-cresol degradation ($k_{app\ 0.1mM}$ = = 0.00960.001 > $k_{app\ 0.25mM}$ = 0.00860.001 > $k_{app\ 0.05mM}$ = 0.00760.001 > $k_{app\ 1.00mM}$ = 0.00660.001 min^{-1}) were lower in relation to phenol constant ($k_{app\ 0.10mM}$ = 0.03760.003 min^{-1}). In fact, under optimal conditions, the complete degradation of a concentrated solution of *o*-cresol (1.05 mM) occurred in less than 300 minutes, about the triple time necessary to phenol degradation (Figure 19). The additional

methyl radical present in *o*-cresol may have produced a greater number of intermediates that competed by hydroxyl radicals and harmed *o*-cresol degradation**.**

Additional experiments were performed to identify main intermediates formed during phenol and cresols degradation in order to highlight degradation mechanisms.

3.4 Identification of intermediates

During electro-Fenton treatment, the oxidation reactions produced intermediates, identified in two stages: identification of aromatics and carboxylics acids. The first one included identification of aromatic intermediates during oxidation of compounds more persistents. It was possible to identify three intermediates for phenol and two for *o*-cresol, but it was not possible to identify aromatic compounds in experiments realized to obtain apparent constants of *m*- and *p*-cresol. In fact, the aromatic intermediates were identified through previous experiments realized to verify the effect of iron concentration in phenol and *o*-cresol degradation.

In the other hand, in second stage, the main carboxylic acids formed during phenol and cresols degradation were identified in separate experiments. Experimental conditions were modified increasing applied current (I = 60 $\rightarrow$ 200 mA) and initial concentration of the substance to be degraded (C_0 = 1.05 $\rightarrow$ 2.50 mM), because carboxylic acids appear as final and more persistant oxidation products of the process.

As follows, the main aromatic compounds produced and destroyed in phenol and *o*-cresol electrochemical degradation are presented.

3.4.1 Evolution of aromatic intermediates

During phenol oxidation by electro-Fenton process, main reactions were successively electrophilic addition of hydroxyl radical on the aromatic ring leading to the formation of polyhydroxylated benzene derivatives, such as hydroquinone and catechol which were oxidized to quinine groups such as p-benzoquinone. The evolution of these substances in aqueous medium is represented in Figure 21.

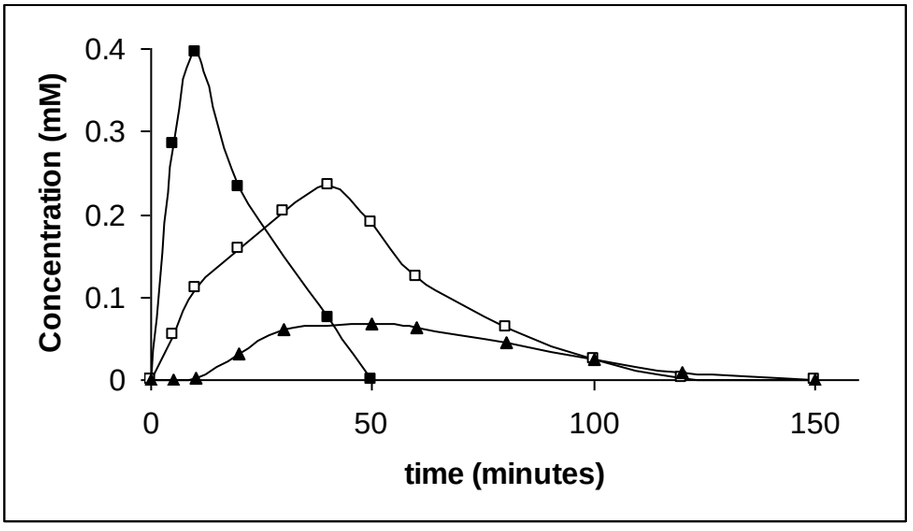

Figure 21. Time-course of aromatic intermediates: (-■-) p-benzoquinone; (-□-) catechol and (-▲-) hydroquinone during the degradation of 1.05 mM phenol aqueous solution by electro-Fenton process. Experimental conditions: $[Fe^{2+}]$ = 0.10 mM, V_0 = 125 mL, pH = 3 and I = 60 mA and Pt (1.5 cm x 2 cm) / CF (7 cm x 8 cm x 0,6 cm) electrodes.

These results corroborate previous studies presented in Table 6. The sum of intermediates maximum concentrations obtained shows that these substances corresponded to the predominant process of phenol degradation (about 70%), being completely degraded in about 150 minutes. The reaction mechanisms that lead to the production of these intermediates are presented in Figure 22 (reactions 63-65).

The *orto* and *para* inductive effect in relation to –OH group (CHANG, 2003) conducted hydroxyls radicals attack, producing catechol and hydroquinone as mainly directed products in phenol oxidation, according to reaction 63. Simultaneously, it can occur hydrogen atom abstraction reactions (reaction 65), but, degradation reaction constants are smaller in comparation to electrophilic addition reactions (BUXTON *et al.*, 1988). The higher oxidative potential of the medium allowed the oxidation of hydroquinone to p-benzoquinone according to reaction 64. The small hydroquinone accumulation in the medium can be explained by its quick transformation to p-benzoquinone and in parallel by its hydroxylation or mineralization reactions. In fact, p-benzoquinone ($k_{1,4\ BQ}$ = 1.2 x 10^9 M^{-1} s^{-1}, ADAMS and MICHAEL, 1967) and hydroquinone (k_{HQ} = 1.0 x 10^{10} M^{-1} s^{-1}, HECKEL and HEINGLEIN, 1966) absolute rate constants of degradation by hydroxyl radicals show that hydroquinone has a greater tendency to be oxidized.

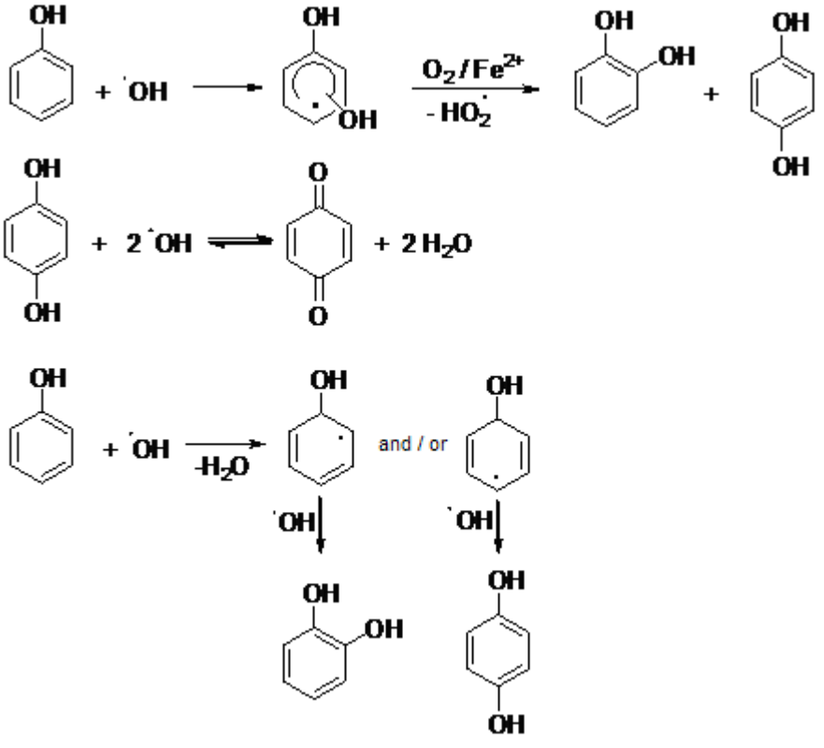

(63)

(64)

(65)

Figure 22. Proposed reaction mechanisms for hydroxyl addition and hydrogen atom abstraction during phenol oxidation by $^{\bullet}$OH radicals.

Figure 23 shows the main aromatic compounds produced and oxidized in *o*-cresol electrochemical degradation. During *o*-cresol electrolysis, the main initial reactions were successively electrophilic additions of hydroxyl radical on the aromatic ring, leading to the formation of 3-methylcatechol and methyl-hydroquinone. This fact is in agreement with the studies presented in Table 6. The mechanisms of the reactions that lead to the production of these intermediates are presented in Figure 24 (reactions 66 and 67).

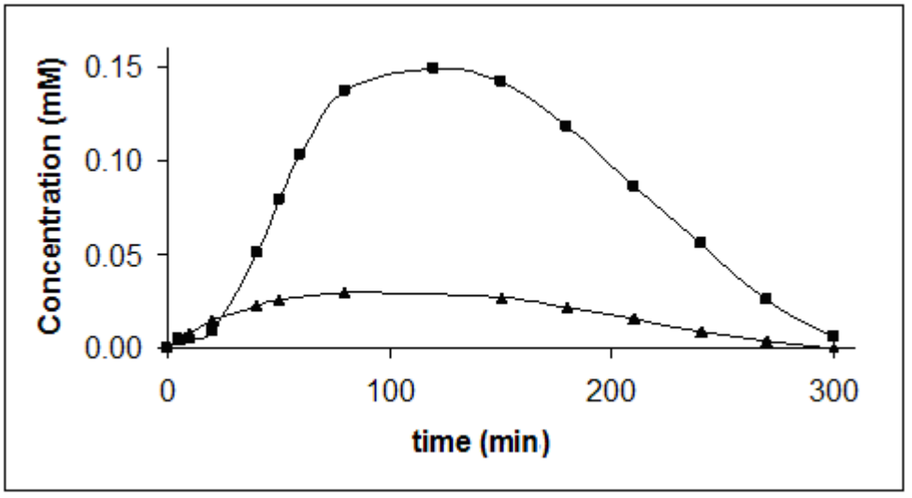

Figure 23. Time-course of aromatic intermediates: (-■-) 3-methyl-catechol and (-▲-) methyl-hydroquinone during the degradation of 1.05 mM *o*-chresol aqueous solution by electro-Fenton process. Experimental conditions: $[Fe^{2+}]$ = 0.10 mM, V_0 = 125 mL, pH = 3 and I = 60 mA and Pt (1.5 cm x 2 cm) / CF (7 cm x 8 cm x 0,6 cm) electrodes.

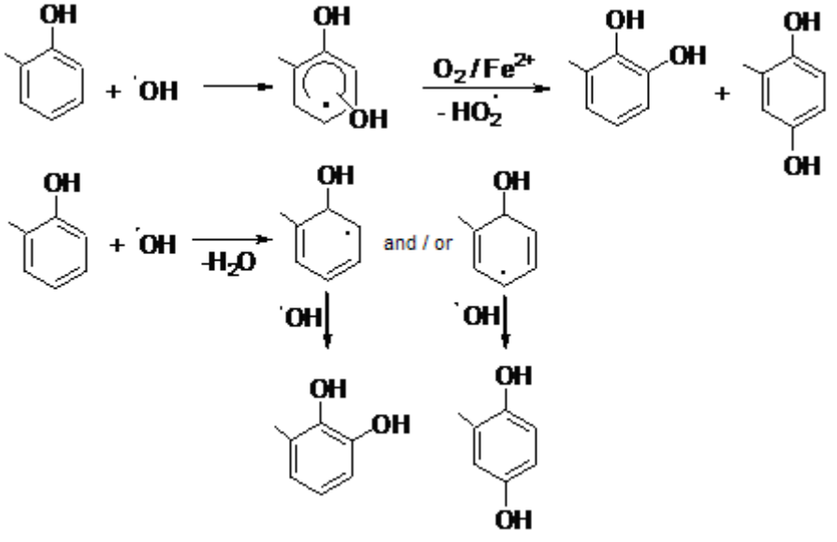

(66)

(67)

Figure 24. Proposed reactions mechanisms of hydroxyl addition on o-chresol aromatic ring by electro-Fenton process.

The *orto* and *para* inductive effect in relation to –OH group (CHANG, 2003), like in phenol's oxidation, directed the hydroxyls attacks according to reactions 66 and 67. The sum of the maximum concentrations obtained (Figure 23) shows that these intermediates represented a higher percentual (58%) of o-cresol degrading process (1,05 mM) and that they were completely degraded in about 300 minutes

As follows, it was possible to present main carboxylic acids produced and oxidized during phenol and cresols electrochemical degradation.

3.4.2. Evolution of carboxilic acids

3.4.2.1. Identified carboxylic acids in phenol oxidation

Phenol's oxidation formed polyhydroxylated derivative and/or quinones. As follows, aromatic ring opening reactions leaded to the formation of carboxylic acids. Figure 25 presents the evolution of the identified carboxylic acids formed during phenol oxidation.

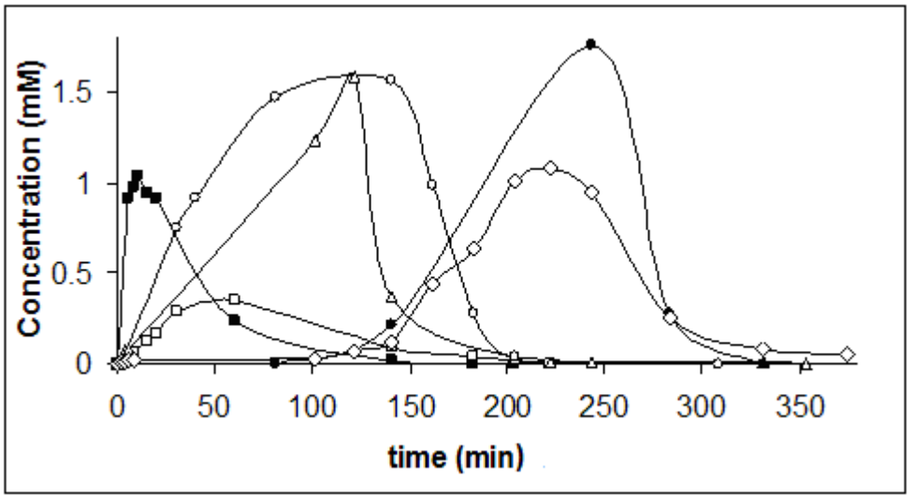

Figure 25. Evolution of carboxylic acids identified during oxidation of phenol by electro-Fenton treatment: maleic (-■-), fumaric (-□-), succinic (-△-), glyoxylic (-○-), formic (-●-) and oxalic (-◇-) acids. Experimental conditions: $[Phenol]_0$ = 2.50 mM, $[Fe^{2+}]$ = 0.10 mM, $[Na_2SO_4]$ = 50 mM, V_0 = 125 mL, I = 200 mA, pH= 3.0 and Pt (1.5 cm x 2 cm) / CF (7 cm x 8 cm x 0,6 cm) electrodes.

Maleic, glyoxylic succinic and fumaric acids were the predominant carboxylic acids formed in the earlier stages of the treatment. Maleic acid reached its maximum concentration at 15 min, being subsequently quickly degraded in about 150 minutes.

Glyoxylic and succinic acids started to be formed in the first minutes and both reached maximum concentrations at 120 minutes. The curves show that the disappearance of glyoxylic and succinic acids was followed by the appearance of formic and oxalic acids as end products, before total mineralization. The transformation of glyoxylic acid into oxalic acid by electrochemical

advanced oxidation methods was already reported by BOYE *et al.* (2002). Traces of malonic, pyruvic and acetic acids were also detected.

In order to clarify the formation mechanism of carboxylic acids, additional oxidation experiments with the most important aromatic intermediates (benzoquinone, hydroquinone and catechol) were carried out at the same experimental conditions during one hour. These results are represented in Figures 26 (a), (b) and (c).

Figure 26 shows the identified acids formed during the oxidation of the main intermediates by hydroxyl radicals. Polyhydroxylated benzenic compounds formed are very unstable which hinders their identification. So, in order to simplify the reaction mechanism, we proposed complete reactions presenting ring opening reactions directly from dihydroxylated derivatives.

During benzoquinone (Figure 26 (a)) and hydroquinone (Figure 26 (b)) oxidation with hydroxyl radicals, glyoxylic and fumaric acids were predominantly formed. Traces of malonic, pyruvic, oxalic (Figures 26 (a) and (b)) and maleic (26 (b)) acids were also detected. Therefore, It could be verified that the same carboxylic acids were essentially formed, confirming of hydroquinone to benzoquinone (reaction 64). Besides, only in these experiments, pyruvic acid could be detected in the earlier minutes. Then, it was proposed that glyoxylic, fumaric and pyruvic acids were directly formed from hydroquinone/benzoquinone destruction.

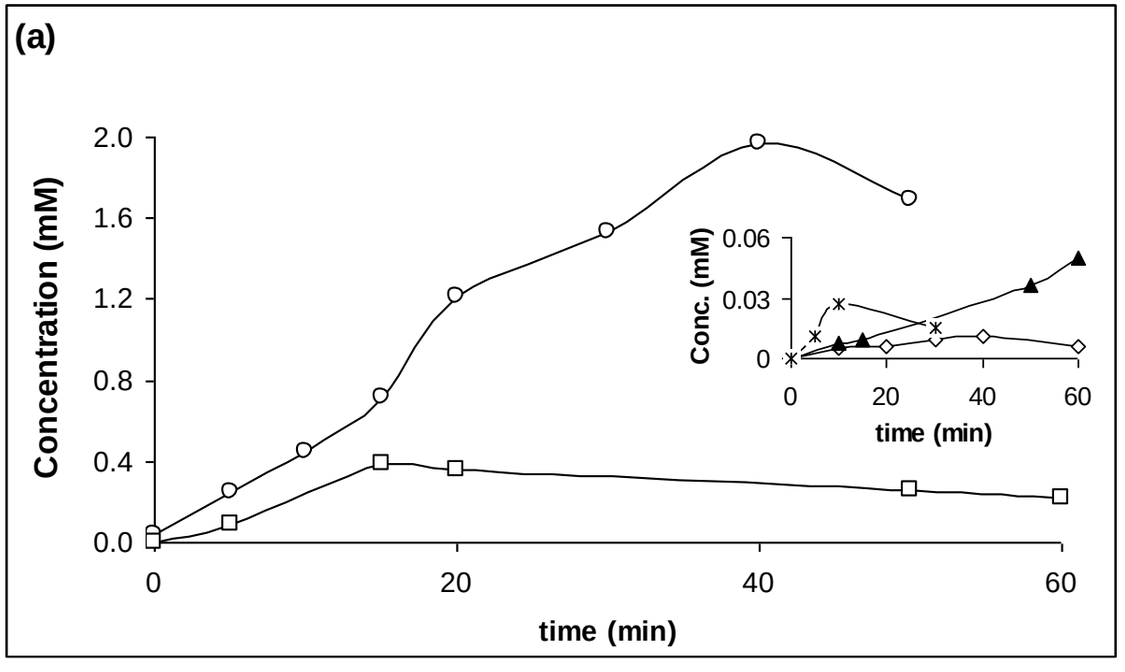

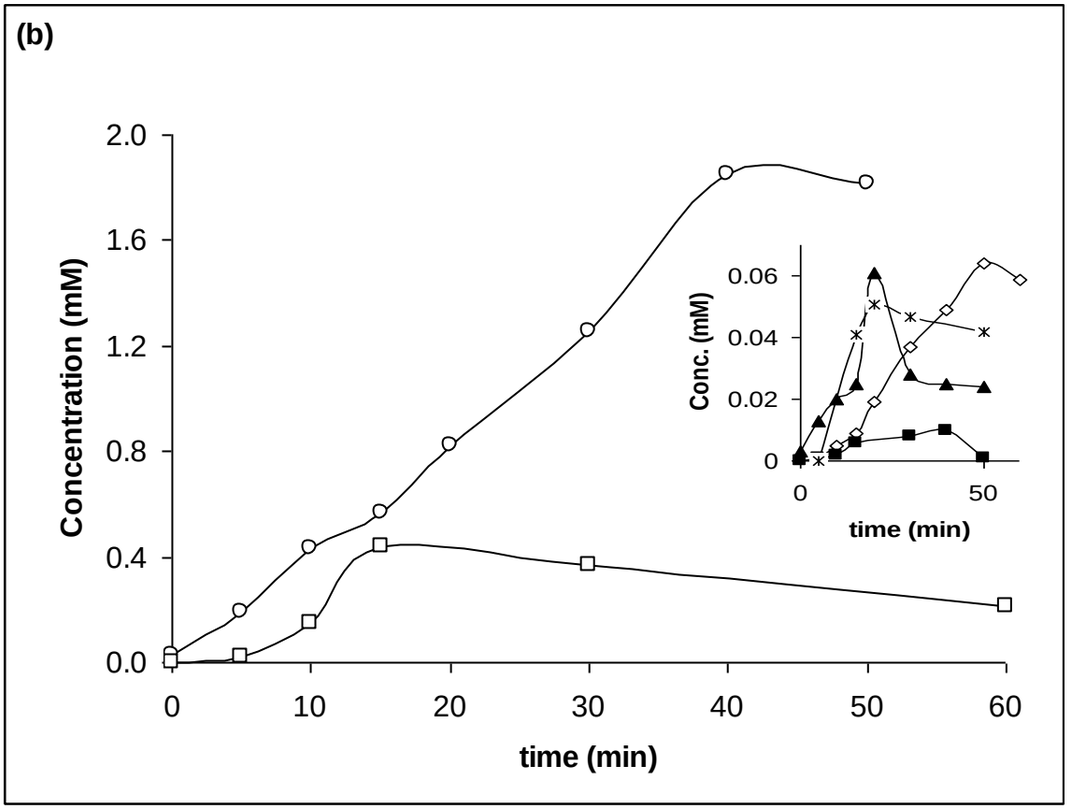

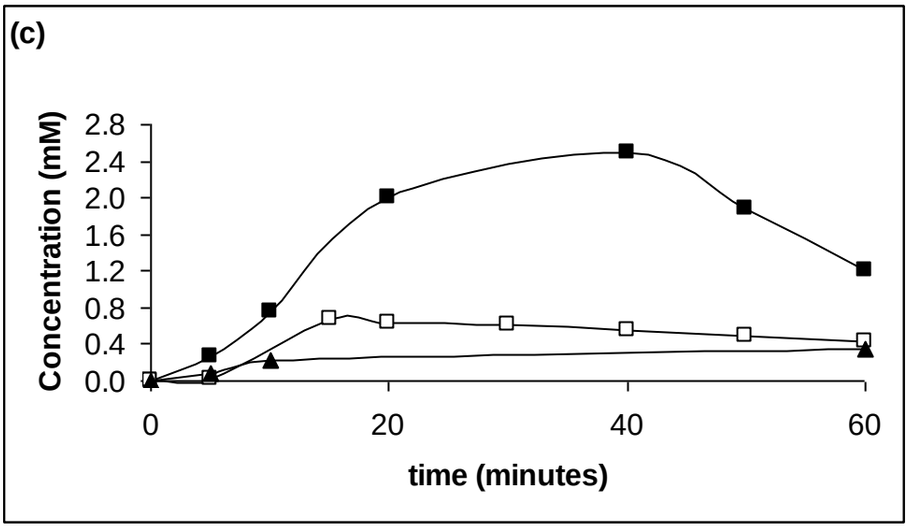

Figure 26. Evolution of carboxylic acids identified (glioxylic: ○, fumaric: □, pyruvic: ▲, malonic: ∗, succinic: △, maleic: ■ and oxalic: ◇) during benzoquinone (a), hydroquinone (b) and catechol (c) degradation by

electro-Fenton process. Experimental conditions: I = 200 mA, V_0 = 125 mL, C_0 = 2.5 mM, $[Fe^{2+}]$ = 0.1 mM, $[Na_2SO_4]$ = 50 mM, pH= 3.0 and Pt (1.5 cm x 2 cm) / CF (7 cm x 8 cm x 0,6 cm) electrodes.

In cathecol oxidation (Figure 26 (c)), the presence of hydroxyl groups in adjacent carbon of benzene ring leaded predominantly to the formation of glyoxylic, fumaric and succinic acids. In these experiments, maleic or succinic acids concentrations were lower. However, both were predominantly formed during the first minutes of phenol degradation (Figure 25). So, they were possibly formed by other intermediates not accumulated in the medium.

Maleic acid, for instance, can be formed by hydroxyls radicals attack to 1, 2, 3-tri-hydroxybenzene, produced by cathecol degradation, according to reaction 68 (Figure 27).

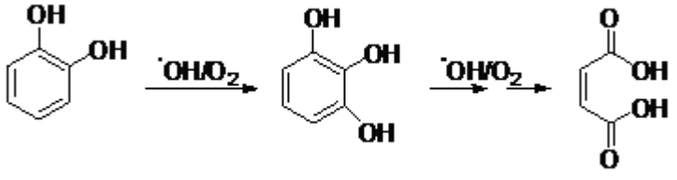

(68)

Figure 27. Proposed reactions mechanisms of maleic production due to hydroxyl attack and catechol aromatic ring cleavage by electro-Fenton process.

In order to highlight the mechanisms of carboxylic acids degradation by electro-Fenton process, other experiments were done, degrading each acid identified for one hour. Table 12 presents the products identified during the degradation of each acid.

Table 12. Products identified in earlier stages of carboxylic acids degradation by electro-Fenton process. Experimental conditions: $[C_0]$ = 0.5 mM, $[Fe^{2+}]$ = 0.1 mM, I = 60 mA, V_0 = 330 mL, pH = 3 and Pt / CF electrodes.

Carboxylic acid precursor	Predominant products identified
Maleic	Glyoxylic, Acetic, Oxalic, Formic
Fumaric	Glyoxylic, Oxalic, Formic
Succinic	Malonic, Oxalic
Malonic	Oxalic
Pyruvic	Acetic, Oxalic
Glyoxylic	Oxalic, Formic
Acetic	Oxalic, Formic
Oxalic	None
Formic	None

Considering the reactions with hydroxyls radicals (reactions 63 to 65 and 68), the identification and evolution of intermediates (Figures 21, 25 to 27 and Table 12) and the molecular structures of compounds, it was proposed a mineralization reaction pathway of phenol, presented in Figure 28.

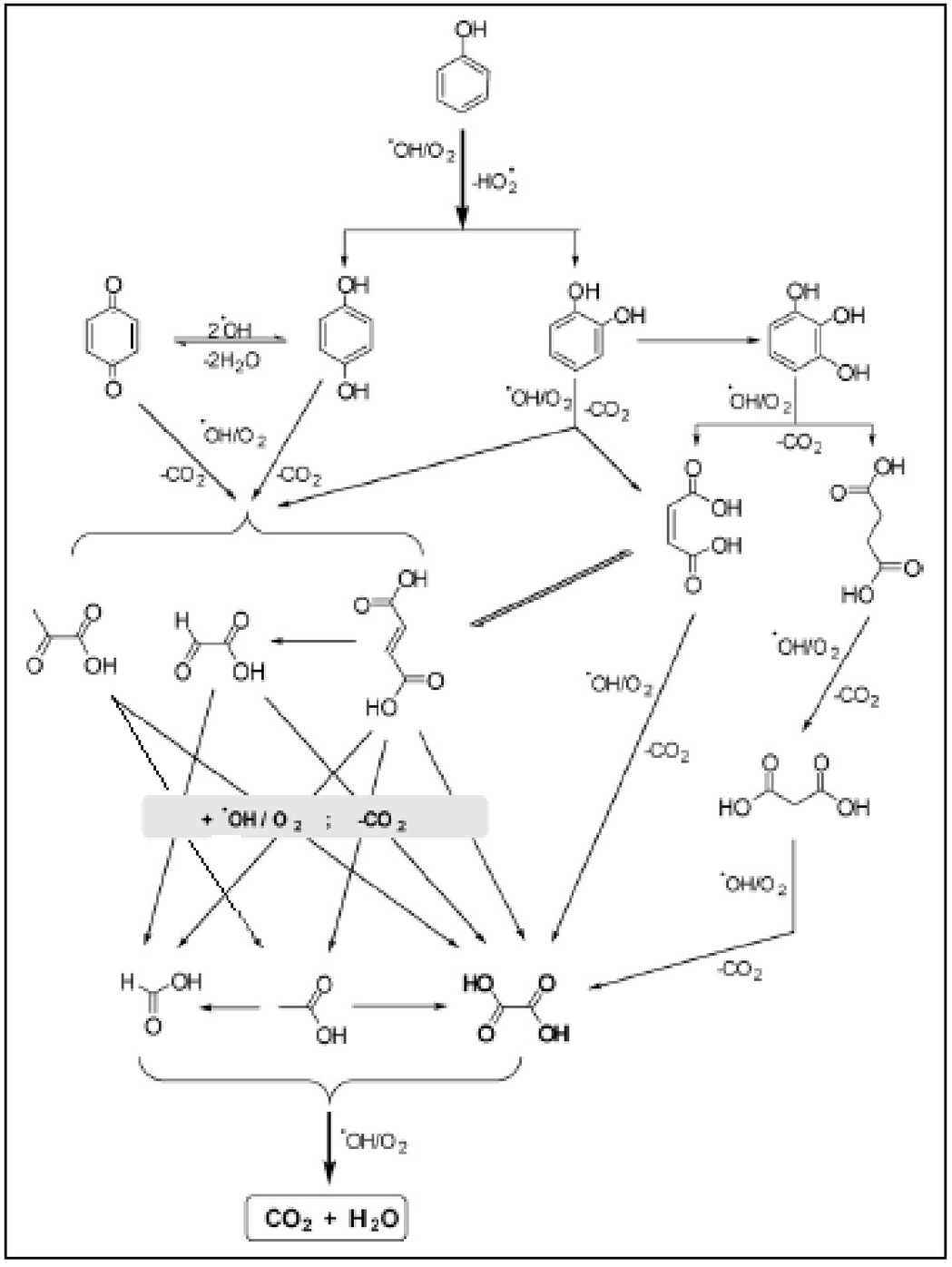

Figure 28. General reaction sequence proposed for the mineralization of phenol in aqueous acid medium by hydroxyl radicals generated in electro-Fenton process.

This mechanism shows the sequence of intermediates produced, emphasizing the high oxidative power of electro-Fenton process. As it can be seen, phenolic compounds are destructed in initial stages, becoming possible to stop the process after total mineralization. Then, it is recommended to complete carboxylics acid treatment with biological process.

Therefore, this mechanism is a significant data of this work because it allows elucidating all intermediates identified. By the fact that electro-Fenton process is a EAOP based on the attack of hydroxyl radicals in acid medium in the presence of the dissolved oxygen, the mechanism presented can help to detail phenol degradation mechanisms by others AOP's at similar conditions.

3.4.2.2 Idenfified acids in cresols oxidation

Figure 29 presents carboxylic acids evolution in *o*-cresol electrolysis.

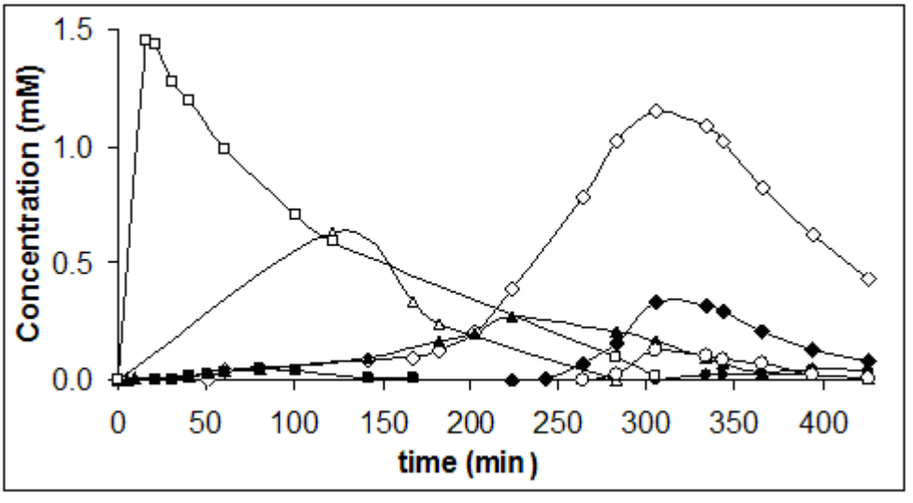

Figure 29. Evolution of carboxylic acids identified during oxidation of *o*-cresol by electro-Fenton treatment: fumaric: (□), succinic: (△), maleic: (■), piruvic: (▲), glioxylic: (○), oxalic: (◇), acetic: (◆) and formic: (●) acids. Experimental conditions: $[o\text{-chresol}]_0$ = 2.50 mM, $[Fe^{2+}]$ = 0.10 mM, $[Na_2SO_4]$ = 50 mM, V_0 = 125 mL, I = 200 mA, pH= 3.0 and Pt (1.5 cm x 2 cm) / CF (7 cm x 8 cm x 0,6 cm) electrodes.

During *o*-cresol electrolysis, fumaric and succinic acids were predominantly formed in initial stages, but there were also traces of piruvic and maleic. Fumaric acid presented maximum concentration (1,45 mM) in 15 minutes of reaction, being totally degraded in 300 minutes. Piruvic acid started to be formed at the first minutes and achieved maximum concentration (0.269 mM) in 223 minutes of reaction. These acids are formed by the breaking of aromatic rings. Maleic, fumaric

and piruvic acids, for instance, can be formed by hydroxyls radicals attack to 3-methylcatechol, according to Figure 30 (reaction 69). Oxalic, acetic and glyoxylic acids are predominant formed in final stages, reaching maximum concentrations in 300 minutes of reaction.

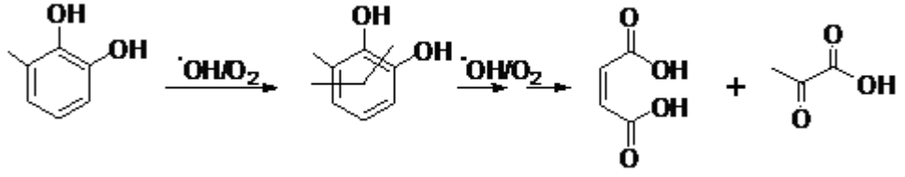

(69)

Figure 30. Proposed reactions mechanisms of maleic and pyruvic production due to hydroxyl attack and 3-methyl-catechol aromatic ring cleavage by electro-Fenton process.

During o-cresol degradation, it was verified a predominance production of fumaric (Figure 29, t = 15 min, [fumaric] ≅ 1.5 mM) in comparison to maleic acid (Figure 25, t = 15 min, [maleic] ≅ 1.0 mM) produced in phenol degradation. It emphasizes the tendency of a major production of intermediates during *o*-cresol degradation, probably due to additional methyl group. Besides, the high values of maleic and fumaric absolute constants by hydroxyl radical attack ($k \cong 10^9$ M^{-1} s^{-1}, BUXTON *et al.*, 1988) and the greater concentrations of maleic and fumaric acids obtained during o-cresol degradation may justify the faster degradation of phenol.

Considering the reactions with hydroxyls radicals (reactions 66, 67 and 69), identification and evolution of intermediates (Figures 23 and 29 and Table 12) and molecular structures of compounds, it was proposed a mineralization reaction pathway of o-cresol, presented in Figure 31.

This mechanism elucidates all intermediates identified during o-cresol degradation by electro-Fenton process. This result is significant, because there are few data in literature showing mechanisms for o-cresol degradation by hydroxyl radicals attack in acid medium (Figure 7)**.** Then, the presented mechanism can help to detail o-cresol degradation mechanisms by others AOP's at similar conditions.

Two other additional experiments allowed identifying some acids formed in *m*- and *p*-cresol degradation. These results, presented in Figures 32 and 33, allowed understanding the higher aparent rate constants produced during *m*- and *p*-cresol degradation (Figure 20).

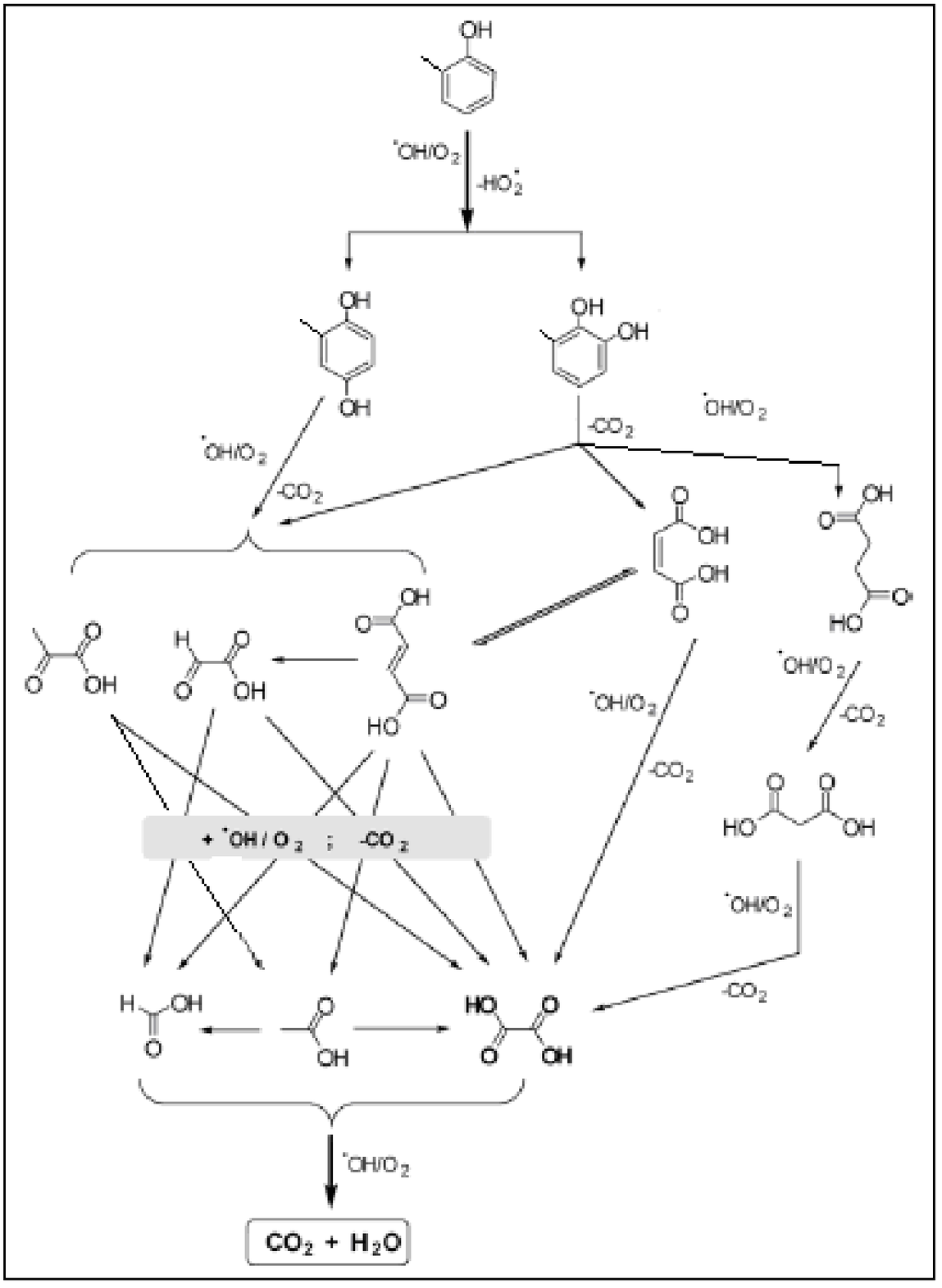

Figure 31. General reaction sequence proposed for the mineralization of *o*-cresol in aqueous acid medium by hydroxyl radicals generated by electro-Fenton process.

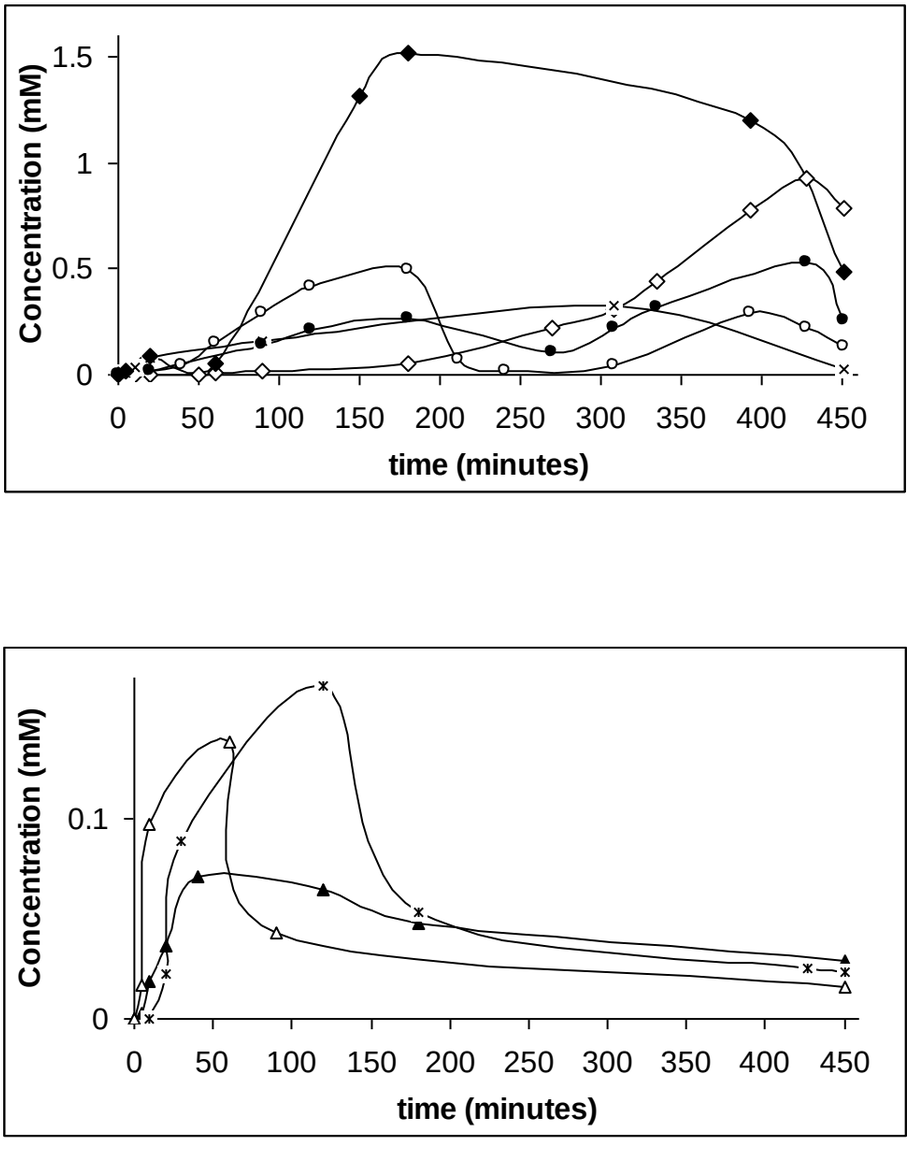

Figure 32. Evolution of carboxylic acids identified (succinic: △, malonic: ∗, piruvic: ▲, glycolic: x, glyoxylic: ○, acetic: ◆, oxalic: ◇ and formic: ●) during oxidation of *m*-cresol by electro-Fenton treatment. Experimental conditions: I = 200 mA, V_0 = 125 mL, C_0 = 2.5 mM, $[Fe^{2+}]$ = 0.1 mM, $[Na_2SO_4]$ = 50 mM, pH= 3.0 and Pt (1.5 cm x 2 cm) / CF (7 cm x 8 cm x 0,6 cm) electrodes.

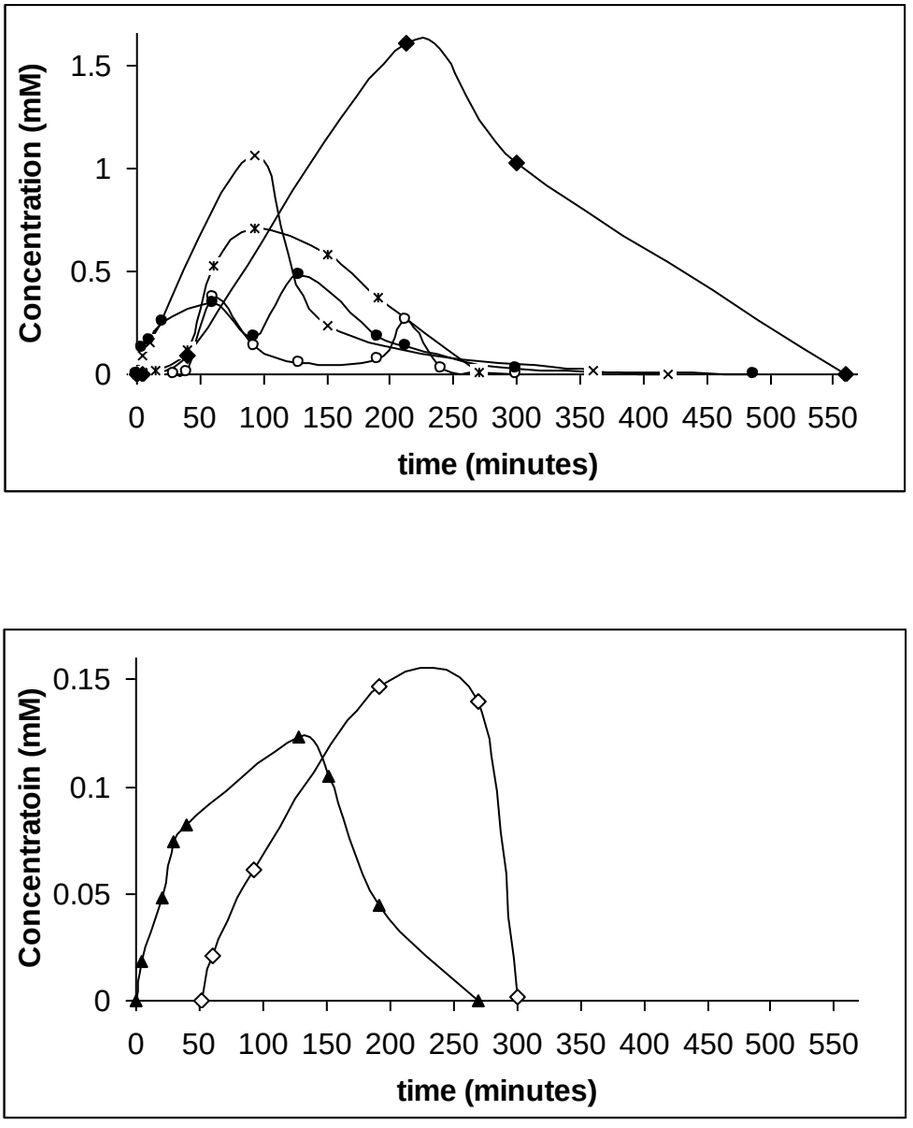

Figure 33. Evolution of carboxylic acids identified (glycolic: x, malonic: ∗, formic: ●, glyoxylic: ○, acetic: ◆, piruvic: ▲ e oxalic: ◇) during oxidation of *p*-cresol by electro-Fenton treatment. Experimental conditions: I = 200 mA, V_0 = 125 mL, C_0 = 2.5 mM, $[Fe^{2+}]$ = 0.1 mM, $[Na_2SO_4]$ = 50 mM, pH= 3.0 and Pt (1.5 cm x 2 cm) / CF (7 cm x 8 cm x 0,6 cm) electrodes.

The predominant acids produced in first stages of m-cresol degradation by electro-Fenton process (Figure 32) were glycolic, succinic, malonic and piruvic acids. These acids were rapidly converted in glyoxilic, acetic, oxalic and formic, as it can be seen by their low accumulation. After 450 minutes, high concentrations of acetic and oxalic acids showed their greater persistency to total mineralization.

The main acids in first stages of p-cresol degradation (Figure 33) were glicolic, malonic, piruvic and formic acids. The presence of formic acid in the first minutes and in two peaks show that it could be produced initially due to the degradation of other acids, like glioxylic and acetic acids. After 125 minutes, acetic acid was predominant, being completely degraded after 550 minutes.

The acids formed in initial stages of *m*- and *p*-cresol degradation (succinic, glicolic, malonic and piruvic, according to Figures 32 and 33) are more persistent (10^7 M^{-1} s^{-1} < k < 10^8 M^{-1} s^{-1}, BUXTON *et al.*, 1988) than the predominant acids presented in the first stages of phenol (Figure 25: maleic) and *o*-cresol degradation (figure 29: fumaric, k ≅ 10^9 M^{-1} s^{-1}, BUXTON *et al.*, 1988). Thus, maleic and fumaric presence could harm complete degradation of phenol and o-cresol, explaining major persistency of these compounds in comparison to *m*- and *p*-cresol.

The experiments that aimed to study the effects of current density and reactional volume on mineralization rates of phenol and cresols are presented as follows.

3.5 Influence of current density and volume

These experiments were conducted in two phases. Initially, the effects of current density and reactional volume in samples containing phenol or o-cresol separately were studied applying electro-Fenton process at the same current. Subsequently, the effect of current density was studied applying electro-Fenton process in a sample containing equimolar concentrations of phenol, *o*- *m*- and *p*-cresol at different currents.

During experiments to evaluate phenol and o-cresol isolated mineralization, the optimized electrocatalitics conditions were maintained ([Fe^{2+}] = 0.1 mM, pH=3) with start concentrations equal to 1mM for each chemical substance (phenol or *o*-cresol). In these cases, during phenol experiments, there were changes in current densities and reaction volumes. Current was kept constant (I = 300 mA) and current density was changed through different superficial areas of carbon felt cathode. The first one had dimension of 7 cm x 8 cm x 0.6 cm (j = 5.4 mA/cm^2), while the second had dimension of 7 cm x 16 cm x 0.6 cm (j = 2.7 mA/cm^2). Both electrodes were totally immersed in solutions. Electro-Fenton process was monitored by sample collection and TOC measurements. Additionally, it was realized a control experiment with 1 mM of phenol and no current. The measures of TOC in function of electrolysis time are presented in Figure 34 and allowed comparing rates obtained during phenol and *o*-cresol degradation. It was also possible to verify the influence of current density, volume and adsorption on carbon-felt by mineralization rates obtained during phenol degradation by electro-Fenton process.

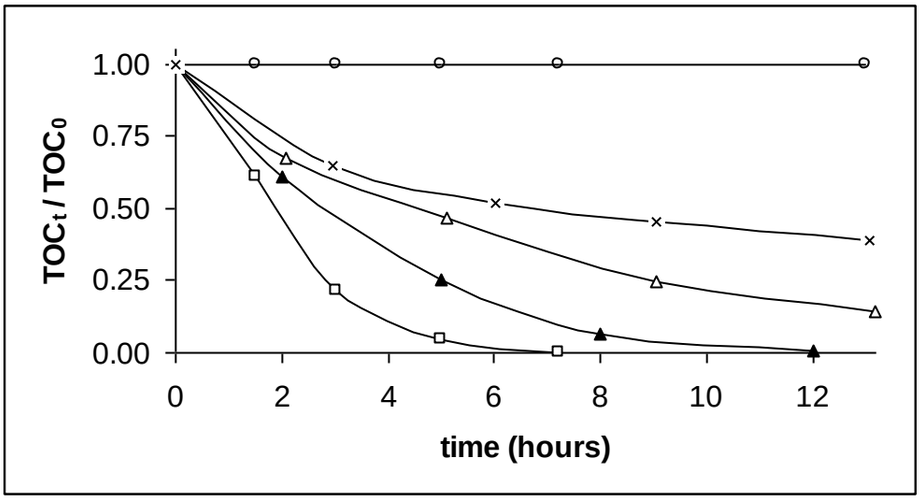

Figure 34. TOC removal during phenol (○, △, ▲, □) and *o*-cresol (x) degradation by electro-Fenton process changing the volume of reaction medium (150 mL: ○, ▲ and □; 400 mL: x and △) and/or current density (j = 0 mA/cm^2: ○; j = 2.7 mA/cm^2: □ ; j = 5.4 mA/cm^2: x, △ and ▲). Experimental conditions: I = 300 mA, $C_0 \cong 1$ mM (with theoretical TOC_0 = 72 mg/L), [Fe^{2+}] = 0.1 mM, [KCl] = 75 mM, pH= 3.0 and Pt (1.5 cm x 2 cm) / CF (7 cm x 8 cm x 0,6 cm: △; ▲, x e 7 cm x 16 cm x 0,6 cm: ○, □) electrodes.

There was no mineralization in control experiment (○). TOC reduction was not significant (< 0.2%), showing that phenol was not adsorbed by carbon-felt, even under critical conditions (small volume, great superficial area and long time reaction).

The comparison between TOC removal rates of phenol (△) and *o*-cresol (x) for 13 hours, under the same experimental conditions, presented a greater efficiency for phenol (86.1 %) than *o*-cresol (61.2%). These results emphasize the greater oxidation rates obtained for phenol during kinetic experiments (Figures 19 e 20). In fact, solutions containing equimolars start concentrations (1 mM) of phenol and *o*-cresol provided a greater concentration of TOC for *o*-cresol because this molecule has a greater number of carbon atoms ($[TOC]_{0\ o\text{-cresol}}$ = 81.19 mg/L and $[TOC]_{0\ fenol}$ = 71.21 mg/L). However, the increase of this difference along the experiment shows that o-cresol degradation was slower. This fact can be explained by the production of great concentrations of persistant intermediates like piruvic, oxalic and acetic acids, observed in *o*-cresol degradation through electro-Fenton process, observed in Figure 29.

During phenol degradation experiments (△, ▲ and □), it was observed that, even with a constant current, it was possible to enhance the eficiency of phenol mineralization rates reducing the volume of reactional medium (△ and ▲) and the current density (▲ and □).

The reduction in solution initial volume decreased phenol total mass, increasing the amount of TOC to be removed. This fact shows the importance to present the treated volume in electrochemical process, data often ignored by literature.

The increase of efficiency with the reduction of current density demands special attention. In fact, electrochemical production of hydrogen peroxide, generally presented by Equation 37, occurrs in four stages, being limited from the first one (MIOMANDRE *et al.*, 2005). These stages are presented from Equations (70) to (73).

$O_2 + e^- \rightarrow O_2^{\bullet -}$ $k = 1.9 \times 10^{10}\ M^{-1}\ s^{-1}$ (BUXTON *et al.*, 1988) (70)

$O_2^{\bullet -} + H^+ \rightarrow HO_2^{\bullet}$ $pK = 4.8$ (71)

$HO_2^{\bullet} + e^- \rightarrow HO_2^-$ $k = 1.3 \times 10^{10}\ M^{-1}\ s^{-1}$ (BUXTON *et al.*, 1988) (72)

$HO_2^- + H^+ \rightarrow H_2O_2$ $pK = 11.63$ (73)

Thus, the increase on working electrode surface (carbon felt: 7 cm x 8 cm x 0,6 cm $\rightarrow$ 7 cm x 16 cm x 0,6 cm) practically doubled the quantity of oxygen dissolved and ferric ion in contact with cathode, increasing peroxide production (PIMENTEL *et al.*, 2008) and electrochemical regeneration of ions ferrous. An improvement in diffusion process can also be observed from limit current (i_{lim}), according to Equation 50. Considering that carbon-felt is a three dimensional electrode, an increase in electrode surface reduced the current density applied and increased the limit current (Equation 50). Probably, current efficiency could be improved because the current density applied was reduced and brought closer to limit current (FOCKEDEY and VAN LIERDE, 2002). This increase is probably limited to currents greater than limit current (equation 50). Thus, this result suggests that while current applied is inferior to limit current, electro-Fenton process is controled by charge transfer. When current is increased and current exceeds limit current, electro-Fenton process becomes controlled by mass transfer process. Then, when the surface of the

working electrode is defined, the electro-Fenton process tends to be maximized when the applied a current is equal to limit current (i_{lim}).

In best conditions (□), with a current density equal to 2.7 mA/cm^2, it was possible to obtain complete mineralization of 1 mM of phenol aqueous solution in seven hours. In two hours of experiment, 56% of TOC was removed, which is a great result when compared with efficiencies frequently presented in literature (Table 8: ESPLUGAS *et al.*, 2002).

Subsequently, two experiments were realized to clarify the effect of the increase in current density by the change of current in a sample containing high concentration of phenol and cresols. Figure 35 presents the results of these experiments.

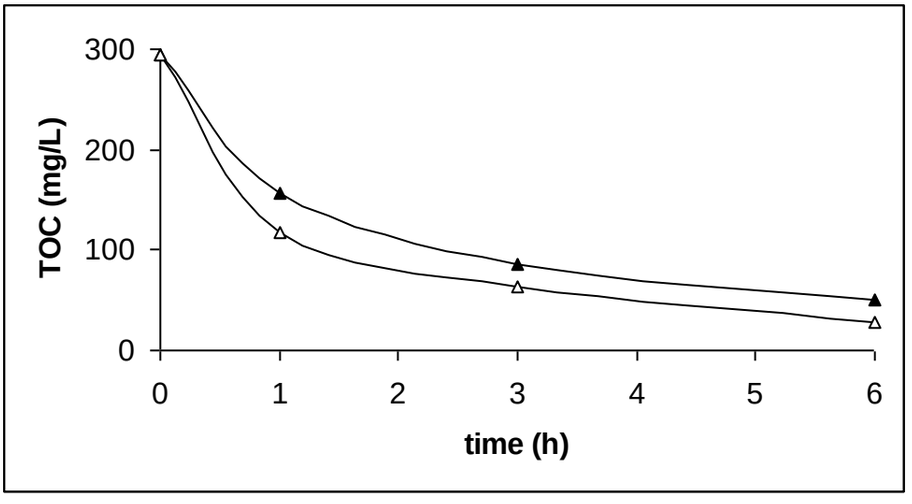

Figure 35. Effect of current increase (▲: I = 250 mA, j = 4.5 mA/cm^2 and △: I = 500 mA, j = 9.0 mA/cm^2) on mineralization of solution containing equimolar concentrations of phenol and cresols ([phenol]$_0$ = [*o*-cresol]$_0$ = [*m*-cresol]$_0$ = [*p*-cresol]$_0$ ≅ 1 mM). Experimental conditions: TOC$_0$ ≅ 324 mg/L, V$_0$ = 100 mL, [Fe^{2+}] = 0.1 mM e [KCl] = 75 mM, pH= 3.0 and Pt (1.5 cm x 2 cm) / CF (7 cm x 8 cm x 0,6 cm) electrodes.

When a current equal to 250 mA (▲) was applied to an equimolar solution containing 4 mM of phenol and cresols, it was observed a TOC removal of 83% after 6 hours of experiment. When the current was doubled to 500 mA (△), it was possible to remove 90% of COT at the same time. Therefore, electro-Fenton process was efficient to treat solutions containing phenol and/or cresols concentrations until 4 mM. This small efficiency increase obtained demonstrated that, in this case, probably, both currents applied were above the limit current. In fact, the current densities applied in these experiments were higher (j = 4.5 e 8.9 mA/cm^2) to current density that allowed the best result (Fig. 34: j = 2.7 mA/cm^2).

After electro-Fenton process optimization in synthetic samples, it was evaluated its performance to treat a sample containing real effluent.

3.6 Application of electro-Fenton process in aircraft stripping process effluent

Ten liters of a real effluent from aircraft striping process, made in Parque de Material Aeronáutico do Galeão in Rio de Janeiro, were collected and transported to Université Paris-Est Marne-la-Vallée. Preliminary chemical analysis of collected samples revealed a basic medium (pH = 9.04 - 9.1), containing extremely high concentrations of organic matter (COT_0 = 5280 – 5312 mg/L), total chrome (75.0 mg/L) and hexavalent chrome (49.5 mg/L).

Considering that the use of iron concentrations between 0.1 and 0.25 mM in previous experiments showed close efficiencies during phenol (Figure 19) and *o*-cresol (Figura 20) degradation and as the concentrations of organic matter in real effluent were higher than concentrations of synthetic effluent, it was decided to add ferrous concentrations equal to 0,2 mM to treat real effluent.

Four electrochemical experiments were done to optimize the efficiency of the electro-Fenton process to treat real effluent, presented in Figure 36.

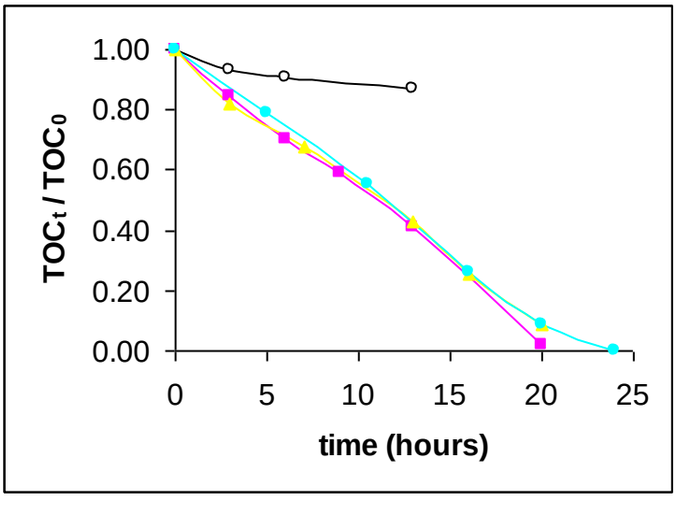

Figure 36. TOC removal from real effluent by electro-Fenton process (I = 500 mA, V_0 = 250 mL and pH = 2.9 - 3) in electrochemical cells of Pt (1.5 cm x 2 cm) / CF (17 cm x 4 cm x 0.6 cm): (○) TOC_0 = 5300 mg/L and BDD (4 cm x 6 cm) /CF (17 cm x 4 cm x 0.6 cm): (■) TOC_0 = 5280 mg/L; (▲) TOC_0 = 5312 mg/L and (●) TOC_0 = 4950 mg/L. Experimental conditions: addition of 0.2 mM of Fe^{2+} (○, ■); addition of 0.2 mM of Fe^{2+} with previous removal of chrome (●) and without addition of iron (▲).

In these experiments, it was studied the effect of an electrochemical cell containing carbon felt as cathode (17 cm x 4 cm x 0.6 cm) and replacing Pt anode (1.5 cm x 2 cm) by boron-doped diamond (4 cm x 6 cm). Besides, the oxidation power of the process was verifified under three different situations: isolated action of iron; combined action of chrome and other present metals; and combined action of iron, chrome and other methals present in the medium.

In experiment without chrome, chrome was previously removed by classic reduction process of hexavalent to trivalent chrome in pH 3 (adding hydrocloridric acid and sodium metabisulfite). Then, trivalent chrome was precipitated in pH 9 (by addition of sodium hydroxide). The supernatant was filtered in double paper and pH was reduced once more by hydrocloridric addition.

In experiment conducted by electro-Fenton process in Pt/CF cell (○), the TOC removal was too low (13%). The experiment had to be finished in 13 hours due to a polymeric film formation in the process which became the electrode surface passive. The polymers formation is often observed during electrochemical degradation of solutions with extremely high concentrations of phenols (ZAREIE *et al.*, 2001; SANTOS *et al.*, 2002; ANDREESCU *et al.*, 2003; LI *et al.*, 2005). So, new reactors had to be tested.

There are few electrochemical studies where the efficiency of different combinations of cathodes (carbon-felt or oxygen difused) and anodes (BDD or Pt) is compared. However, Pt/carbon felt and BDD/carbon-felt cells have presented, respectively, the better results (Figure 8). In these studies, Pt/CF cell presented the best results because it favours a major regeneration of ferrous ion, increasing hydroxyls radical's production (Equation 5).

According to the authors, BDD/FC cell did not allow a greater production of hydroxyls radicals because it promoted a major re-oxidation of ferrous to ferric ion. It is important to observe that in all these studies, 50 mM sodium sulphate was added to increase conductivity. Higher presence of sodium sulphate concentration in BDD/CF systems were the main explanation to the losses of eficiency in these reactors. This higher concentration promoted re-oxidation of ferrous to ferric ion by the equations 37 and 74, presented as follows.

$$2HSO_4^- \rightarrow S_2O_8^{2-} + 2H^+ + 2e^- \quad (37)$$

$$S_2O_8^{2-} + 2Fe^{2+} \rightarrow 2SO_4^{2-} + 2Fe^{3+} + 2e^- \quad (74)$$

On the other hand, in real effluent treatment, (Figure 36), the replacement of Pt anode (○) by BDD (■), under the same experimental conditions, increased significantly the efficiency of electro-Fenton process, removing about 98% of TOC in 20 hours of reaction. It wasn't necessary to add any electrolyte and typical sulphates concentrations in this effluent are very low (Table 1). In fact,

according to OTURAN and BRILLAS (2007), theoretically, substitution of Pt anode by BDD increases strongly electro-Fenton process efficiency, because additional hydroxyls radicals are produced in anode. So, probably, the major oxidant power of BDD anode increased hydroxyls radicals' production in anode through reaction 24.

$$BDD(H_2O) \rightarrow BDD(^{\bullet}OH) + H^+ + e^- \quad (24)$$

Polymers weren't formed in experiments with BDD/CF cell. Probably, supplementary hydroxyls radicals transfered by anodic via avoided it. It is important to remind that when higher electric charges are applied in BDD anode, there is ozone production (reaction 36), promoting additional oxidative processes (reaction 10 and direct oxidation).

$$3H_2O \rightarrow O_3 + 6H^+ + 6e^- \quad (36)$$

$$O_3 + Fe^{2+} + H_2O \rightarrow O_2 + FeOH^{2+} + {}^{\bullet}OH \quad (10)$$

On the other hand, other experiments using BDD/FC cell removed about 91% of TOC in 20 hours of experiment, by adding ferrous ion and previous removal of chrome (●) or even without addition of any transition metal (▲).

The great removal of TOC obtained in these experiments showed that the effluent naturally presents transition metal (s) that allowed act in the process without adding any catalyst (▲). In fact, Table 1 shows typical characterization of this effluent and other metals. Chrome removal did not increase efficiency of the process, although, in this case, it was necessary to add ferrous ion, because chrome precipitation probably promoted removal of others transition metals naturally present. So, the procedure that allowed greater efficiency was the pH reduction by adding 0.2 mM of ferrous ion without removing chrome (■).

However, BDD/FC cell (11.8 V) increased significantly the voltage in relation to Pt/FC cell (3.8 V), leading to a considerable increase of electric consumption.

CHAPTER IV: CONCLUSION

In optimum experimental conditions, electro-Fenton process allowed to obtain total mineralization of phenol. Ferrous iron ions were the most effective catalysts with optimum concentration of 0.1 mM. Fixing constant currents and pH value about 3, smaller volumes and greater cathode surfaces allowed faster degradation. These results presented tips to design, to compare and to optimize electrochemical reactors. It is important to remind that these optimum catalytic conditions were obtained considering phenol degradation. During electro-Fenton degradation of some other compounds, using iron as catalyst may lead to formation of complexes, changing iron concentration in the media. In these cases, other metal cations may present better results as catalyst.

During kinetic experiments involving cresols degradation, catalyst optimum concentration obtained was also equal to 0.1 mM of Fe^{2+}. The apparent rate constants obtained during the degradation of 1.05 mM of these compounds were equal to 0.0326 0.001 min^{-1} (*m*-cresol), 0.0246 0.001 min^{-1} (*p*-cresol) and 0.0096 0.001 min^{-1} (o-cresol). It confirmed the major persistence of *o*-cresol between the cresols (BUXTON *et al.*, 1988; RODER *et al.*, 1999).

Phenol oxidation by hydroxyl radicals also followed a pseudo-first order kinetics with an apparent rate constant of 0.037 min^{-1} under the same experimental conditions (pH=3, V_0=125 mL, I=60 mA, $[phenol]_0$=1.05 mM, [Fe]=0.1mM).

Using competition kinetics method, the absolute rate constant between the hydroxyl radicals and the compounds (pH = 3) found to be (2.62 $\pm$ 0.23) x 10^9 M^{-1} s^{-1} to phenol and (3.70 6 0.19) x 10^9 M^{-1} s^{-1} for *o*-cresol.

Hydroxylation of phenol generated benzoquinone, catechol and hydroquinone as the most important intermediates (about 70%). Maleic, fumaric, succinic, glyoxylic were predominantly formed in the beginning, while oxalic and formic were the final products. These intermediates were also completely mineralized at the end of treatment. High mineralization rates observed in first hours of treatment can be justified by higher reaction rate constant of hydroxyl radicals with aromatics in comparison with carboxylic acids and the formation of stables ferri-oxalate complexes.

During *o*-cresol electrolysis, the main initial reactions (about 58%) were successively electrophilic additions of hydroxyl radical on the aromatic ring, leading to the formation of 3-methylcatechol and methyl-hydroquinone. Fumaric and succinic acids were predominantly formed in initial stages, but there were also traces of piruvic and maleic. Oxalic, acetic and glyoxylic acids were predominant formed in final stages, reaching maximum concentrations in 300 minutes of reaction.

The predominant acids produced in first stages of m-cresol degradation by electro-Fenton process were glycolic, succinic, malonic and piruvic acids. These acids were rapidly converted in glyoxilic, acetic, oxalic and formic, as it could be seen by their low accumulation. After 450 minutes, high concentrations of acetic and oxalic acids showed their greater persistency to total mineralization.

The main acids in first stages of p-cresol degradation were glicolic, malonic, piruvic and formic acids. After 125 minutes, acetic acid was predominant, being completely degraded after 550 minutes.

During real effluent treatment, the replacement of Pt anode by BDD, under the same experimental conditions, increased significantly the efficiency of electro-Fenton process, removing about 98% of TOC in 20 hours of reaction. The presence of chrome did not harm the efficiency of the process. High mineralization rates evidenced the efficiency of the electro-Fenton as an advanced oxidation process to treat stripping aircraft wastewater.

REFERENCES

AL-EKABI, H.; SERPONE, N.; PELIZZETTI, E.; MINERO, C.; FOX, M.A., DRAPER, R.B. Kinetic Studies in Heterogeneous Photocatalysis. II: TiO_2-Mediated Degradation of 4-Chlorophenol Alone and in a Three-Component Mixture of 4-Chlorophenol, 2,4-Dichlorophenol, and 2,4,5-Trichlorophenol in Air-Equilibrated Aqueous Media", *Langmuir*, 5(1), 250-255, 1989.

ANDREESCU, S.; ANDREESCU, D.; SADIK, O. A. A new electrocatalytic mechanism for the oxidation of phenols at platinum electrodes. *Electrochemistry Communications*, 5, 681-688, 2003.

ANIPSITAKIS, G. P.; DIONYSIOU D. D. Transition metal/UV-based advanced oxidation technologies for water decontamination. *Applied Catalysis B: Environmental*, 54, 155-163, 2004.

ARAÑA, J.; REONDÓN, E. T.; RODRIGUEZ, J. M. D.; MELLIAN, J. A. H.; DÍAZ, O. G.; PEÑA, J. A. Highly concentrated phenolic wastewater by the photo-Fenton reaction, mechanism study by FTIR-ATR. *Chemosphere*, 44, 1017-1023, 2001.

AHAMAD, P.Y.A.; KUNHI, A. A. M. Degradation of high concentration of cresols by *Pseudomonas sp CP4*. *World Journal of Microbiology and Biotechnology*, 15 (2), 321-327, 1999.

ARQUIAGA, M. C.; CANTER, L. W.; ROBERTSON, J. L. Microbiological characterization of the biological treatment of aircraft paint stripping wastewater. *Environmental Pollution*, 89 (2), 189-195, 1995.

AZEVEDO, E. B. *Identificação e toxicidade de intermediários formados na degradação fotocatalítica e na ozonização de fenol em meio salino.* Tese (Doutorado em Engenharia Química) — Departamento de Engenharia Química, Universidade Federal do Rio de Janeiro, Rio de Janeiro, 188 f., 2003.

BAIRD, C. *QUÍMICA AMBIENTAL.* 2ª ed. Porto Alegre: Editora Bookman, 511-512, 2002.

BARRET, K. A.; MCBRIDE, M.B. Oxidative Degradation of Glyphosate and Aminomethylphosphonate by Manganese Oxide. *Environmental Science & Technology*, 39, 9223-9228, 2005.

BELTRAN, F. J. Ozone-UV radiation-hydrogen peroxide oxidation technologies, in: M.A. Tarr (Ed.), *Chemical Degradation Methods for Wastes and Pollutants — Environmental and Industrial Applications*, Marcel Dekker, Inc., New York, USA, 1-77, 2003.

BOYE, B.; DIENG, M. M.; BRILLAS, E. Degradation of herbicide 4-chlorophenoxyacetic acid by advanced electrochemical oxidation methods. *Environmental Science & Technology*, 36(13), 3030-3035, 2002.

BOYE, A. M.; DIENG, M. M.; BRILLAS, E. Anodic Oxidation. electro-Fenton and photoelectro-Fenton treatments of 2.4.5-trichlorophenoxyacetic acid. *Journal of Electroanalytical Chemistry*, 557, 135-146, 2003.

BRASIL. *Resolução nº 357 do Conselho Nacional do Meio Ambiente, de 17 mar. 2005.* Dispõe sobre a classificação dos corpos de água e diretrizes ambientais para o seu enquadramento, bem como estabelece as condições e padrões de lançamento de efluentes e dá outras providências. Disponível em: <http://www.caema.ma.gov.br>. Acesso em: 3 abr. 2007.

BREMNER, D. H.; BURGESS, A. E.; HOULLEMARE, D.; NAMKUNG, K-C. Phenol degradation using hydroxyl radicals generated from zero-valent iron and hydrogen peroxide. *Applied Catalysis B: Environmental*, 63, 15-19, 2006.

BRILLAS, E., MUR, E., CASADO, J. Iron (II) catalysis of the mineralization of inaniline using a carbon-PTFE O_2-fed cathode. *Journal of the Electrochemical Society*, 143, L49-L53, 1996.

BRILLAS, E.; SAULEDA, R.; CASADO, J. Peroxi-coagulation of aniline in acidic medium using and oxygen diffusion cathode. *Journal of the Electrochemical Society*, 144, 2374-2379, 1997.

BRILLAS, E.; CASADO, J. Aniline degradation by Electro-Fenton and peróxi-coagulation processes using a flow reactor for wastewater treatment. *Chemosphere*, 47, 241-248, 2002.

BRILLAS, E.; BAÑOS, M.A.; GARRIDO, J.A. Mineralization of herbicide 3.6-dichloro-2-methoxybenzoic acid in aqueous medium by anodic oxidation. electro-Fenton and photoelectro-Fenton. *Electrochimica Acta*, 48, 1697,2003.

BRILLAS, E.; BOYE, B.; DIENG, M. M. General and UV-assisted cathodic Fenton treatments for the mineralization of herbicide MCPA. *Journal of the Electrochemical Society*, 150, E583-E589, 2003.

BRILLAS, E.; BOYE, B.; SIRÉS, I.; GARRIDO, J.A.; RODRÍGUEZ, R.M.; ARIAS, C.; CABOT, P.L.; COMNINELLIS, CH. Electrochemical destruction of chlorophenoxy herbicides by anodic oxidation and electro-Fenton using a boron-doped diamond electrode. *Electrochimica Acta*, 49, 4487, 2004a.

BRILLAS, E.; BAÑOS, M. A.; CAMPS, S.; ARIAS, C.; CABOT, P. L.; GARRIDO, J. A.; RODRÍGUEZ, R. M. Catalytic effect of Fe^{2+}. Cu^{2+} and UVA light on the electrochemical degradation of nitrobenzene using an oxygen-diffusion cathode. *New Journal of Chemistry*, 314-322, 2004b.

BRILLAS, E.; SIRÉS, I.; ARIAS, C.; CABOT, P. L.; CENTELLAS, F.; RODRÍGUEZ, R. M.; GARRIDO, J. A. Mineralization of paracetamol in aqueous medium by anodic oxidation with a boron-doped diamond electrode. *Chemosphere*, 58, 399-406, 2005.

BRILLAS, E.; BAÑOS, M. A.; SKOUMAL, M.; CABOT, P. L.; GARRIDO, J. A.; RODRÍGUEZ, R. M. Degradation of the herbicide 2.4-DP by anodic oxidation. electro-Fenton and photoelectro-Fenton using platinum and boron-doped diamond anodes. *Chemosphere*, 68, 199-209, 2007.

BUDAVARI, S., O'NEIL M. J., SMITH A., HECKELMAN P. E. *The Merck index*. New Jersey: Merck & Co. Inc., 1150, 1989.

BUXTON, G. V., GREENSTOCK, C. L.; HELMAN, W. P. and ROSS, A. B. Critical Review of Rate Constants for Reactions of Hydrated Electrons. Hydrogen Atoms and Hydroxyl Radicals ($HO^{\bullet}$ / $O^{\bullet -}$) in Aqueous Solution. Journal of Physical Chemistry, 17(2), 517, 518, 702, 706, 728, 1988.

CANTON, C.; ESPLUGAS, S.; CASADO, J. Mineralization of phenol in aqueous solution by ozonation using iron or copper salts and light. *Applied Catalysis B: Environmental*, 43, 139-149, 2003.

CATURLA, F.; MARTIN-MARTINEZ, J., M.; MOLINA-SABIO, M.; RODRIGUEZ-REINOSO, F., TORREGROSA, R. Adsorption of substituted phenols on activated carbon. *Journal of Colloid and Interface Science***,** 124, 528-534, 1988.

CANTON, C; ESPLUGAS, S.; CASADO, J. Mineralization of phenol in aqueous solution by ozonation using iron or copper salts and light. *Applied Catalysis B: Envinronmental*, 43, 139-149, 2003.

CHANG, R. *Química*. 5ª ed. Portugal: Editora McGraw-Hill de Portugal Ltda., 5-6, 863, 1994.

CHEN, J.; LIU, M.; ZHANG, J.; XIAN, Y.; JIN, L. Electrochemical degradation of bromopyrogallol red in presence of cobalt ions. *Chemosphere*, 53, 1131-1136, 2003.

COMINELLIS, Ch. Electrocatalysis in the electrochemical conversion/ combustion of organic pollutants for waste water treatment. *Electrochimica Acta*, 39, 1857-1862, 1994.

DABROWSKI, A.; PODKOSCIELNY, P., HUBICKI, Z.; BARCZAK, M. Adsorption of phenolic compounds by activated carbon - a critical review. *Chemosphere*, 58, 1049-1070, 2005.

DEICHMANN W, KEPLINGER ML. Phenols and phenolic compounds. In: Clayton GD & Clayton FE ed. *Patty's industrial hygiene and toxicology*, 3rd ed. New York: John Wiley and Sons, 2A, 2567-2627, 1981.

DIAGNE, M.; OTURAN, N. e OTURAN, M.A. Removal of methyl parathion from water by electrochemically generated Fenton's reagent. *Chemosphere*, 66, 841-848, 2007.

DUTTA K.; MUKHOPADHYAY B.; HATTACHARJEE S. Chemical oxidation of methylene blue using a Fenton-like reaction. *Journal of Hazardous Material*, B84, 57-71, 2001.

ECKENFELDER, W., W. *Industrial water pollution control*. 3ª ed. USA: Editora McGraw-Hill Ltda., 124, 469, 2000.

EDELAHI, M. C.; OTURAN, N.; OTURAN, M. A.; PADELLEC, Y.; BERMOND, A.; KACEMI, K. Degradation of diuron by electro-Fenton process in aqueous solution. *Environmental Chemistry Letters*, 1, 233-236, 2004.

ESPLUGAS, S.; GIMÉNEZ, J. ; CONTRERAS, S.; PASCUAL, E.; RODRÍGUEZ. M. Comparison of different advanced oxidation processes for phenol degradation. *Water Research*, 36, 1034-1042, 2002.

FENTON, H. J. H. Oxidation of tartaric acid in presence of iron. *Journal of the Chemical Society Transactions*, 65, 897-910, 1894.

FIEGE, H., BAYER, A. G. Cresols and xylenols. In: Gerharte W ed. *Ullman's encyclopedia of industrial chemistry*, 5th ed. New York, VCH Publishers, vol 8A, 25-59, 1987.

FIESER, L.F. An indirect method of studying the oxidation-reduction potentials of unstable systems including those from the phenols and amines. *Journal of American Chemical Society*, 52, 5204-5241, 1930.

FLOX, C.; GARRIDO, J. A.; RODRÍGUEZ, R. M.; CENTELLAS, F.; CABOT, P. L.; ARIAS, C., BRILLAS, E. Degradation of 4.6-dinitro-o-cresol from water by anodic oxidation with a boron-doped diamond electrode. *Electrochim. Acta*, 50, 3685-3692, 2005.ica

FLOX, C.; GARRIDO, J. A.; RODRÍGUEZ, R. M.; CENTELLAS, F.; CABOT, P. L.; ARIAS, C., BRILLAS, E. Electrochemical combustion of herbicide mecoprop in aqueous medium using a flow reactor with a boron-doped diamond anode. *Chemosphere*, 64, 892-902, 2006.

FLOX, C.; CABOT, P. L.; CENTELLAS, F.; GARRIDO, J. A.; RODRÍGUEZ, R. M.; ARIAS, C.; BRILLAS, E. Solar photoelectro-Fenton degradation of cresols using a flow reactor with a boron-doped diamond anode. *Applied Catalysis B: Environmental*, 75, 17-28, 2007.

FLYVBJERG, J.; J0RGENSEN, C.; ARVIN, E.; JENSEN, B. K.; OLSEN, S. K. Biodegradation of ortho-Cresol by a Mixed Culture of Nitrate-Reducing Bacteria Growing on Toluene. *Applied and Environmental Microbiology*, 59(7), 2286-2292, 1993.

FOCKEDEY, E.; VAN LIERDE, A. Coupling of anodic and cathodic reactions for phenol electro-oxidation using three-dimensional electrodes. *Water Research*, 36, 4169-4175, 2002.

FRANCE. *Décret no 2001-1220 de la Présidance de la République*, du 20 décembre 2001. Relatif aux eaux destinées à la consommation humaine, à l'exclusion des eaux minérales naturelles.

FUNDAÇÃO CENTRO TECNOLÓGICO DE MINAS GERAIS. Lagoa Santa: *Projeto da Estação de Tratamento do Parque de Material Aeronáutico de Lagoa Santa (PAMA-LS)*. Certificado de Ensaios n^{o} 204725, 2000.

GANDINI, D.; MAHÉ, E.; MICHAUD, P. A.; HAENNI, W.; PERRET, A.; COMNINELLIS, C. Oxidation of carboxylic acids at boron-doped diamond electrodes for wastewater treatment. Journal of Applyed Electrochemistry, 30, 1345-1350, 2000.

GATTRELL, M.; KIRK, D. W. A study of the oxidation of phenol at platinum and preoxidized platinum surfades. *Journal of Electrochemistry Society*, 140 (6), 1534-1540, 1993.

GHAEMI, M.; BIGLARI, Z.; BINDER, L. Effect of bath temperature on electrochemical properties of the anodically deposited manganese dioxide. *Journal of Power Sources*, 102, 29-34, 2001.

GLAZE, W. H.; KANG, J.W.; CHAPIN, D.H. The chemistry of water treatment processes involving ozone, hydrogen peroxide and ultraviolet irradiation. *Ozone Science & Engineering*, 9, 335-352, 1987.

GRANT, T., M.; KING, C., J. Mechanism of irreversible adsorption of phenolic compounds by activated carbons. *Industrial & Engineering Chemistry Research*, 29, 264-271, 1990.

HANNA, K.; CHIRON, S.; OTURAN, M. A. Coupling enhanced water solubilization with cyclodextrin to indirect electrochemical treatment for pentachlorophenol contaminated soil remédiation. *Water Research*, 39, 2763-2773, 2005.

HANS, B. H. Paint Stripping with Nontoxic Chemicals. *Metal Finishing*, 93(4), 34-38, 1995.

HSU, Y. C.; CHEN, J. H.; YANG, H. C. Calcium enhanced COD removal for the ozonation of phenol solution. *Water Research*, 41, 71-78, 2007.

INIESTA, J.; MICHAUD, P.A.; PANIZZA, M.; CERISOLA, G.; ALDAZ A; COMINNELLIS, C, H. Electrochemical oxidation of phenol at boron-doped diamond electrode. *Electrochimica Acta*, 46, 3573-3578, 2001.

INTERMETA ENGENHARIA E CONSULTORIA. Lagoa Santa: Estudo de Tratabilidade, 13, 2001.

IRMAK, S.; YAVUZ, H. I.; ERBATUR, O. Degradation of 4-chloro-2-methylphenol in aqueous solution by electro-Fenton and photoelectro-Fenton processes. *Applied Catalysis B: Environmental*, 63, 243-248, 2006.

JUANG, R.,S.; TSENG, R., L.; WU, F., C.; LEE, S. H. Liquid-phase adsorption of phenol and its derivatives on activated carbon fibers. *Separation Science and Technology*, 31, 1915-1931, 1996.

KAVITHA, V.; PALANIVELU, K. The role of ferrous in Fenton and photo-Fenton processes for the degradation of phenol. *Chemosphere,* 55, 1235-1243, 2004.

KAVITHA, V.; PALANIVELU, K. Destruction of cresols by Fenton oxidation process. *Water Research*, 39, 3062-3072, 2005.

KURAMOCHI, H.; MAEDA, K.; KAWAMOTO, K. Water solubility and partitioning behavior of brominated phenols. *Environmental Toxicology and Chemistry*, 23(6), 1386-1393, 2004.

KUSIC H., KOPRIVANAC N., BOZIC, A. L. Minimization of organic pollutant content in aqueous solution by means of AOPs: UV- and ozone-based technologies. *Chemical Engineering Journal*, 123, 127-137, 2006.

LADISLAV S. A. *et al.* Degradation of high-molecular-weight hyaluronan by hydrogen peroxide in the presence of cupric ions. *Carbohydrate Research*, 341, 639-644, 2006.

LAURINDO, E. A.; AMARAL, F. A.; SANTOS, M. L.; FERRACIN, L. C.; CARUBELLI, A.; BOCCHI, N.; ROCHA-FILHO, R. C. *Produção de dióxido de manganês eletrolítico para uso em baterias de lítio.* São Paulo: Química Nova, 22(4), 1999.

LEMASTERS, G. K.; OLSEN, D. M.; YIIN, J. H.; LOCKEY; J. E.; SHUKLA, L.; SELEVAN, S. G.; SCHRADER, S. M.; TOTH, G. P.; EVENSON, D. P.; HUSZAR, G. B. Male reproductive effects of solvent and fuel exposure during aircraft maintenance. *Reproductive Toxicology*, 13(3), 155-166,1999.

LI, X. Y.; CUI, Y. H.; FENG, Y. J.; XIE, Z. M.; GU, J. D. Reaction pathways and mechanisms of the electrochemical degradation of phenol on different electrodes. *Water Research*, v. 39, 1972-1981, 2005.

MACIEL,R.; SANT-ANNA, G. L. J.; DEZOTTI, M. Phenol removal from high salinity effluents using Fenton's reagent and photo-Fenton reactions. *Chemosphere*, 57, 711-719, 2004.

MAEDA, M.; ITOH, A.; KAWASE, K. Kinetics for aerobic biological treatment of o-cresol containing wastewaters in a slurry bioreactor: biodegradation by utilizing waste activated sludge. *Biochemical Engineering Journal*, 22, 97-103, 2005.

MARR, J.C.A.; HANSEN, J.A.; MEYER, J.S.; CACELA, D.; PODRABSKY, T.; LIPTON, J.; BERGMAN, H.L. Toxicity of cobalt and copper to rainbow trout: application of a mechanistic model for predicting survival. *Aquatic Toxicology*, 43, 225-238, 1998.

MEHROTRA, I.; KUMAR, P.; GALI, V. *Treatment of phenolic wastewater using upflow anaerobic sludge blanket reactor.* Proceedings of National Conference on Biological Treatment of Wastewater and Waste Air, Regional Research Laboratory (CSIR), Trivandrum, India: 2003.

MIOMANDRE, F. ; SADKI, S.; AUDEBERT, P. ; MEALLET-RENAULT, R. In: *Électrochimie - Des concepts aux applications*, Dunot, Paris, 82, 2005.

NEUDER, H.; SIZEMORE, C.; KOLODY, M.; CHIANG, R.; LIN, C. T. Molecular design of in situ phosphatizing coatings (ISPCs) for aerospace primers. *Progress in Organic Coatings*, 47, 225-232, 2003.

NEYENS, E.; BAYENS, J. A review of classic Fenton's peroxidation as an advanced oxidation technique. *Journal of Hazardous Materials*, B98, 33-50, 2003.

NUNES, J. A. *Tratamento físico-químico de águas residuárias industriais.* 3ª ed. Brasil: Gráfica e Editora Triunfo Ltda, 99-102, 2001.

OTURAN M.A., PINSON J. Polyhydroxylation of salicylic acid by electrochemically generated OH radicals. *New Journal of Chemistry*, 16, 705-710, 1992.

OTURAN, M.A.; PINSON, J.; BIZOT, J.; DEPREZ, D.; TERLAIN, B. Reaction of inflammation inhibitors with chemically and electrochemically generated hydroxyl radicals. *Journal of Electroanalytical Chemistry*, 334, 103-109, 1992.

OTURAN, M. A. e PINSON J. Hydroxylation by Electrochemically Generated OH Radicals. Mono- and Polyhydroxylation of Benzoic Acid: Products and Isomers' Distribution. *Journal of Physical Chemistry*, 99, 13948-13954, 1995.

OTURAN , M.A.; AARON, J.J.; OTURAN, N.; PINSON, J. Degradation of chlorophenoxyacid herbicides in aqueous media, using a novel electrochemical methode. Pestic. Sci. 55, 558-562, 1999.

OTURAN, M.A. An ecologically effective water treatment technique using electrochemically generated hydroxyl radicals for in situ destruction of organic pollutants. Application to herbicide 2.4-D. *Journal of Applyed Electrochemistry*, 30, 477-478, 2000.

OTURAN, M.A.; PEIROTEN, J.-L.; CHARTRIN, P.; AUREL, J.A. Complete destruction of p-nitrophenol in aqueous medium by electro-Fenton methode. *Environmental Science & Technology*, 34, 3474, 2000.

OTURAN, M. A.; OTURAN, N.; LAHITTE C.; TREVIN S. Production of hydroxyl radicals by electrochemically assisted Fenton's reagent. Application to the mineralization of an organic micropollutant. pentachlorophenol. *Journal of Electroanalytical Chemistry*, 507, 96-102, 2001.

OTURAN, M. A.; PEIROTEN, J.; CHARTRIN, P.; ACHER, A. J. Complete Destruction of p-Nitrophenol in Aqueous Medium by Electro-Fenton Method. *Environmental Science & Technology*, 34, 3474-3479, 2002.

OTURAN, M. A.; BRILLAS, E. Electrochemical Advanced Oxidation Processes (EAOPs) for Environmental Applications. *Portugaliae Electrochimica Acta*, 25, 1-18, 2007.

OTURAN, N.; OTURAN, M.A. Degradation of three pesticides used in viticulture by electrogenerated Fenton's reagent. *Agronomy for Sustainable Development*, 25, 267-270, 2005.

OKAMOTO, K., YAMAMOTO, Y., TANAKA, H., TANAKA, M., ITAYA, A. Heterogeneous photocatalytic decomposition of phenol over TiO_2 powder. Bulletin of *Chemical Society of Japan*, 58(7), 2015-2022, 1985.

PENETONE CORPORATION. USA: *Material Safety Data Sheet - Formula 423*, 1-5, 2004.

PERRON, N.; WELANDER, U. Degradation of phenol and cresols at low temperatures using a suspended-carrier biofilm process. *Chemosphere*, 55, 45-50, 2004.

PIGNATELLO, J.J. Dark and photoassisted Fe^{3+}-catalyzed degradation of chlorophenoxy herbicides by hydrogen peroxide. *Environmental Science Technology*, 26 (5), 944-951, 1992.

PIMENTEL, M.; OTURAN, N.; DEZOTTI, M.; OTURAN, M. A. Phenol degradation by advanced electrochemical oxidation process electro-Fenton using a carbon felt cathode. *Applied Catalysis B: Environmental*, *(DOI: org/10.1016/j.apcatb.2008.02.011).*

PUMA, P. T. L.; RHODES, B. S. Chromate Content versus Particle Size for Aircraft Paints. *Regulatory Toxicology and Pharmacology*, 36, 318-324, 2002.

QIANG, Z.; CHANG, J. H.; HUANG C. P. Electrochemical regeneration of Fe^{2+} in Fenton oxidation processes. *Water Research*, 37, 1308-1319, 2003.

RICHTER, C. A.; NETTO, J. M. A. *Tratamento de água.* 5ª ed. São Paulo: Editora Edgar Blücher Ltda., 55-56, 1991.

RODER, M.; WOJNAÁROVITS, L.; FÖLDIÁK, G.; EMMI, S. S.; BEGGIATO, G.; D'ANGELANTONIO, M. Addition and elimination kinetics in OH radical induced oxidation of phenol and cresols in acidic and alkaline solutions. *Radiation Physics and Chemistry*, 54, 475-479, 1999.

SÁNCHEZ, L.; A, DOMÈNECH, X.; CASADO, J.; PERAL, J. Solar activated ozonation of phenol and malic acid. *Chemosphere*, 50, 1085-1093, 2003.

SANTOS, A.; YUSTOS, P.; QUINTANILLA, A.; RODRÍGUEZ, S.; GARCÍIA-OCHOA, F. Route of the catalytic oxidation of phenol in aqueous phase. *Applied Catalysis B: Environmental,* 39, 97-113, 2002.

SHREVE, R. N.; BRINK Jr, J. A. *INDÚSTRIA DE PROCESSOS QUÍMICOS.* 4ª ed. Rio de Janeiro: Editora Guanabara Koogan S. A., 341, 355, 1997.

SIRÉS, I.; OTURAN, N.; OTURAN, M. A.; RODRÍGUES, M. A.; GARRIDO, J. A.; BRILLAS, E. Electro-Fenton degradation of antimicrobials triclosan and triclocarban. *Electrochimica Acta*, 52, 5493-5503, 2007b.

SIRÉS, I.; GARRIDO, J. A.; RODRÍGUEZ, R. M.; BRILLAS, E.; OTURAN, N.; OTURAN, M. A. Catalytic behavior of the Fe^{3+}/Fe^{2+} system in the electro-Fenton degradation of the antimicrobial chlorophene. *Applyed Catalysis B: Environ*mental, 72, 382-394, 2007a.

SOLOMONS, T. G. Compostos Aromáticos. In. *Química Orgânica.* 6ª ed. Rio de Janeiro: LTC Livros ténicos e Científicos Editora S. A., 2, 279, 636-637, 1996.

SKOUMAL, M.; CABOT, P.; CENTELLAS, F; ARIAS, C.;RODRÍGUEZ R. M., GARRIDO, J. A.;BRILLAS E. Mineralization of paracetamol by ozonation catalyzed with Fe^{2+}, Cu^{2+} and UVA light. *Applied Catalysis B: Environmental,* 66, 228-240, 2006.

TORRES, R. A.; TORRES, W.; PERINGER, P.; PULGARIN, C. Electrochemical degradation of p-substituted phenols of industrial interest on Pt electrodes. Attempt of a structure-reactivity relationship assessment. *Chemosphere,* 50, 97-104, 2003.

TRYBA, B.; MORAWKSKY, A. W.; INAGAKI, M.; TOYODA, M. The kinetics of phenol decomposition under UV irradiation with and without H_2O_2 on TiO_2. Fe-TiO_2 and Fe-C-TiO_2 photocatalysts. *Applyed Catalysis B: Environmental*, 65, 86-92, 2006.

TÜRK, H.; ÇIMEN, Y. Oxidation of 2,6-di-tert-butylphenol with tert-butylhydroperoxide catalyzed by cobalt(II) phthalocyanine tetrasulfonate in a methanol–water mixture and formation of an unusual product 4,4′-dihydroxy-3,3′,5,5′-tetra-tert-butylbiphenyl. *Journal of Molecular Catalysis A: Chemical*, 234 (1-2), 19-24, 2005.

UNITED NATIONS ENVIRONMENT PROGRAME; INTERNATIONAL LABOUR ORGANISATION; WORLD HEALTH ORGANIZATION. Environmental Health Criteria 168 - Chresol. In: International Programme on Chemical Safety, 1995.

UNITED NATIONS ENVIRONMENT PROGRAME; INTERNATIONAL LABOUR ORGANISATION; WORLD HEALTH ORGANIZATION. Environmental Health Criteria 161 - Phenol. In: International Programme on Chemical Safety, 1994.

UNITED NATIONS ENVIRONMENT PROGRAME; INTERNATIONAL LABOUR ORGANISATION; WORLD HEALTH ORGANIZATION. Environmental Health Criteria 164 - Methylene chloride. In: International Programme on Chemical Safety, 1996.

UNITED NATIONS ENVIRONMENT PROGRAME; INTERNATIONAL LABOUR ORGANISATION; WORLD HEALTH ORGANIZATION. 2.4.6-tribromophenol and other simple brominated phenols. In: Concise International Chemical Assessment Document 66, 2005.

VIDIC, R.D., SUIDAN, M.T., BRENNER, R.C. Oxidative coupling of phenols on activated carbon: impact on adsorption equilibrium. Environmental Science & Technology, 27, 2079-2085, 1993.

VOEVODIN, N. N.; BALBYSHEV, V.N.; DONLEY, M.S. Investigation of corrosion protection performance of sol-gel coatings on AA2024-T3. *Progress in Organic Coatings*, 2004.

WU, M. S.; CHIANG, P. C. J. Electrochemically deposited nanowires of manganese oxide as an anode material for lithium-ion batteries. *Electrochemistry Communications,* 8, 383-388, 2006.

ZAREIE, M. H.; KÖRBAHTI, B. K.; TANYOLAÇ, A. Non-passivating polymeric structures in electrochemical conversion of phenol in the presence of NaCl. *Journal of Hazardous Materials,* B87, 199-212, 2001.

ZAZO, J. A.; CASAS, J. A.; MOHEDANO, A. F.; GILARRANZ, M. A.; RODRIGUEZ, J. J. Chemical Pathway and Kinetics of Phenol Oxidation by Fenton's Reagent. *Environmental Science & Technology*, 39(23), 9295 -9302, 2005.

ZHOU, G. M.; HERBERT, H. P. Co-degradation of phenol and m-cresol in a uasb reactor. *Bioresource Technology*, 61, 47-52, 1997.

GLOSSARY

Advanced Oxidative Processes – Technologies for the production of chemical radicals with high power oxidizer (hydroxyl radical - $^{\bullet}OH$), intended or mineralization and the degradation of toxic organic compounds.

Aircraft Stripping – It is the process of removing ink, held across aircraft, aiming to verify the existence of points of corrosion in the structure and to maintain security.

Degradation – Elimination of a chemical compound, turning it into another compound. The rate of degradation of a compound is defined by the percentage of compost removed in an instant t.

Mineralization – Elimination of an organic compound, through the transformation of that product and any derivatives the carbon dioxide (CO_2). The rate of mineralization is defined by the percentage of total organic carbon (TOC) removed an instant t.

Phenols – Any organic compound, containing beyond the structure of phenol, other radical added (R-phenol) for the replacement of one or more atoms of hydrogen.

Total Organic Carbon (COT) – Chemical analysis that measures the concentration of carbon on the organic compounds present.

Wastewater/effluent – Liquid generated in any activity from the use of the water supply or any other product.

Annexes

Annexe 1: Evolution of reverse-phase HPLC chromatograms (detection at 280 nm) during electro-Fenton treatment of 1.05 mM phenol aqueous solution. Experimental conditions: pH=3, I = 60 mA, V_0 = 125 mL, [Fe] = 0.1mM, Pt (1.5 cm x 2 cm) / CF (7 cm x 8 cm x 0,6 cm) electrodes. HPLC analysis conditions: Purospher RP-C18 column, eluent: water/methanol/acetic acid (79.2/19.8/1, v/v), flow rate: 0.8 mL/min.

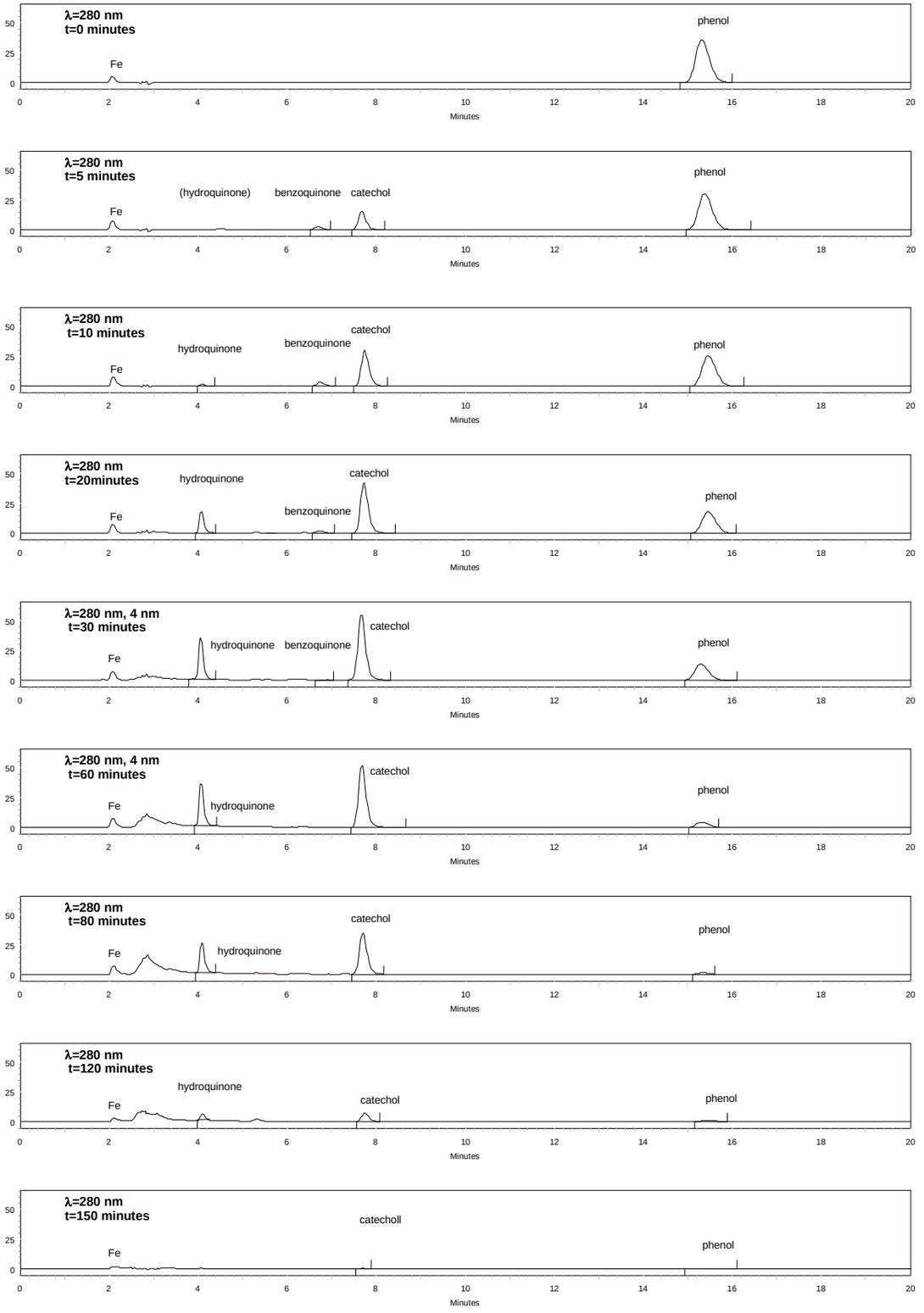

Annexe 2: Main chemical composition of removers used in paint stripper processes

MATERIAL SAFETY DATA SHEET

Penetone® Corporation, 700 Gotham Parkway, Carlstadt, NJ 07072

FORMULA 423

Page: 1 of 5
Date Prepared: February 23, 2004
MSDS No.: 3262-402O

SECTION 1 PRODUCT IDENTIFICATION & EMERGENCY INFORMATION

PRODUCT NAME: FORMULA 423
GENERAL USE: Heavy duty paint stripper and coating remover
PRODUCT DESCRIPTION: Paint stripper
GENERIC INGREDIENTS: Methylene chloride, cresols, phenol, water, and surfactant

EMERGENCY TELEPHONE NUMBERS: **PENETONE 201-567-3000**
CHEMTREC 800-424-9300

SECTION 2 HAZARDOUS INGREDIENT SECTION

This product is hazardous as defined in 29 CFR1910.1200.

OSHA HAZARD: CORROSIVE

OSHA HAZARDOUS INGREDIENTS

		EXPOSURE LIMITS 8 hrs. TWA (ppm)		
	CAS#	OSHA PEL	ACGIH TLV	Supplier
Methylene chloride	75-09-2	25 (125 STEL)	50	---
Cresol	1319-77-3	5 (skin)	5 (skin)	---
Phenol	108-95-2	5 (skin)	5 (skin)	---